

Neuronal mechanisms for evaluating the visual scene across eye movements

by

Trinity B. Crapse

Philosophy, B.A., University of South Carolina, 2000

**Submitted to the Graduate Faculty of
Arts and Sciences in partial fulfillment
of the requirements for the degree of
Doctor of Philosophy**

University of Pittsburgh

2010

UNIVERSITY OF PITTSBURGH
SCHOOL OF ARTS AND SCIENCES

This dissertation was presented

by

Trinity B. Crapse

It was defended on

September 23, 2010

and approved by

Aaron Batista, Ph.D. Dept. of Bioengineering

Committee Chairperson: Carol Colby, Ph.D. Dept. of Neuroscience

Neeraj Gandhi, Ph.D. Dept. of Otolaryngology

Outside Examiner: Richard Krauzlis, Ph.D. Salk Institute for Biological Studies

Erik Reichle, Ph.D. Dept. of Psychology

Dissertation Advisor: Marc Sommer, Ph.D. Dept. of Neuroscience

NEURONAL MECHANISMS FOR EVALUATING THE VISUAL SCENE ACROSS EYE MOVEMENTS

Trinity B. Crapse, Ph.D.

University of Pittsburgh, 2010

As a foveate animal, the primate must redirect its gaze with saccadic eye movements to subject different objects to high resolution analysis. Though beneficial in extending the range of visual analysis, the saccade-and-fixate oculomotor strategy poses a problem to the visual system as it performs its analyses. Each saccade results in a whole-field displacement of the visual image across the retina. Nevertheless, we experience a stable visual percept, implying a brain mechanism for visuo-spatial correction. The experiments reported here examine the neural mechanisms underwriting this correction.

In the first study, we sought to understand how the frontal eye field (FEF) gains access to information about ipsilateral space. Information about all of space, not just the contralateral hemifield, is a prerequisite for omnidirectional processes such as spatial remapping, a putative mechanism of visual stability. We found that one source of ipsilateral information is the superior colliculus (SC) on the opposite side of the brain.

In the second study, we set out to test a major prediction of one theory of visual stability. This theory invokes the function of neurons with shifting receptive fields (RFs) as a mechanism for achieving transaccadic visual stability. Shifting RFs effectively sample the same region of space twice, presaccadically and postsaccadically, and a percept of stability may rely on how well the samples match. This theory has the salient prediction that neurons in areas where shifting RFs are found should be sensitive to changes that occur to stimuli during saccades. We tested this prediction by recording from FEF neurons while monkeys performed a task during which a probe changed along a particular dimension during a saccade.

In a final study, we sought to bridge the neuron-behavior gap by recording from FEF neurons while monkeys performed a visual stability judgment task that probed their capacity to detect changes occurring during saccades. We found that monkeys are clearly able to discern whether a stimulus is stable or unstable during a saccade and moreover that FEF neural activity is predictive of monkey psychophysical performance.

Table of Contents

1. General Introduction.....	1
1.1 Visual stability and corollary discharge.....	1
1.2 The frontal eye field.....	7
1.3 Shifting receptive fields.....	11
1.4 The superior colliculus.....	15
1.5 Summary and Research Objectives.....	16
2. Frontal eye field neurons with spatial representations predicted by their subcortical input.....	19
2.1 Introduction.....	19
2.2 Materials and Methods.....	22
2.2.1 Surgery and region identification.....	22
2.2.2 Behavioral tasks.....	22
2.2.3 Neurophysiology.....	24
2.2.4 Data Analysis.....	25
2.2.5 Statistics.....	26
2.3 Results.....	27
2.3.1 Excitatory activation of the FEF from the two SCs.....	27
2.3.2 Route of activation from the contralateral SC.....	30
2.3.3 Response fields of FEF neurons driven from one SC.....	31
2.3.4 RFs of FEF neurons driven from both SCs.....	35

2.3.4.1	The RFs are lateralized, pandirectional, monolobed, and independent of relative weightings of SC inputs.....	35
2.3.4.2	The movement fields and visual fields are relatively broad and misaligned.....	38
2.3.5	Visual and saccadic activity.....	42
2.4	Discussion.....	45
2.4.1	Overview.....	45
2.4.2	Properties of FEF neurons with input from the opposite SC.....	45
2.4.3	Structure-function relationship in the SC-FEF circuit.....	48
2.4.4	Special case of bilateral SC input.....	50
2.4.5	Conclusion.....	52
3.	Frontal eye field neurons assess visual stability across saccades.....	53
3.1	Introduction.....	53
3.2	Methods.....	56
3.2.1	Surgery and region identification.....	56
3.2.2	Behavioral tasks.....	57
3.2.3	Data analysis.....	59
3.2.4	Tuning curve analysis.....	60
3.2.5	Saccade endpoint analysis.....	61
3.2.6	Statistics.....	62
3.3	Results.....	62
3.3.1	FEF neurons can detect intrasaccadic translations of a visual stimulus.....	62
3.3.2	Translation tuning was not a passive mapping of the future field.....	72

3.3.3	Translation tuning is not exclusive to neurons that remap.....	74
3.3.4	The neurons detect other transaccadic changes as well.....	75
3.4	Discussion.....	77
3.4.1	Overview.....	77
3.4.2	The variety of translation tuning curves.....	77
3.4.3	A perpendicular translation tuning advantage.....	78
3.4.4	The future field mapping hypothesis.....	79
3.4.5	A generalized change detection capability.....	80
3.4.6	Change detection is performed even by neurons without shifting RFs	82
3.4.7	Conclusion.....	84
4.	Frontal eye field activity predicts performance in a visual stability judgment task...	85
4.1	Introduction.....	85
4.2	Methods.....	86
4.2.1	Surgery and region identification.....	86
4.2.2	Behavior.....	86
4.2.2.1	Visual stability judgment task.....	86
4.2.2.2	Other tasks.....	88
4.2.3	Physiology.....	89
4.2.4	Data Analysis.....	89
4.2.4.1	Behavior.....	89
4.2.4.2	Neurons.....	90
4.3	Results.....	91

4.3.1	Behavior.....	91
4.3.2	Neurons.....	97
	4.3.2.1 On hit trials, FEF neurons are tuned for translations	97
	4.3.2.2 Early trial activity is predictive of psychophysical performance	100
	4.3.2.3 Reaction time is correlated with time of peak firing rate.....	103
4.4	Discussion.....	105
	4.4.1 Overview.....	105
	4.4.2 Monkeys distinguish true displacement of a visual stimulus from illusory, saccade-induced displacement.....	105
	4.4.3 Perpendicular translations are more salient than parallel translations..	106
	4.4.4 Reaction times are inversely proportional to translation amount and are predicted by time of peak firing rate.....	107
	4.4.5 FEF reafferent responses represent prediction error.....	108
	4.4.6 Monkey performance is predicted by an attention-like elevation of reafferent visual responses.....	109
	4.4.7 Conclusion.....	110
5.	General Discussion	
	5.1. Overview.....	112
	5.2. A large-scale theory of visual stability.....	115
	5.2.1 Prediction and the brain.....	115
	5.2.2 A prediction map in primate FEF.....	116
	5.2.3 Computational basis of the prediction map.....	119

5.2.4 Physiological mechanism of the prediction map.....	120
5.2.5 The sequence of events.....	121
5.2.6 Site of prediction error calculation.....	124
5.2.7 Relation to previous FEF studies.....	125
5.2.8 Empirical tests of the prediction map theory.....	126
5.3 Summary and Conclusion.....	128
6. Bibliography.....	130

List of Tables

Table 1. Distribution of FEF neuron types activated from each SC.....	43
Table 2. Number of FEF neurons with maximal activity for a given translation.....	67

List of Figures

Figure 1. The double step task.....	4
Figure 2. An eye field in the frontal lobe.....	8
Figure 3. Shifting receptive fields.....	12
Figure 4. Three hypothetical routes for a crossed SC to FEF connection.....	20
Figure 5. Orthodromic activation of FEF neurons.....	29
Figure 6. FEF neurons orthodromically activated from (A) the contralateral SC only and (B) the ipsilateral SC only.....	32
Figure 7. Totality of individual neuronal tunings for all 3 classes.....	33
Figure 8. Population results for tuning curves in all three samples of neurons.....	34
Figure 9. Individual response fields for the BothSC neurons.....	37
Figure 10. Shapes of the tuning curves.....	40
Figure 11. Activity profiles of the neurons.....	44
Figure 12. The ambiguity inherent in any visual change.....	54
Figure 13. Saccadic translation task.....	62
Figure 14. Three example neurons tested on the saccadic translation task.....	63
Figure 15. Ramp/Curvature indices for the two populations of neurons tested on the parallel and perpendicular versions of the task.....	65
Figure 16. Max-Min indices for the parallel and perpendicular tested samples.....	66
Figure 17. Ranked population of significant neurons.....	68
Figure 18. Temporal characteristics of translation tuning.....	69
Figure 19. Saccadic endpoint analysis.....	70

Figure 20. The RF mapping hypothesis.....	73
Figure 21. FEF responses to transaccadic featural changes.....	76
Figure 22. The visual stability judgment task.....	93
Figure 23. Behavioral performance.....	94
Figure 24. Reaction time distributions.....	95
Figure 25. Spike density functions for an example neuron.....	98
Figure 26. Neuronal population.....	99
Figure 27. Visual neuron response profiles.....	101
Figure 28. Early trial activity is predictive of monkey psychophysical performance....	102
Figure 29. Reaction time is correlated with time of peak firing rate.....	104
Figure 30. The FEF as a prediction map.....	123

Preface

Publications

This dissertation is composed of a general introductory chapter, three separate research chapters, and a general discussion. The research chapters and portions of the general discussion have been published or are being prepared for submission.

Chapter 2: Crapse, T.B. and Sommer, M.A. (2009). Frontal eye field neurons with spatial representations predicted by their subcortical input. *Journal of Neuroscience* 29(16):5308-5318.

Chapter 3: Crapse, T.B. and Sommer, M.A. Frontal eye field neurons assess visual stability across saccades. *In preparation*.

Chapter 4: Crapse, T.B. and Sommer, M.A. Frontal eye field activity predicts performance in a visual stability judgment task. *In preparation*.

Portions of Chapter 5: Crapse, T.B. and Sommer, M.A. (2008) The frontal eye field as a prediction map. *Progress in Brain Research*. 171:383-390.

Acknowledgments

This dissertation represents the labors of some five years. I, of course, did not act alone. A support structure was present without which I could not have completed this work. Many wonderful people were a part of this structure. Firstly, I wish to thank my advisor, Marc A. Sommer. I learned much from Marc. He taught me how to be a scientist. He spent hours upon hours with me, teaching me such things as the basics of primate neurophysiology, and most importantly how to convey my ideas clearly, both in written and spoken forms. I will continue to aspire to be like Marc, a talented master of conveying scientific ideas to a wide audience. Secondly, I wish to thank the monkey labs residing in the Mellon Institute. These include the Colby, Olson, and Lee labs, a special group indeed. I especially wish to thank Carl Olson and Carol Colby. No matter the time of day, I found that I could knock on Carl's door and ask him various questions about how the brain works, or ask him to evaluate an analysis or idea. He was always accommodating and extremely helpful. When times were tough, I would often find myself in Carol's office. She never failed to offer me much needed reassurances, advice, and warm support. She is truly an extraordinary person.

I also wish to thank the remaining members of my committee: Aaron Batista, Neeraj Gandhi, Erik Reichle, and Richard Krauzlis (outside examiner). Their guidance and feedback really improved the quality of the experiments described in this dissertation. Most importantly, they forced me to think about my results in novel ways.

Finally, I wish to thank my family. They may not understand what it is that I do exactly, but they certainly understand that it is important to me. As such, they provided me all the support I could ever ask for.

1.0 General Introduction

1.1. Visual stability and corollary discharge

Imagine a world in which objects appear to leap with every movement we make. Indeed, as far as our sensory receptors are concerned, we inhabit such a world. Consider things from the retina's perspective. Tucked away in the back of the eye, it witnesses a moving world some 2-3 times per second, a result of those frequent eye movements known as saccades. Surprisingly, though, we do not experience such a volatile, unstable world. Instead, we perceive a stable visual world in spite of saccadic interruptions. This is a clear example of the difference between sensation and perception and points to a mechanism within the brain for spatial correction. The question is: how does the brain do it?

The question of how the brain achieves visual stability is an old one with a rich history. Thinkers as far back as antiquity entertained the question and formulated various theories as to how the brain solves the problem. Writing in the 11th century, the Arabian scientist Alhazen showed keen insight when he noted that “the form of a stationary object may move in the eye while the object is at rest, but sight will not in consequence of this perceive the object to be in motion” (Wade and Tatler, 2005) . He concluded that, “sight has become accustomed to the motion of the objects' forms on its surface when the objects are stationary, and therefore does not judge the object to be in motion on account of the motion of its form...” (Wade and Tatler, 2005). A number of centuries later, the physiologist Müller reiterated Alhazen's observation in more modern terms when he noted that “If the image moves over the surface of the retina while the muscles of the eye

are acting at the same time in a manner corresponding to this motion, as in reading, we infer that the object is stationary, and we know we are merely altering the relation of eyes to the object” (Wade and Tatler, 2005). As evidenced by his reference to eye muscles, Müller was convinced that the movement of the eyes themselves played a role in compensatory stabilization mechanisms, but was unsure whether these signals emerged directly from the muscles (inflow) or were generated centrally with each eye movement (outflow).

The polymath Herman von Helmholtz took up the inflow/outflow distinction and became a proponent of the outflow hypothesis, i.e. that signals responsible for visual stabilization are produced within the brain concomitant with each eye movement. He mustered three pieces of evidence to support his claim. First, he cited the ancient observation that passive displacement of the eye results in the apparent motion of the visual image, while active displacement of the eye due to a saccade does not. Second, he noted that afterimages often remain fixed when the eye is moved passively, yet move when the eye is rotated by a saccade. Third, he described individuals with partial paralysis of the eye muscles and related how they experience motion of the world when they attempt to make an eye movement with the paralyzed eye. He concluded that, “These phenomena prove conclusively that our judgments as to the direction of the visual axis are simply the result of the effort of will involved in trying to alter the adjustment of the eyes” (Helmholtz, 1925). The Helmholtzian “effort of will” would be cast later in terms of “efference copy” by von Holst and Mittelstaedt (Holst and Mittelstaedt, 1950a), and “corollary discharge” by Roger Sperry (Sperry, 1950), internal monitoring signals

that are now deemed essential in the process of constructing a stable visual representation despite saccadic eye movements.

Corollary discharges are copies of movement commands that the brain issues with each movement (reviewed by (Crapse and Sommer, 2008b). Unlike the motor commands themselves, which travel out to the periphery to contract the appropriate muscles, corollary discharges travel in the opposite direction, impinging upon sensory brain areas. The corollary discharge information tells the sensory areas about the upcoming movements and allows them to prepare for the sensory consequences of the movement. Corollary discharges have advantages over proprioception and visual reafference, two signals that could contribute to informing a stable representation. Corollary discharges are faster, occurring before a saccade; proprioception and visual reafference become available only after a saccade. And as internal signals, corollary discharges are less subject to noise, injury, or other perturbations that can impair sensory systems.

The specific role of corollary discharges in generating a stable percept is thought to consist in their capacity to rapidly update retinotopic maps within the visual system. The classic example of updating occurs in the context of the double-step task first developed by Hallet and Lightstone (Hallett and Lightstone, 1976). For this task, the experimental subject is required to make two saccades in rapid succession to two sequentially flashed targets (Figure 1). Correct calculation of the second saccade must take into account the vector of the first since the original retinotopic coordinates of the second saccade target are no longer valid. A corollary discharge of the first saccade is considered to be required for appropriate spatial updating of the remembered location of the second saccade target.

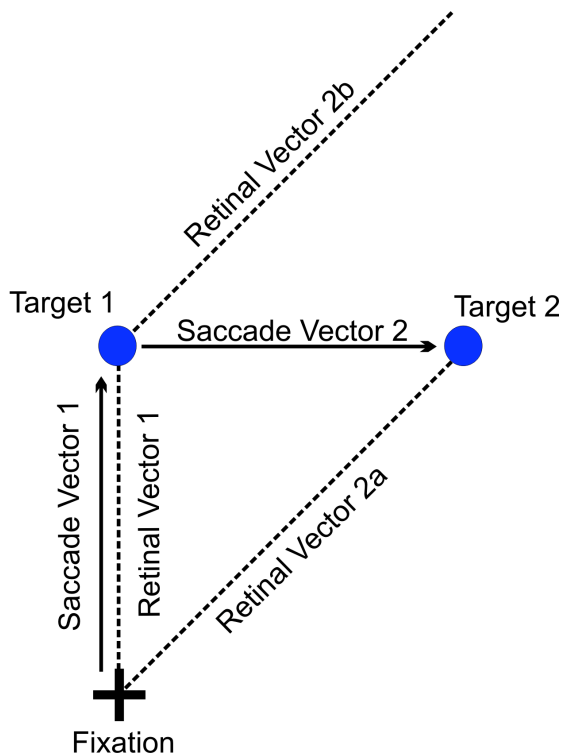


Figure 1. The double step task. A subject must make a pair of saccades to two targets flashed sequentially. The first saccade is easy enough, as it has a vector congruent with retinal vector 1. The second saccade is a bit more complicated since its generation cannot rely solely on retinal vector 2. If it did, the second saccade would follow a trajectory along retinal vector 2b. Something above and beyond retinal error is required for its proper computation, and that something is corollary discharge of saccade vector 1. Inspired by (Schlag and Schlag-Rey, 2002).

While much indirect evidence pointed to the existence and operation of corollary discharges, an actual corollary discharge pathway of saccadic eye movements was not identified until 2002 (Sommer and Wurtz, 2002). Ascending from the superior colliculus (SC), a midbrain structure, to the frontal eye field (FEF) via the mediodorsal nucleus of the thalamus, it was found to convey internal monitoring signals contributing to proper performance of the double-step task. Subsequently, a link between this pathway and visual neurons that appear to mediate the spatial updating process itself was established (Sommer and Wurtz, 2006). Found throughout the visual system, such neurons

presaccadically shift their RFs to that portion of space where the RF will reside after the saccade. By shifting their sensitivity perisaccadically these neurons are thought to perform a pre-emptive updating of the retinotopic, spatial representation thus resulting in a percept of visual stability (Sommer and Wurtz, 2008b). While much is known about the properties of shifting RFs and the corollary discharges that trigger them, several questions remained open.

One question centers around the intriguing observation that shifting RFs can accompany saccades over a broad range of directions and amplitudes (Heiser and Colby, 2006). It is common for single neurons to shift their RFs along with contralateral saccades *and* ipsilateral saccades. As mentioned, the shifting RF process relies on corollary discharges of movement commands, so the implication is that these neurons have access to corollary discharges of both contraversive and ipsiversive saccades. In general, cortical regions are highly lateralized to represent only contralateral space, so what could be the source of the ipsilateral signals? A subcortical source was implicated following a series of experiments performed by Colby and colleagues (Berman et al., 2005; Heiser et al., 2005). They performed a split brain study to determine if shifting RFs that accompany ipsiversive saccades are driven by interhemispheric corollary discharge. It was hypothesized that severing the forebrain commissures would disrupt the signaling and consequently affect the efficacy of ipsiversive RF shifts. Surprisingly, no significant, lasting behavioral deficits ensued. Their results suggest that ipsiversive RF shifts are driven by a corollary discharge of subcortical rather than cortical origin. The identity of the subcortical source remained an open question. A second major question concerns how shifting RFs actually contribute to visual stability. One hypothesis proposes that shifters

perform a comparison operation, by which the similarities between the presaccadic and postsaccadic RF samplings are measured (Crapse and Sommer, 2008c; Sommer and Wurtz, 2006, 2008a). If there is no difference between the two data samples, then nothing must have changed in the visual scene. A percept of stability is the result. If, on the other hand, there is a mismatch, then something must have happened in the environment during the saccade. A prediction of this hypothesis is that the neurons should signal when there is a mismatch between the presaccadic and postsaccadic RF samplings. No investigation had examined the precise computations performed by shifters, however, particularly with respect to their capacity to assess the stability of a visual scene during saccadic eye movements

The objective of the studies presented in this thesis was to achieve a better understanding of the neural mechanisms underlying visual stability. The experiments were designed to provide more insights into the perisaccadic computations performed by FEF neurons, specifically neurons with shifting RFs, and how these computations may ultimately contribute to a sense of visual stability during saccadic eye movements. The general questions that motivated these experiments were: 1. How do FEF shifting RFs gain access to information about all of visual space?, 2. Do FEF shifting RFs perform transaccadic comparisons?, and 3. Do the neuronal reports of such comparisons correlate with perceptions of visual stability? To address these questions we performed single unit recording in the FEF of *Macaca mulatta*, a non-human primate species with a visual system remarkable similar to the human visual system. The FEF, a prefrontal area, was selected as a region of interest because of several features it possesses (reviewed below) that render it a likely candidate for performing visual-stabilization computations. In

chapter 2, we report our investigation of a route by which the FEF could gain access to ipsilateral information, a critical ingredient for generating omni-directional shifting RFs. In chapter 3, we describe the results of an explicit test of the shifting RF comparison hypothesis. In chapter 4, we demonstrate that FEF visual neurons predict monkey performance in a visual stability judgment task. In the final chapter, we attempt to synthesize the results and propose a large-scale theoretical framework describing how shifting RFs and the FEF itself contribute to a percept of visual stability

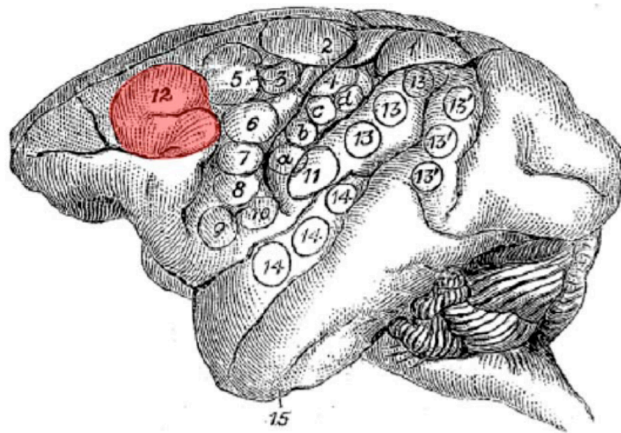
The purpose of the remaining portions of this chapter is to motivate the described experiments by providing appropriate context. I will begin with a brief history of the FEF and provide reasons for why it is a suitable area for investigating questions of visual stability. I will follow with a detailed description of shifting RFs and finish with some remarks about the SC, a critical source of corollary discharges necessary for triggering shifting RFs. I will conclude this chapter by listing the specific aims of my experiments.

1.2 The frontal eye field

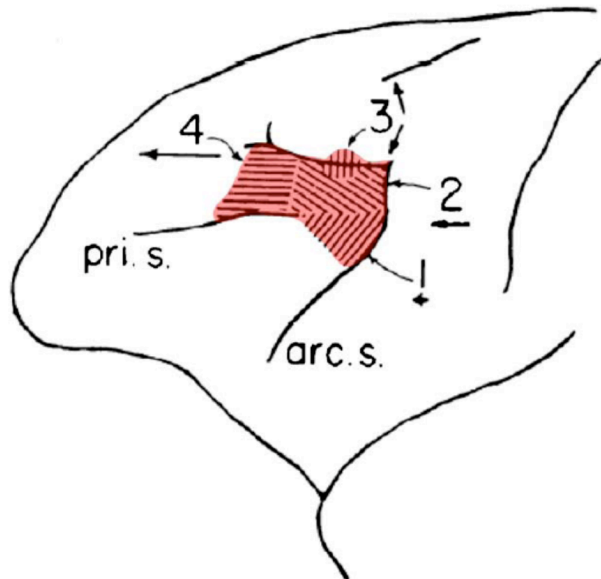
The frontal eye field (FEF) has been historically associated with eye movement generation (Figure 2). In 1875, Ferrier discovered that electrical stimulation around the general area of the arcuate sulcus resulted in the evocation of contraversive eye movements (Ferrier, 1875). Robinson and Fuchs refined this observation nearly a century later (Robinson and Fuchs, 1969). They discovered that electrical stimulation of the FEF elicited fixed-vector saccades, meaning that the direction and amplitude of the elicited saccade was invariant with respect to initial orbital position. They also observed a coarse

topography of elicited saccades in that smaller saccades were evoked from the ventrolateral regions, while larger saccades were evoked from the dorsomedial regions. Bruce and Goldberg later confirmed these findings and went a step further by

A



B



S

Figure 2. An eye field in the frontal lobe. A. Ferrier (1875) identified a zone of cortex, demarcated by circle 12, that produced saccades when electrically stimulated. B. Robinson and Fuchs (1969) found that the amplitude of stimulation-evoked saccades (marked as arrows of different lengths) varied as a function of location along the anterior bank of the arcuate sulcus. From (Amiez and Petrides, 2009).

systematically recording from neurons throughout the FEF (Bruce and Goldberg, 1985; Bruce et al., 1985). They found three general types of visually-guided saccade-related FEF neurons that they classified according to the degree to which the neurons exhibited visual and/or movement related activity: visual, visuomovement, and movement. Based upon these three response types they proposed a model in which the FEF receives visual signals as input and produces saccadic eye movement commands as its sole output. According to this model, the FEF is devoted to a sensorimotor transformation in the service of eye movement generation. The implication of this model is that the FEF is mostly concerned with action and has little to do with perception.

Subsequent work has cast doubt on this simplified model. First, the FEF has been shown to export signals other than those of the purely movement type. For example, Sommer and Wurtz found that the FEF outputs visual and delay period activity in addition to the typical movement activity (Sommer and Wurtz, 2000, 2001). Second, recording, stimulation, and inactivation studies have revealed that the FEF plays a considerable role in attentional allocation. Moore and Fallah, for example, found that subthreshold stimulation of the FEF resulted in an attentional-like improvement in a psychophysical detection task (Moore and Fallah, 2001). Subsequent studies found that this very same stimulation protocol elicits attentional-like effects on the response properties of V4 neurons (Armstrong et al., 2006; Moore and Armstrong, 2003). Third, the work of Schall and colleagues has shown that the response properties of FEF visual neurons can be quite discriminative, exhibiting inferential signals that gauge the relative salience of visual targets (Schall and Thompson, 1999). Taken together, the current best guess of the function of the FEF is that it implements a salience map of the visual scene,

the purpose of which is to select targets for saccadic eye movements (Thompson and Bichot, 2005). The FEF therefore plays a role in perception in addition to the traditionally assumed role in action generation.

Now, what is the evidence that the FEF plays a role in visual stability? The FEF contains two critical ingredients that are thought by current accounts to be key components of a visual stabilization mechanism. First, it receives corollary discharges of eye movement commands from the midbrain (Sommer and Wurtz, 2002). As mentioned, corollary discharges provide advance warning of imminent changes in eye movements and therefore may play a role in compensating for the sensory consequences of movement. Second, the FEF contains a population of neurons with shifting RFs, a putative mechanism of visual stability (Sommer and Wurtz, 2006; Umeno and Goldberg, 1997, 2001). While it is true that many brain areas contain shifting RFs, the FEF is viewed to be unique in that it is the only known cortical recipient of a CD pathway from the brainstem saccade-generating circuitry. Possibly as a result of this direct connectivity, FEF shifters have extremely early shift latencies compared to neurons of other brain areas. Neurons in the FEF start shifting their RFs on average 24 ms relative to saccade onset (Sommer and Wurtz, 2006), while neurons in extrastriate area LIP, for example, start shifting around 80 ms later (Kusunoki and Goldberg, 2003). The early timing of FEF shifters may play a role in the preemptive updating of the visual representation necessary for visual stability. As such, the FEF seems well positioned to play a role in visual stability.

1.3 Shifting receptive fields

Most neurons of the primate visual system are firmly retinotopic; they move only when the eyes move. Other neurons are extremely dynamic in the sense that they alter their visual sensitivity at the time of a saccade. For these neurons, visual responsiveness shifts before the saccade from the neuron's current visual receptive field (RFs) to the location (the future field; FF) where the RF will reside after the saccade (Figure 3). By shifting, these neurons literally take a sneak-peak of what will rest in their RF after the saccade and consequently begin signaling the contents of the postsaccadic RF with latencies far earlier than usual reafferent responses. Such early signaling permits an escape from the time-lags associated with typical visual reafferent processing and may permit a pre-emptive visual-spatial corrective process to occur that compensates for the visual disturbance associated with saccades. The shifting RF process is also called "presaccadic remapping".

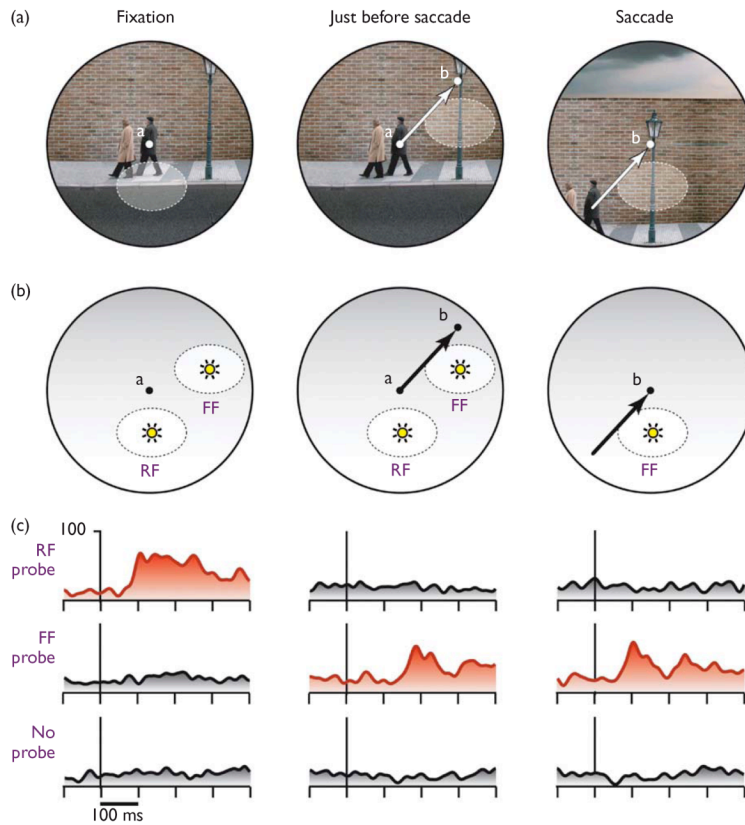


Figure 3. Shifting receptive fields. (A) An example neuron has an RF positioned just below fixation (left). Just before the saccade, the RF shifts to a new position (center). This position corresponds to where the RF will reside following the saccade (right). (B) Shifting RFs can be probed by flashing stimuli in either the presaccadic RF or the postsaccadic RF (FF) at various times relative to the saccade. (c) Activity of an example FEF neuron. Firing rate (in spikes/s) is aligned with probe onset, for the left and middle panels, and with saccade initiation for the right panel. The visual response shifts from the RF to the FF just before the saccade. By sampling the same region of space both before and after the saccade, these neurons are thought to perform a comparative operation that leads ultimately to a sense of visual stability. From (Bays and Husain, 2007).

First identified in area LIP (Duhamel et al., 1992), shifting RFs have been found subsequently in a host of cortical areas: FEF (Sommer and Wurtz, 2006; Umeno and Goldberg, 1997), V4 (Tolias et al., 2001), V3A, V3, and V2 (Nakamura and Colby, 2002). While typically viewed to be similar in operation, there are subtle differences in the nature of the shift amongst these areas. Temporally, there tends to be an increase in shift latency as one moves caudally along the anterior-posterior axis, with FEF neurons

having the shortest latency, and V2 neurons having the longest latency. It should be noted that the neurons become sensitive to visual stimuli at the FF just before the saccade, but the burst of action potentials that signals the shift is time-locked to the onset of the saccade. Shifts are saccade-triggered visual responses, implying that if a saccade were to be aborted, a neuron would withhold its shift signal. This seems advantageous for a transsaccadic visual stability function, since no updating would be needed if the saccade were canceled.

Spatially, the shift tends to move along an axis parallel to the saccade vector, with the exception of shifters in area V4 (Tolias et al., 2001). In that area, the RFs shrink and shift toward the saccade target. As mentioned earlier, shifting RFs are capable of moving into any portion of space, accompanying any direction of saccade. This implies that the neurons are receiving CD and visual information about all of space, not just the contralateral hemifield. Regarding other aspects of the shift, it has been shown that --at least in the FEF--the shift jumps rather than sweeps across the space separating the RF and FF positions (Sommer and Wurtz, 2006), implying a strict dependence on the vector of the imminent saccade.

In terms of function, there is dispute in the field as to what purpose predictive shifting actually serves (Bays and Husain, 2007). As delineated above, a prominent theory maintains that shifting RFs play a causal role in visual stability. Presaccadic samples are compared to postsaccadic samples and if the two are in concordance then a percept of stability eventuates. While influential, this view has been called into question. Some theorists maintain that predictive remapping plays a more active role in *action* rather than *perception*. The evidence arrayed against the perceptual role of predictive

remapping includes the observation that under certain circumstances we retain very little information across saccades (O'Regan and Levy-Schoen, 1983). Moreover, we are often blind to events that occur to a scene during saccades (Simons and Rensink, 2005). If shifters are performing a detailed comparison of the pre-saccadic and post-saccadic scenes, then why are we so forgetful across saccades, and how is saccadic change blindness possible? One possible reason is that presaccadic remapping only occurs for stimuli to which attention has been allocated (Wurtz, 2008). In fact, Gottlieb and colleagues found about a decade ago that attention is absolutely necessary for the shift operation to occur; no attention, no shift (Gottlieb et al., 1998). In light of this result, it is not surprising that we do not retain much information across fixations or that we are blind to changes that occur during saccades. The system can only allocate attention to select regions of the visual scene and as a result only remap and compare select regions of the visual scene.

As for its putative contribution to motor control, some theorists maintain that a primary function for remapping could be for sensorimotor adaptation (Bays and Husain, 2007). Due to injury and aging, the oculomotor system must constantly calibrate its motor signals to achieve the desired movement goal. For eye movements, saccadic adaptation is the means by which the system corrects systematic errors resulting from mismatches in movement endpoint and saccade target. The idea is that if any sort of presaccadic-postsaccadic comparison operation is being performed, it is within this context. This view is on shaky ground, however, because with the exception of V4, shifting RFs shift along an axis parallel to the saccade vector. The mechanism required for saccadic adaptation would necessitate shifters that shift toward the saccade target, not

parallel to it. I think, therefore, that, the current data favor a perceptual function for shifting RFs.

1.4 The superior colliculus

Perched on the roof of the midbrain, the SC is one of the most well understood areas of the vertebrate brain (Hall and Moschovakis, 2004). As a sensorimotor structure, the SC possesses a laminated architecture featuring precisely aligned maps of contralateral space that vary in sensory to motor properties as a function of depth: neurons in the superficial layers encode purely sensory attributes while motor properties become increasing dominant in the deeper layers (Schiller and Koerner, 1971; Sparks, 2002; Wurtz and Goldberg, 1972). Recording, stimulation, and inactivation studies have revealed that neurons in the intermediate and deep layers are causally involved in saccade generation (Sparks and Hartwich-Young, 1989). Aside from receiving dense cortical inputs (Lynch and Tian, 2005), the SC provides inputs of its own to the cortex via feedback projections, one of which targets the FEF (Benevento and Fallon, 1975; Lynch et al., 1994). This particular pathway, emerging from the intermediate layers, targets deep layer III/layer IV of the FEF (Giguere and Goldman-Rakic, 1988) via a relay node in mediodorsal thalamus. Functionally, the pathway has been shown to convey corollary discharges (Sommer and Wurtz, 2004a, b) that are important for triggering shifting RFs of FEF neurons (Sommer and Wurtz, 2006). There is also anatomical evidence of crossed connections linking SC to cerebral cortex (Clower et al., 2001; Preuss and Goldman-

Rakic, 1987) and these could hypothetically convey CD of ipsiversive saccades, a necessary ingredient for omni-shifting RFs.

1.6 Summary and Research Objectives

In sum, neurons that presaccadically shift their receptive fields are found throughout the primate brain, including the FEF (Sommer and Wurtz, 2006; Umeno and Goldberg, 1997) and constitute a putative mechanism for visual stability. Since they effectively sample the same region of space twice, they are proposed to perform a comparison operation. The comparison operation may inform a percept of stability but the comparison hypothesis has never been tested, nor is it known how these neurons are able to shift omnidirectionally.

In the studies described here, I have made an attempt to provide deeper insights into shifting RF function through a circuit level investigation of omni-shift capability and a mechanistic exploration of the computations performed by the shift operation itself, an explicit test of the comparison hypothesis. These experiments involved recording from FEF neurons physiologically identified as receiving input from a given SC (chapter 2), recording from FEF visual neurons while stimuli changed during a saccade (chapter 3), and recording from FEF neurons while monkeys performed a visual stability judgment task that assessed their visual percept across saccades (chapter 4). I now describe the specific aims and hypotheses for each chapter.

Specific aim of chapter 2. *Determine how each FEF receives information about ipsilateral space, a prerequisite for omni-directional shifting receptive fields.* Neurons in

the FEF, as in most of cerebral cortex, primarily represent contralateral space. Yet many FEF neurons engage in sophisticated functions that require flexible spatial representations such as shifting receptive fields and vector subtraction. Such functions require knowledge about all of space, including the ipsilateral hemifield. How does the FEF gain access to ipsilateral information? We hypothesized that one source of ipsilateral information may be the opposite superior colliculus (SC) in the midbrain. To test this hypothesis we physiologically identified neurons in the FEF that receive input from the opposite SC, same-side SC, or both. We deduced that these neurons would carry signals appropriate for generating omni-directional shifts, specifically that the laterality of an FEF neuron's response field would reflect the laterality of the SC from which it received input. In toto, signals from these two pathways could provide the necessary ingredients critical for shifting a receptive field into any portion of space.

Specific aim of chapter 3: *Determine if FEF neurons assess the visual stability of the world across saccades.* A long-standing hypothesis of shifting RFs is that they compare a presaccadic sample with a postsaccadic sample, thereby measuring whether any change occurred during the saccade. A percept of stability could be founded on how well the two samples match. We set out to test this hypothesis by recording from FEF visual neurons while monkey's performed a task designed to probe an FEF neuron's capacity to compare visual space across saccades. We intrasaccadically manipulated the position or visual feature of a task-irrelevant probe so that the presaccadic state of the probe differed from the postsaccadic state. We predicted that FEF neurons would signal whether the stimulus changed and by how much it did so.

Specific aim of chapter 4: *Determine if FEF activity predicts performance in a visual stability judgment task.* The experiment of chapter 3 left open a number of questions. First, do monkeys in fact experience a stable visual world? Specifically, are they able to distinguish true displacement of an external visual stimulus from saccade-induced displacement? Second, if they are adept at such judgments, is behavioral performance predicted by visual responses of FEF neurons? While the chapter 3 experiments unveiled signals suitable for behavioral detection, the probes used in those experiments were task-irrelevant. It therefore remained unknown whether those signals exerted any influence on the monkey's perception. To address this, we designed a behavioral paradigm requiring monkeys to explicitly report whether a stimulus moved as they executed scanning saccades. Consistent with its postulated role in visual stability, we deduced that FEF neuronal activity would be predictive of monkey psychophysical performance.

2.0 Frontal eye field neurons with spatial representations predicted by their subcortical input

2.1 Introduction

Previous reports indicate that the frontal eye field (FEF), a cortical region involved in vision and eye movements, codes predominately for contralateral space (Bruce and Goldberg, 1985; Bruce et al., 1985; Schall et al., 1995a; Tehovnik et al., 2000). However, some FEF neurons possess ipsilateral response fields (RFs), and many FEF neurons perform operations that require visual and motor information about both hemifields. These operations include shifting RFs (Sommer and Wurtz, 2006; Umeno and Goldberg, 1997, 2001) and vector subtraction (Goldberg and Bruce, 1990; Tian et al., 2000). What are the sources of the ipsilateral information, and how does it reach the FEF?

There are a number of potential routes for ipsilateral signals to reach the FEF. One route would be the corpus callosum, which could provide signals from the FEF on the opposite side of the brain (Gould et al., 1986; Pandya and Vignolo, 1971). This scenario is unlikely because functions such as omni-shifting RFs and transhemifield saccadic sequences survive transection of the corpus callosum (Berman et al., 2007; Berman et al., 2005; Colby et al., 2005; Heiser et al., 2005) and the result of one FEF acting upon the other seems to be mostly inhibitory (Izawa et al., 2004; Schlag et al., 1998; Seidemann et al., 2002). While this does not exclude the possibility that the opposite FEF is partially involved in providing ipsilateral signals, it does suggest that the

main function of interhemispheric FEF connections is to enforce motor act consensus (Schlag et al., 1998).

Ascending pathways from subcortical structures may also provide ipsilateral information. One candidate is the superior colliculus (SC) on the opposite side of the brain (Fig. 4). The SC, a sensorimotor structure in the midbrain, is interconnected with the FEF (Fries, 1984; Lynch et al., 1994; Stanton et al., 1988). Each SC codes for contralateral space (Schiller and Koerner, 1971; Wurtz and Goldberg, 1972) and is known to excite FEF neurons on the same side of the brain via a relay in the mediodorsal (MD) nucleus of the thalamus (Sommer and Wurtz, 1998, 2004a). Similarly, signals from the opposite SC could reach the FEF, and do so by way of at least three possible routes (outlined in Fig. 4). Physiological techniques provide a feasible means to test these anatomical possibilities.

Hypothetical routes for
crossed connection

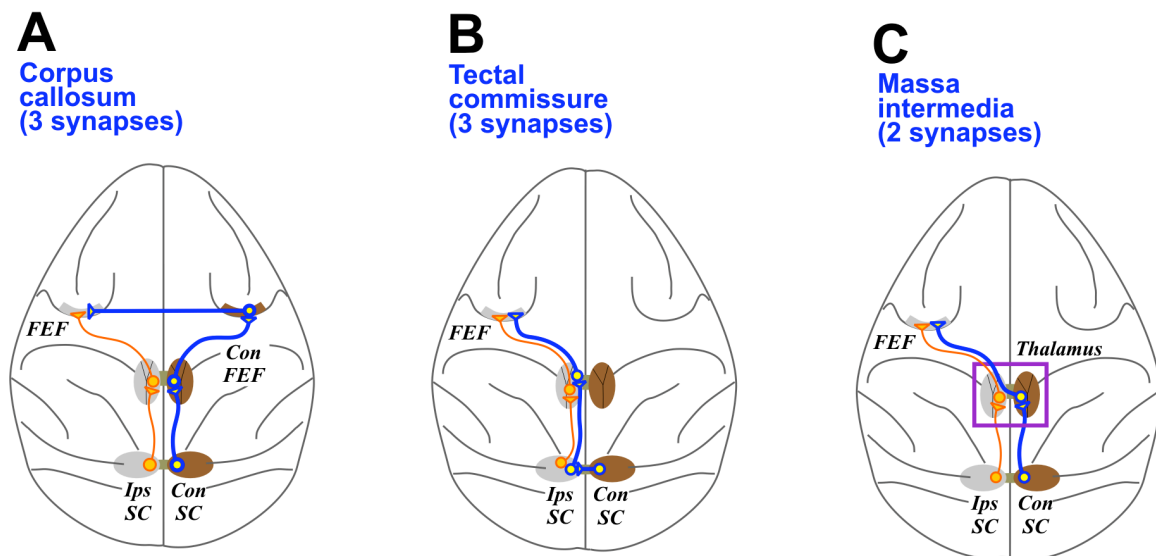


Figure 4: Three hypothetical routes for a crossed SC to FEF connection. Blue pathways show the possible crossed routes and orange pathways the known uncrossed route. (A) Corpus callosum hypothesis. According to this hypothesis, ipsilateral information reaches the FEF by way of a tri-synaptic pathway: the contralateral SC (Con SC) excites the contralateral FEF (Con FEF) which in turn transcallosally excites the FEF of the opposite hemisphere. (B) Tectal commissure hypothesis. Like the corpus callosum hypothesis, this hypothesis implies at least three synaptic interruptions but differs at the point of decussation: the tectal commissure. After crossing to the ipsilateral SC (Ips SC), the ipsilateral coding signals would ascend to the FEF adjacent to the pathways that encode contralateral space. (C) Massa Intermedia hypothesis. This hypothesis predicts that the ipsilateral signals cross at the level of the mediodorsal (MD) thalamus via a commissural track known as the massa intermedia. Upon crossing, the MD relay neuron would ascend directly to the FEF. This third pathway consists of only two synapses thus implying a faster transmission time compared to the pathways of the corpus callosum and tectal commissure hypotheses. intermedia (Olszewski, 1952). Anatomically, a crossed thalamo-cortical projection to prefrontal cortex has been demonstrated (Preuss and Goldman-Rakic, 1987), and consists of only two synapses, implying a faster transmission time compared to the corpus callosum or tectal commissure mediated pathways, both of which require at least three synapses (Lamantia and Rakic, 1990; Swadlow et al., 1978; Takahashi et al., 2007). In principle these pathways are not mutually exclusive; all could be functional to varying degrees.

The objectives of this study were three-fold. First, we aimed to determine whether FEF neurons receive input from the contralateral SC and which of the three crossed pathways likely provided the input. Second, we sought to characterize the signals conveyed by the crossed pathway and understand how they relate to the spatial representations of recipient FEF neurons. Specifically, we examined whether the inputs were excitatory and whether the recipient FEF neurons were tuned for ipsilateral space. Third, we aimed to compare the FEF neurons that received input from the crossed pathway with those that received input from the same-side SC pathway, to clarify how inputs from the two SCs may interact to provide the FEF with information about all of space.

2.2. Materials and Methods

2.2.1 Surgery and region identification

In four monkeys (*Macaca mulatta*) we implanted scleral search coils for measuring eye position, recording chambers for accessing FEF and SC, and a post for immobilizing the head during recording experiments (for details, see Sommer MA and Wurtz RH, 2004a). The locations of FEF and SC were determined stereotaxically and verified by physiological means: the recording of saccade related neurons and the evocation of saccades at $< 50 \mu\text{A}$ threshold (Bruce and Goldberg, 1985). One or more tungsten microelectrodes for stimulation were semi-chronically implanted in the intermediate layers of each SC (termed “ipsilateral” and “contralateral” relative to the recorded FEF). We positioned the stimulating electrodes near the middle of each SC, i.e. around 12 deg. amplitude and within a few degrees of the horizontal meridian on the topographic map. We recorded from single FEF neurons by conventional extracellular means while attempting to activate them with SC simulation (single biphasic pulse, 0.15 ms/phase).

2.2.2 Behavioral tasks

During recording sessions each monkey sat in a primate chair facing a tangent screen onto which visual stimuli were back projected. Once a neuron was sufficiently isolated, we characterized its activity with several oculomotor tasks (described below). In all tasks the monkey was required to fixate a spot of light projected onto the center of the screen.

Then, with timings that depended on task contingency, the monkey was required to execute an appropriate eye movement for a liquid reward.

First, we determined the directional tuning of the response field (RF) with a direction series task. The monkey made saccades to targets in 8 different locations, along cardinal axes and diagonals, using an amplitude that seemed optimal from initial qualitative testing. Second, with the preferred direction of the RF determined, we aligned targets along this direction during an amplitude series task. The monkey made saccades of 8 different amplitudes (2, 5, 10, 20, 30, 40, 50 and 60 deg.) along the preferred direction of the neuron. If the optimal amplitude for evoking a maximal response differed substantially from that estimated with initial qualitative testing, we repeated the direction series task at the newly determined amplitude. We iterated between these tasks, if necessary, to firmly establish the range and center of the neuronal RF. Both the direction series and amplitude series tasks involved visually-guided saccades; the fixation spot disappeared and, simultaneously, a single visual target appeared. Saccades were made after a reaction time (typically 150-250 ms) with no imposed delay.

After determining the center of the neuron's RF, we had monkeys make memory-guided saccades to that location. The monkey fixated a spot of light, then a target flashed for 50 ms at the center of the RF. The monkey was not allowed to look at the target location until the fixation spot disappeared 500-1000 ms later. Then the monkey had to make a saccade to the remembered location of the target (for details see Sommer and Wurtz, 2004a). The memory-guided task was used because it permitted temporal dissociation of visual responses from saccadic responses (Hikosaka and Wurtz, 1983; Mays and Sparks, 1980).

2.2.3 Neurophysiology

We recorded only from single FEF neurons activated orthodromically from the left or right SC. Our search strategy was to inspect the multiunit activity while stimulating one or the other SC. If we detected signs of stimulation-triggered activation, we manipulated the electrode depth in order to isolate one of the activated neurons. If we succeeded in isolating an activated neuron, we mapped its RF and studied its other task-related properties. Otherwise, we moved on. A neuron was considered orthodromically activated if it discharged consistently ($\geq 1/2$ stimulation attempts) at a comparable latency (variability of ~ 2 -4ms). Detailed procedures are described elsewhere (Sommer and Wurtz, 1998, 2004a). To rule out antidromic activation we only accepted neurons that failed the collision test. Once orthodromic activation of a neuron was suitably verified from one SC, we would attempt to activate the neuron from the other SC. Our searching current was 600 μA , but if a neuron was activated from one SC and apparently not the second SC, we tried current levels up to 1500 μA in the second SC before concluding that the FEF neuron could not be activated from it.

Our strategy did not permit quantification of the fraction of activated vs. non-activated neurons. Qualitatively, SC-activated neurons seemed to be in the minority, around 1 out of every 15 neurons encountered. Since we mapped RFs only after identifying a neuron as activated, we could not estimate the fraction of FEF neurons with ipsilaterally tuned RFs that were not drivable from the contralateral SC. All questions like these, relating to non-activated neurons, are not answerable with our techniques.

2.24 Data Analysis

All neuronal data were converted from raw spike rasters to average firing rates during defined task epochs for off-line analysis. Our first goal was to determine if an orthodromically activated neuron was significantly task modulated, and if so, in which aspect of the task it was modulated. To determine this, we divided each memory-guided task trial into a series of analysis epochs. A neuron was considered visual if it exhibited neuronal activity during a visual epoch (50-150 ms after target onset) that was significantly greater than baseline activity (300-0 ms before target onset). A neuron was considered to be movement related if it exhibited activity during a saccadic epoch (50 ms before to 50 ms after saccade initiation) that was significantly greater than both the intervening delay epoch (last 300 ms of the delay period) and the baseline epoch.

Our second goal was to determine the spatial tuning curves of the task-modulated neurons. For this, we divided each directional series task trial into visual and saccadic epochs as defined above, and measured mean firing rates as a function of visual target location and saccade direction (Sommer and Wurtz, 2004a). The visual and saccadic activities for each direction were individually compared and the maximum value of each comparison was used for constructing the final tuning curve. The resultant tuning curve was thus a composite representing the boundary of the visual field and movement field. For some analyses (see Results) we considered the separate visual and movement fields independently, in neurons that had both fields.

Using the tuning curves, we constructed an index for each neuron that summarized the laterality of its RF. First, we found the average firing rate for saccades made to targets in contralateral space (FR_C) and ipsilateral space (FR_I). Vertical targets were excluded, so each of the averages included three target locations (at the diagonal and horizontal directions). Then we calculated an RF Laterality Index (RFLI) as the contrast ratio of the average firing rates: $(FR_C - FR_I) / (FR_C + FR_I)$. The RFLI ranged from -1 (completely ipsilateral tuning) to 1 (completely contralateral tuning) with 0 representing symmetric tuning. We used the RFLI to determine if biases in the laterality of a neuron's RF varied continuously with biases in the laterality of its collicular inputs. An SC Laterality Index (SCLI) compared the current thresholds for activating a neuron from contralateral SC (I_C) versus ipsilateral SC (I_I) using the contrast ratio $(I_I - I_C) / (I_I + I_C)$. The SCLI ranged from -1 (activation was from ipsilateral SC only) to 1 (activation was from contralateral SC only). Neurons activated from both SCs had SCLI values between -1 and 1, and the special case of SCLI = 0 represented equal activation from the two SCs. To analyze if RF laterality was related to input laterality from the two SCs, we performed a Spearman correlation test on the RFLI and SCLI data.

2.2.5 Statistics

All data were statistically analyzed using conventional parametric, nonparametric, and circular statistics with $p < 0.05$ as the criterion for significance.

2.3 Results

2.3.1 Excitatory activation of the FEF from the two SCs

We recorded from single neurons throughout the FEF and attempted to orthodromically activate them by stimulating each SC. The FEF was sampled from the ventrolateral small saccade zone (approximately 2 deg. amplitude saccades) to the dorsomedial large saccade zone (approx. 30 deg. amplitude saccades) as determined by the eccentricities of visuomovement response fields and the vectors of stimulation-evoked saccade (Bruce & Goldberg 1985; Bruce et al. 1985; Sommer & Wurtz 2000, 2004). Successful orthodromic activation of an FEF neuron provided physiological evidence for connectivity (Sommer and Wurtz, 1998, 2002, 2004a, b, 2006). We were able to orthodromically activate a total of 55 FEF neurons. Of these, 12 were driven from the contralateral SC alone (*ConSC-only* neurons), 16 from both SCs (*BothSC* neurons), and 27 from the ipsilateral SC alone (*IpsSC-only* neurons). All three types of neurons were found throughout the FEF, presumably in layer IV, the principal thalamic recipient zone (Giguere and Goldman-Rakic, 1988). All of the neurons were identified as receiving input from the SC, but none seemed to project to the SC (i.e. all of the neurons were orthodromically but not antidromically activated from the SC; also found by Sommer and Wurtz, 2004a).

Every instance of detected orthodromic activation from the SC was excitatory as evidenced by the reliable evocation of short-latency spikes. We found no evidence for stimulation-evoked inhibition. Although we feel confident that we could have identified

stimulation-evoked pauses in the spontaneous activity of most of the neurons (the average baseline firing rate of the drivable neurons was 17 sp/s), it is possible that some inhibition occurred that escaped our detection. Figure 5A depicts example action potential waveforms from a ConSC-only neuron. The stimulus artifact is at time zero. This neuron fired with a latency of 5.8-6.8 ms in response to stimulation from the contralateral SC (top), but not from the ipsilateral SC (bottom). IpsSC-only neurons showed similar activations but solely from stimulation of the ipsilateral SC (not shown). We refer to these neurons as Con- or Ips- “only” although the failure to activate them from the other SC is a negative result and should be interpreted cautiously, e.g. larger currents may have revealed activation (we tried up to 1.5 mA; for more about this issue, see penultimate paragraph of Discussion).

Other FEF neurons, in contrast, were clearly activated from both SCs. The action potentials from one example are shown in Figure 5B. This neuron fired 0.9 ms later for Contra SC stimulation (top) than for Ipsi SC stimulation (bottom). Our first main result, therefore, was that FEF neurons may be orthodromically activated from the contralateral SC, the ipsilateral SC, or both, and that this activation is excitatory.

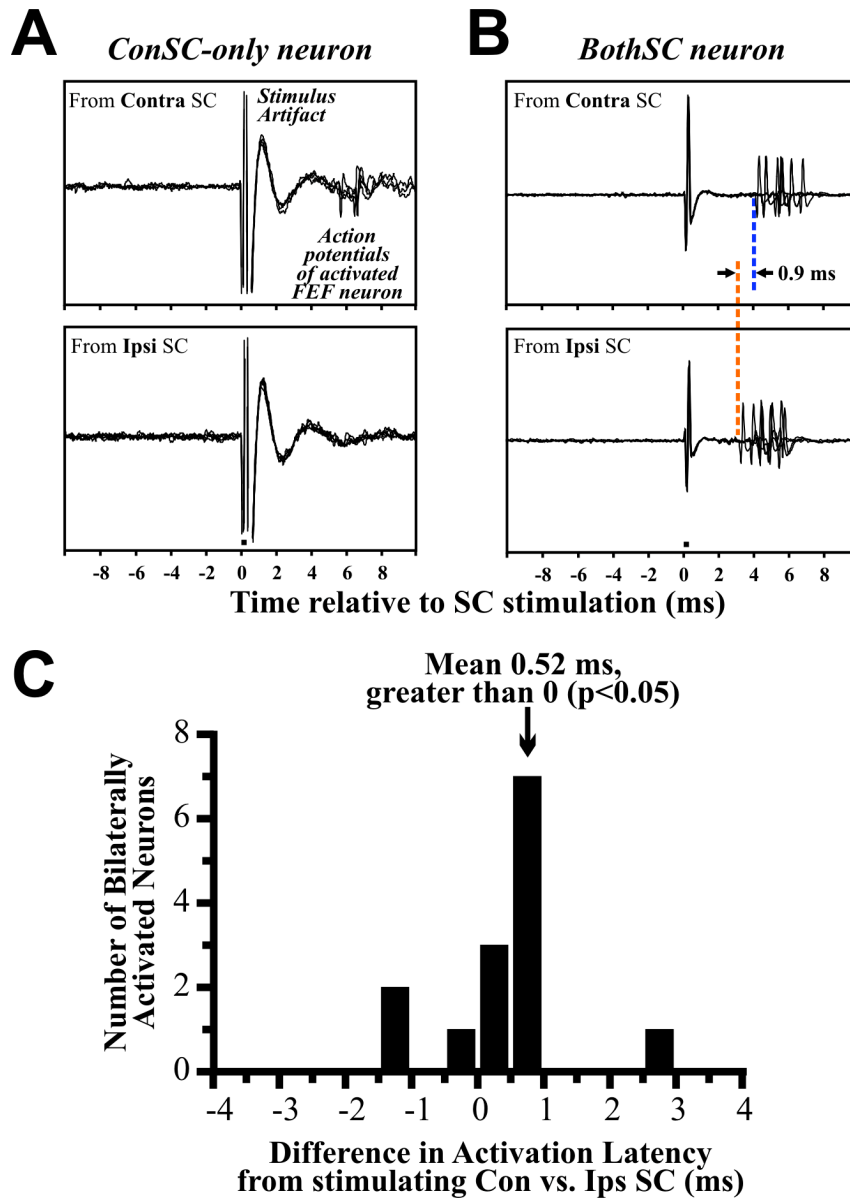


Figure 5: Orthodromic activation of FEF neurons. (A) Some neurons were activated from only one SC. Action potentials evoked from such a neuron are shown. It fired in response to stimulation of the contralateral SC (top) but not the ipsilateral SC (bottom). Small bar below lower stimulus artifact represents duration of SC stimulation (0.3 ms). (B) Other neurons were activated from both SCs. The minimal activation latency from each SC was measured using dozens of trials (only a few are shown here for clarity). This example neuron fired 0.9 ms later for Contra SC stimulation than for Ipsi SC stimulation. (C) Comparison of activation latencies for 14 neurons activated from both SCs. On average the activation took 0.52 ms longer from the contralateral SC, significantly longer than from the ipsilateral SC. The slightly longer time is expected from a longer axonal length required to cross hemispheres, but it does not seem long enough to suggest additional synapses.

2.3.2 Route of activation from the contralateral SC

Input to the FEF from the contralateral SC could ascend by way of at least three potential routes. Three synapses are predicted by the corpus callosum hypothesis (Fig. 4A) and tectal commissure hypothesis (Fig. 4B) but only two synapses for the massa intermedia hypothesis (Fig. 4C). The same-side pathway (from the ipsilateral SC) involves two synapses as well, and thus the massa intermedia hypothesis predicts that activation latencies from the contralateral SC should exceed activation latencies from the ipsilateral SC by only a small amount attributable to different axon lengths. In contrast, the other two hypotheses predict that activation latencies from the contralateral SC should exceed activation latencies from the ipsilateral SC by a larger amount, attributable to both longer axons plus an extra synapse.

To test among these three hodological hypotheses we analyzed the activation latencies of the neurons. We focused on the BothSC neurons since they could be activated through both the same-side and crossed pathways and thus provide the most direct temporal comparison of same-side vs. crossed connectivity. We found that signals from the contralateral SC took an average of 3.87 ms to reach the BothSC neurons while signals from the ipsilateral SC took an average of 3.35 ms, resulting in a significant average latency difference of 0.52 ms (t-test, $p < 0.05$; Fig. 5C). This latency difference implies slightly longer axons. At an estimated conduction speed of 15 m/s, for example, the extra 0.52 ms would imply an extra 7.8 mm, approximately the distance needed to traverse the massa intermedia (Olszewski, 1952). The latency difference seems far too short, however, to account for the additional synapse in the other two potential paths.

Transmission times across the corpus callosum or tectal commissure and through a synapse are on the order of 1-10 ms (Swadlow et al., 1978; Takahashi et al., 2007). Our data suggest that the primary, functional route from the contralateral SC to the FEF (although not necessarily the only route) involves a thalamic crossing-point with no extra synapses.

2.3.3 Response fields of FEF neurons driven from one SC

Next we evaluated whether structure predicted function in the sense that the laterality of connections from the SCs predicts the laterality of an FEF neuron's RF. We did not examine finer details such as the correspondence between stimulation location within an SC map and RF direction of activated FEF neurons. Examining such details would have necessitated systematic changes in stimulating electrode locations across the topographic maps of both SCs (Robinson, 1972), which seemed like too much of a risk in an already challenging experiment.

Each SC represents contralateral visual space and saccades, and therefore the most parsimonious prediction was that FEF neurons with solely crossed SC input would have ipsilateralized fields, FEF neurons with solely same-side input would have contralateralized fields, and FEF neurons with convergent input from both SCs would have bilateralized fields (i.e. fields that extend equally into either hemifield). While we recorded from identified FEF neurons, monkeys performed oculomotor tasks designed to characterize each neuron's visuosaccadic activity and its spatial tuning (see Methods for details of measuring visual and movement fields).

We began our analysis with the simplest sets of FEF neurons, those activated from only one SC. Figure 6A shows data from an example ConSC-only neuron (pathway

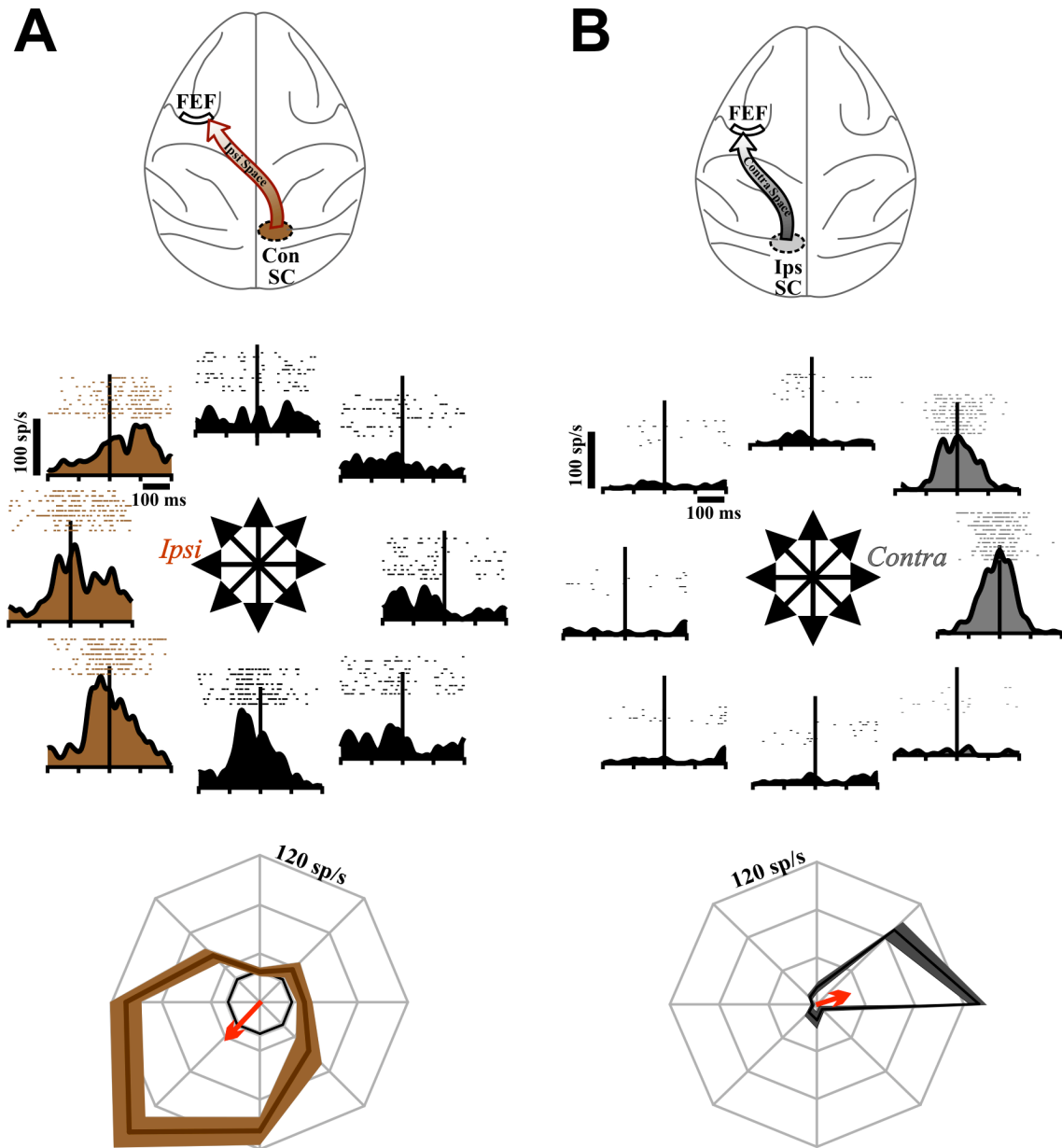


Figure 6: FEF neurons orthodromically activated from (A) the contralateral SC only and (B) the ipsilateral SC only. In both panels, diagrams show route of activation at top. Below that is a directional series depicting the firing rates for an example single neuron. Rasters and spike density functions are aligned to saccade onset. Brown shading emphasizes the ipsilateral directions in panel A and grey shading the contralateral directions in B. At bottom are polar plots that summarize the example data (colored curves, mean \pm SE). Arrows represent the mean tuning vectors in each case. Inner concentric curves (where visible) show baseline firing rates.

depicted at top). Shown are the raw activity plots for visually-guided saccades in eight

directions (middle) as well as a summary tuning curve (bottom). The neuron exhibited a spatially selective increase in firing rate for visuosaccadic tasks and coded predominately for *ipsilateral* space (relative to the recorded FEF). Most neurons of the ConSC-only set (11/12) had RFs tuned ipsilaterally (all summary tuning curves are shown in Fig. 7). To

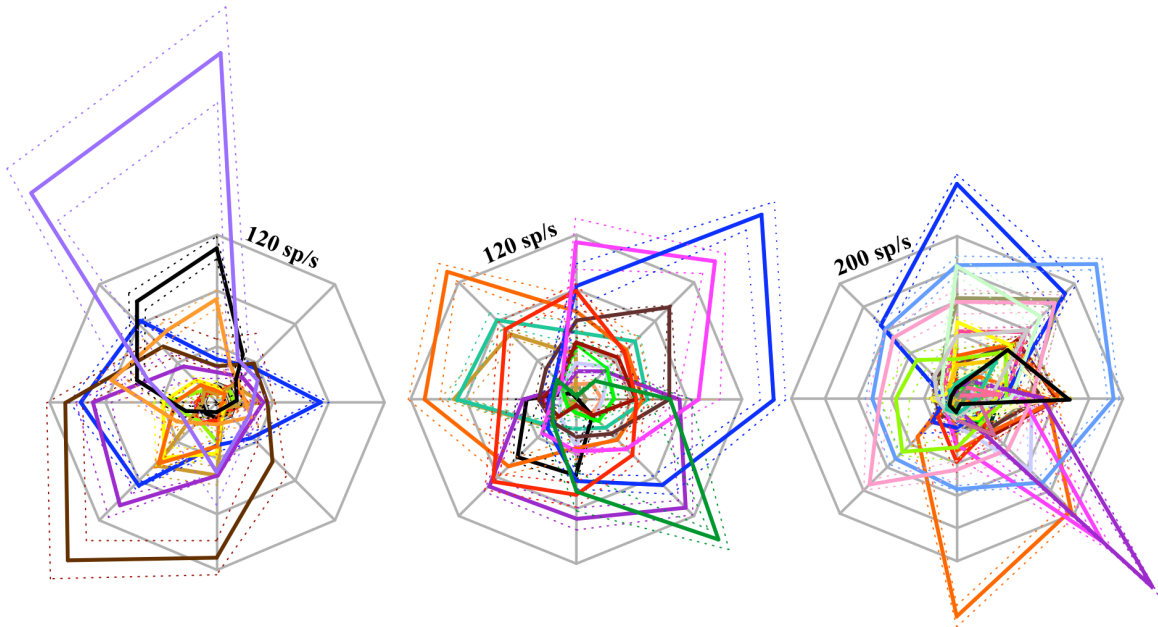


Figure 7: Totality of tunings for all 3 classes. Polar plots showing every tuning curve for neurons in the ConSC-only sample (left; n=12), BothSC sample (middle; n=16), and IpsSC-only sample (right; n=27).

quantify this RF laterality, we represented each tuning curve with its mean vector (Fig. 6, bottom, red arrow) and plotted the vectors from the entire population (Fig. 8A, left). The average mean vector for the ConSC-only group (brown arrow) was 10.7 spikes/s in magnitude (represented by vector length), which was significantly different from zero ($p < 0.01$; the significance of a mean vector is established by constructing the 99% confidence ellipse of the tips of all the vectors and showing that zero falls outside of the ellipse) (Batschelet, 1981). The mean vector was directed almost purely ipsilaterally (angle was 169.9 deg.). For confirmation of this circular statistics approach, we also constructed a more traditional population tuning curve (Fig. 8B, left) by averaging all of

the individual tuning curves. This population tuning curve was significantly biased (ANOVA, $p < 0.01$) toward ipsilateral space. We also normalized the curves to remove any influences of neurons with particularly high firing rates and found a comparable bias (ANOVA, $p < 0.01$) for ipsilateral space (Fig. 8C).

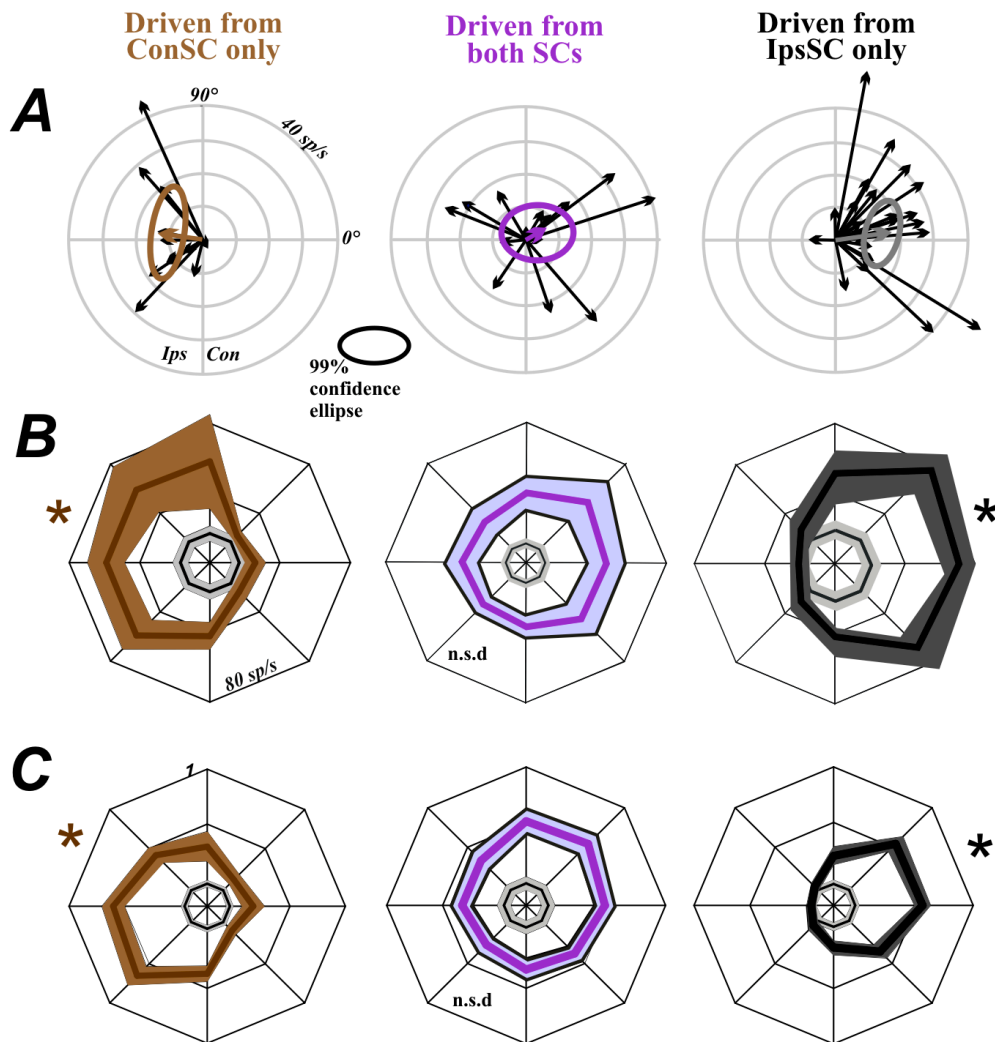


Figure 8: Population results for tuning curves in all three samples of neurons. (A) The mean tuning curve vectors for all individual neurons (thin black arrows) are shown, along with the overall resultant mean vectors and 95% confidence ellipses for each sample (bold colored arrows and ellipses). (B) The population average tuning curves for each sample (mean and SE), calculated from raw firing rate data. (C) The population tuning curves for each sample (mean and SE), calculated from normalized data in which each neuron's activity was set to 1.0 for the direction associated with maximal firing. Asterisks, $p < 0.01$ by

ANOVA for the entire tuning curve. Grey inner concentric curves show baseline firing rates. See text for details.

Results from an example IpsSC-only neuron are represented in Figure 6B. This neuron coded for *contralateral* space and movements, activity reflective of sole input from the SC of the same side. Nearly all of the IpsSC-only FEF neurons (25/27) had contralateral fields. The mean vector for this set of neurons was significant (amplitude 13.97 spikes/s, $p < 0.01$) and directed almost purely contralaterally (angle 8.17 deg., Fig. 8A, right). This tuning was confirmed in the population average curve (Fig. 8B & 8C, right; ANOVA $p < 0.01$).

These results support the parsimonious structure-function hypothesis: FEF neurons have lateralized RFs that are directed in strict accordance with their SC input laterality. Neurons with only crossed input had ipsilateralized fields and neurons with only same-side input had contralateralized fields. Next we examined whether this structure-function relationship extended to BothSC neurons, those with bilateral SC input.

2.3.4 RFs of FEF neurons driven from both SCs

2.3.4.1 The RFs are lateralized, pandirectional, monolobed, and independent of relative weightings of SC inputs

The simplest hypothesis is that convergent input from both SCs would cause recipient FEF neurons to have bilateral RFs. The possible shapes of such RF structures include omnidirectional (circular with no distinct lobes), vertically oriented (one lobe on the vertical axis), or bilobed (two similar lobes with one pointing left and one pointing right).

We studied the RF structure of BothSC neurons and found, first, that RF tuning was not omnidirectional. It was spatially biased for most (15/16) of the BothSC neurons (ANOVA, $p < 0.05$ criterion; Fig. 7, center, and Fig. 9). The individual tuning directions covered virtually every portion of space (Fig. 8A, middle), however, so that the mean vector of the population was not significant (99% confidence ellipse included zero) and the average tuning curve of the population was unbiased (ANOVA, $p > 0.05$; Fig. 8B & 8C, middle). Hence the RFs of BothSC neurons are lateralized and pandirectional, i.e. they *collectively* represent all directions.

Second, we tested if the range of tuning directions exhibited a bias toward vertical orientations. Such an effect might be expected because the vertical meridian of the visual field is common to both SCs. To search for a vertical tuning bias, we calculated the angles of the RF mean vectors in two ways: relative to the horizontal axis and relative to the vertical axis. A vertical bias would be evident in a significantly smaller average angle relative to vertical than to horizontal. No significant difference was found, however (average angle relative to horizontal, 40.7 degrees; average angle relative to vertical, 49.3 degrees; t-test $p=0.293$).

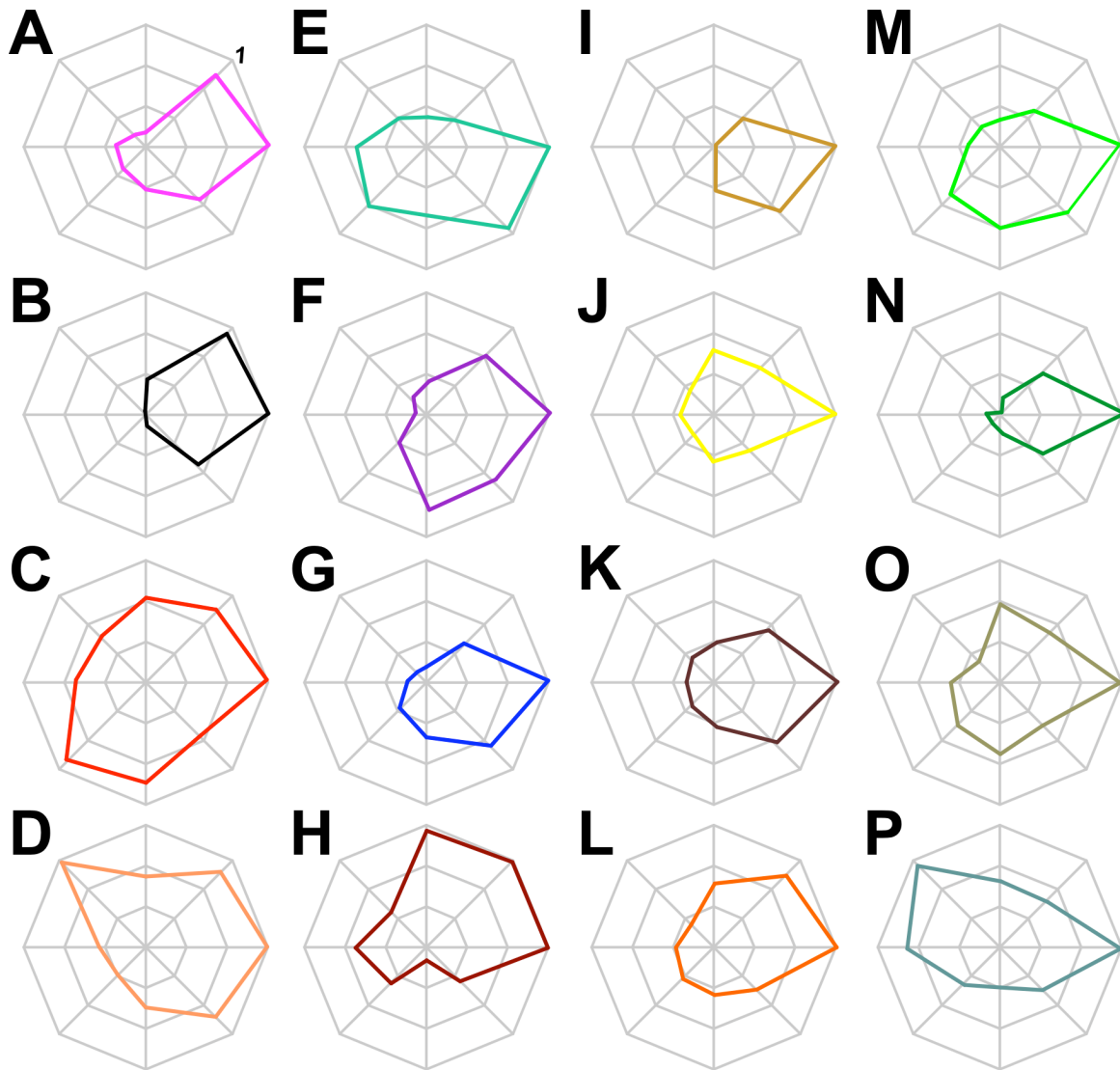


Figure 9: Individual response fields for the BothSC neurons. Each response field is normalized and rotated to emphasize its shape. These are the same data from Fig. 7, middle, but here the tuning curves are spread out for easier inspection.

Third, we searched for signs of bilobed RFs, which might be expected from summing sharply tuned directional information from the two SCs. It was clear from a qualitative inspection of the data, however, that bilobed RFs (similar extensions into contralateral

and ipsilateral space) were present in only a small fraction of neurons, perhaps three of the sixteen (Fig. 9C, D, and P).

Finally, we tested if the direction of RF laterality in individual BothSC neurons was related to the weighting of input from the two SCs. Some BothSC neurons were activated from one SC with much lower current threshold than from the other SC, implying stronger input from the first SC. In principle this could explain how direction tuning is determined in BothSC neurons. Those neurons with ipsilaterally tuned RFs, for example, might have stronger input from the contralateral SC. To test this hypothesis, we calculated for each neuron a RF Laterality Index (RFLI) and a SC Laterality Index (SCLI; see Methods). The critical test was on BothSC neurons, which had SCLI values between -1 and 1. If RF laterality varies smoothly with bias of SC input, then in the BothSC class there should be an inverse correlation between RFLI and SCLI. We found no correlation, however ($p=0.80$). To check the method, we calculated the RFLI index for the groups in which SCLI = 1 (ConSC-only neurons) or -1 (IpsSC-only neurons). Confirming the reliability of the indices, the RFLI of ConSC-only neurons was significantly less than zero (median -0.628; Wilcoxon signed rank sum test, $p < 0.001$) and the RFLI of IpsSC-only was significantly greater than zero (median 0.892; $p < 0.001$).

2.3.4.2 The movement fields and visual fields are relatively broad and misaligned

Overall, then, the RF shapes of BothSC neurons can be described as follows: they are lateralized, can point in any direction independently of SC input strength, and are monolobed. These findings refute our hypothesis that the RFs would be bilateral. The RF shapes of BothSC neurons were remarkably similar to the RF shapes of neurons driven

from only one or the other SC (ConSC-only and IpsSC-only neurons). This unexpected result led us to ask, does the second SC input received by the BothSC neurons have *any* discernable influence on RF structure?

To answer this question we compared the tuning curves of BothSC neurons with the tuning curves of IpsSC-only and ConSC-only neurons. First we normalized each RF to its maximal firing rate, so that we could focus on RF shape regardless of absolute intensity of activity (Fig. 10A). For comparison, we pooled IpsSC-only and ConSC-only neurons into one “unilaterally driven” category. Then we rotated every curve so that its best direction was aligned to the right (Fig. 10B, top) and computed the average for the curves (Fig. 10B, bottom). It appeared that BothSC neurons (Fig. 10B, left) had broader tuning curves (larger areas) than neurons with unilateral SC input (Fig. 10B, right). To quantify this difference, we represented the area enclosed by each individual tuning curve as a ratio of the maximal possible area it could enclose (i.e., an equilateral octagon of radius 1). The distributions of these relative areas, expressed as percentages of maximal area, are shown in Figure 10C. We found that the average area of tuning curves for BothSC neurons (Fig. 10C, left) was 29% of maximal, significantly larger (t-test, $p < 0.005$) than the average area of neurons with unilateral SC input (19% of maximal; Fig. 10C, right). This suggested that the BothSC tuning curves were broader than the others.

To study this breadth result in more detail, we analyzed the component visual receptive fields and movement fields. Until this point we have considered the visual receptive fields and movement fields together, as a composite field (see Methods), because we were interested in the basic issue of tuning laterality. But the relatively broad

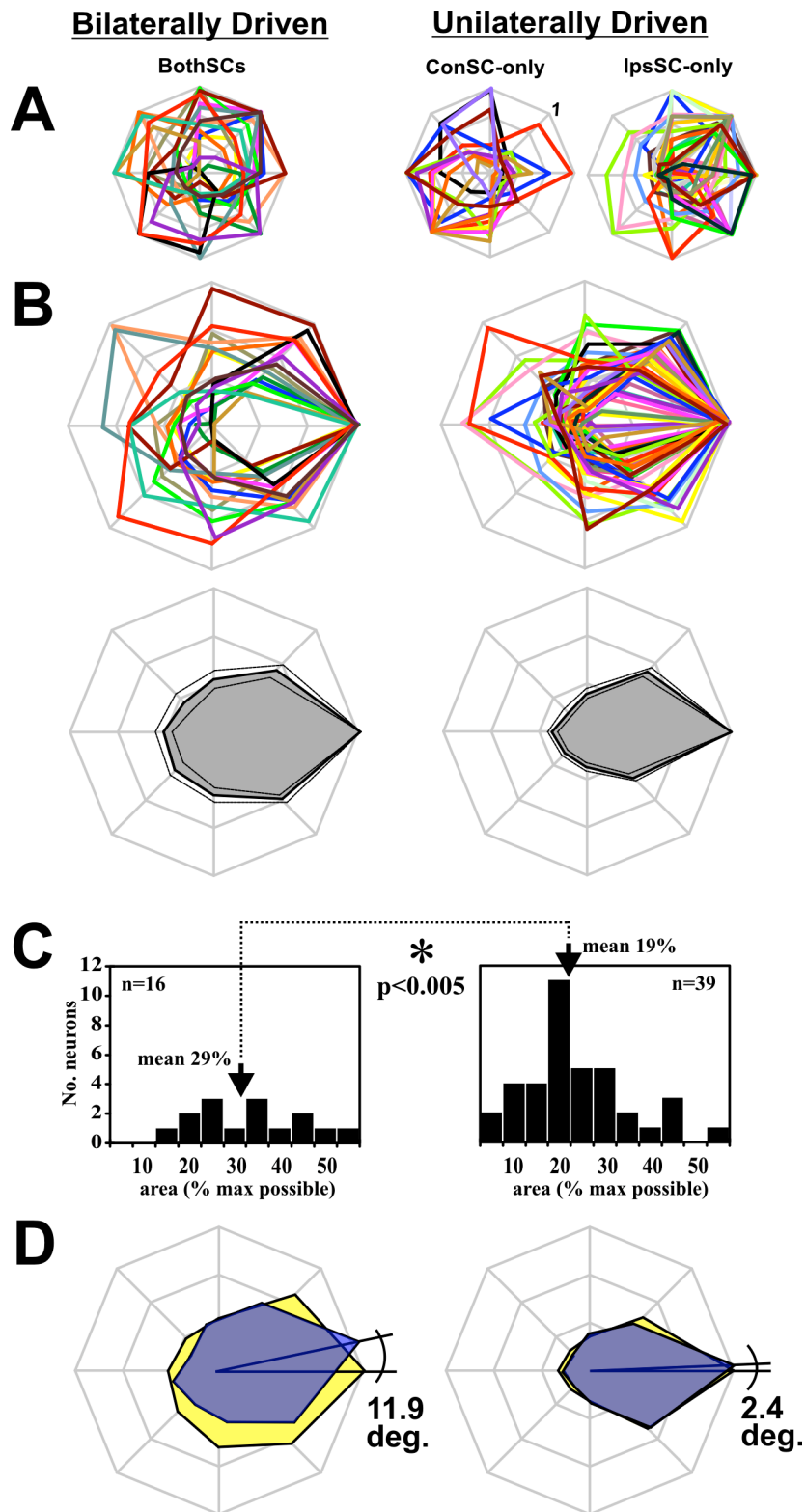


Figure 10: Shapes of the tuning curves. (A) Normalized tuning curves for neurons in all three samples. (B) *Top*: Same tuning curves but rotated with peak firing rate to the right. The ConSC-only and IpsSC-only populations are combined to form a single Unilaterally Driven category. *Bottom*: Average tuning curve for BothSC (left) and Unilaterally Driven (right) categories (mean and SEs). (C) Histograms of the relative

areas enclosed by the tuning curves, expressed as a percentage of the maximal possible area. The average relative area enclosed by BothSC neuron response fields (left) was significantly larger ($p < 0.005$) than that enclosed by Unilaterally Driven neuron response fields (right). (D) Average tuning curves of the visual receptive fields (yellow) and movement fields (blue) for neurons that had both. The angles depict the average VM differences, which are standardized to appear as counterclockwise angular rotations of the movement fields (on a neuron-by-neuron basis a movement field could be rotated either clockwise or counterclockwise relative to the visual receptive field).

composite fields of BothSC neurons raised the question of whether their individual visual and movement fields were unusually broad, or just less well-aligned in neurons with both fields. We found, first, that the individual visual receptive fields were in fact broader for BothSC neurons ($n=14$ neurons with a visual receptive field, 32% of maximal possible area) than for unilaterally driven neurons ($n=36$, 19%; $p=0.002$). The movement fields were broader, as well ($n=13$ BothSC neurons, and $n=19$ unilaterally-driven neurons; 30% vs. 20% of maximal possible area, respectively; $p=0.023$). These differences in breadth can be seen in Figure 10D which shows the average visual receptive field (yellow) and movement field (blue) for BothSC (left) and unilaterally-driven neurons (right). The differences in breadth were not related to trivial factors such as general firing rate differences between the BothSC and unilaterally-driven neurons (ANOVAs, $p > 0.10$ for both peak firing rate and baseline firing rate).

Finally, we quantified the alignment of visual fields and movement fields for each neuron that had both fields (“visuomovement” neurons as discussed in the next section; BothSC neurons, $n=11$; unilaterally driven neurons, $n=16$). We calculated the *VM difference*, i.e. the difference in angle between the preferred directions of the visual field and movement field (Fig. 10D). Although the VM difference was always small, quantitatively it was larger for BothSC neurons (median 11.9 deg.; see Fig. 10D, left) than for unilaterally driven neurons (median 2.4 deg.; $p < 0.001$; Fig. 10D, right).

In summary, the composite RFs of BothSC neurons were relatively broad, as were the component visual receptive fields and movement fields. In visuomovement BothSC neurons, the fields were relatively misaligned. These results suggest that the impact of the second SC input on BothSC neurons frees the directional range of tuning at the expense of sharp tuning and tight alignment of the visual and motor components of the RFs.

2.3.5 Visual and saccadic activity

As implied in our analysis of separate visual and movement fields above, we categorized the neurons of each population according to the types of task-related signals they carried. We found that, regardless of SC input laterality or RF laterality, the FEF neurons could be visual-only, movement-only, or visuomovement in nature (Bruce and Goldberg, 1985) (Table 1). We found no neurons that were unmodulated. The ConSC-only and IpsSC-only groups were each divided between approximately equal numbers of visual and visuomovement neurons. The BothSC group had an apparent bias for more visuomovement neurons, but this was not significant (Fisher exact test, $p=0.104$). While many neurons had saccade-related activity, pure movement neurons (those lacking any visual response) were rare ($n=5$), consistent with previous results (Sommer and Wurtz, 2004a).

Table 1. Distribution of FEF neuron types activated from each SC

FEF Neuron Type	ConSC-only	BothSC	IpsSC-only	Totals
Visual	6	3	14	23
Movement	2	2	1	5
Visuomovement	4	11	12	27
Totals	12	16	27	55

We examined the timing of activity in the neurons, since prior reports of ipsilateral tuning in the FEF have emphasized postsaccadic activity (Bruce and Goldberg, 1985; Goldberg and Bruce, 1990) (but see Schlag et al., 1998). Figure 11A depicts the average activity profiles of ipsilaterally tuned neurons and contralaterally tuned neurons. Figure 11B is the same except that it was constructed from normalized firing rate data. The main point is that, regardless of tuning laterality, the average saccade-aligned activity (Fig. 11A & B, right) was presaccadic: it started before and peaked near saccade initiation. Visual responses, as well, were comparable regardless of response field laterality (Fig 11A & B, left).

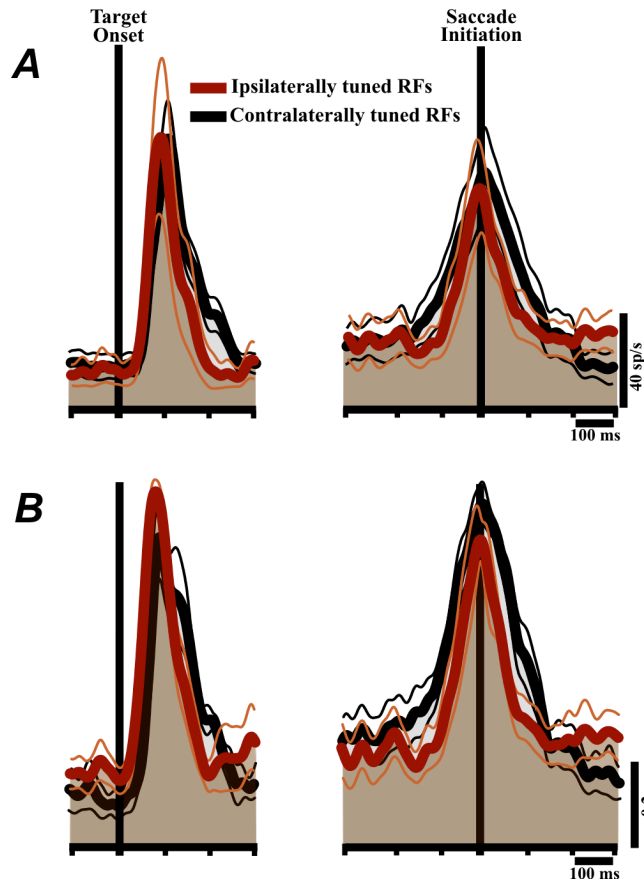


Figure 11: Activity profiles of the neurons, aligned to visual target onset (left) and saccade initiation (right). (A) The average activity profiles of ipsilaterally tuned and contralaterally tuned neurons. (B) Same as panel A, but for each neuron the activity profile was normalized to the peak firing rate within the respective (visual or presaccadic) epoch before averaging. Neurons pooled for this analysis were those with a significant visual (left) or saccade-related response (right). The ipsilaterally tuned data were from ConSC-only neurons and the contralaterally tuned data from IpsSC-only neurons. Scales at lower right.

The visual and presaccadic bursts of contralaterally tuned neurons appeared to be slightly wider than those of ipsilaterally tuned neurons (Fig. 11A, averages of raw activity; Fig. 11B, averages of peak-normalized activity). To test for significance, we measured the width of each burst at half-height. For the visual burst, the width difference was significant in the normalized data (Mann-Whitney rank sum; $p < 0.05$) although not in the raw data ($p = 0.3$). For the saccadic bursts, the width difference was significant in both the raw ($p < 0.005$) and normalized data ($p < 0.001$).

2.4 Discussion

2.4.1 Overview

In this study we provided evidence for a functional crossed pathway linking the opposite SC to the FEF. We identified FEF neurons that receive input from the contralateral SC and compared them with FEF neurons receiving input from the ipsilateral SC. We found that the connections were excitatory and that the activation latencies implied a thalamic decussation point for the crossed pathway. FEF neurons with SC inputs were found to have lateralized, presaccadic RFs that in toto represented visual stimuli and saccades in all directions. In large part the laterality of each neuron's RFs was predicted by its SC input laterality. The exception to this rule occurred for FEF neurons with bilateral SC input.

2.4.2 Properties of FEF neurons with input from the opposite SC

Many neurons in the FEF seem to have simple representations of stimulus locations or saccadic vectors, and they do this primarily for contralateral space. Other FEF neurons, however, exhibit more complex signals. They may have presaccadically shifting RFs or activity attributable to vector subtraction, phenomena that occur for any direction. Such neurons require information about contralateral *and* ipsilateral visual targets and saccades. It has been unknown how neurons with such properties gain access to

ipsilateral information. A main result of our study was to show that one physiologically-defined set of neurons in the FEF, those with SC input, have clear presaccadic, ipsilateral information. We found that as long as a neuron could be driven from the contralateral SC, it could have an ipsilateral RF. If it was driven *exclusively* from the contralateral SC, the chance of it having an ipsilateral RF was nearly 100%, while if it was driven from both the contralateral *and* ipsilateral SC the chance dropped to about 50%. If we could not drive it from the contralateral SC, the chance of it having an ipsilateral RF approached zero. These data suggest that the opposite SC sends information that may be used by FEF neurons with ipsilateral spatial representations.

Neurons in the primate cerebral cortex receive many inputs from numerous parts of the brain (Douglas and Martin, 2004; Felleman and Van Essen, 1991), so there was little reason to expect that the RF tuning of FEF neurons would be predicted almost entirely by a single subset of their inputs, the afferents arriving from a structure of the midbrain, the SC. Nonetheless, that is what we found. The clear structure-function relationship, illustrated in Figure 8, is a deceptively simple result with intriguing implications. One is that the SC inputs may dictate the RF laterality of the FEF neurons by serving as powerful drivers for the neurons (Sherman and Guillery, 1998). An alternative possibility is that the SC inputs do not dictate the RF laterality, but seek out and connect with FEF neurons that have compatible RF lateralities. In this case, the inputs could exert their influence in a more subtle, context-dependent way. These hypotheses are testable by recording from FEF neurons with crossed SC input, then inactivating the crossed pathway (e.g. at the level of the SC or thalamus) and studying how the FEF RFs change. Similar experiments were performed on the same-side SC-FEF

pathway (Sommer and Wurtz, 2006). In that circuit, it appeared that the SC input did not create the classical FEF RFs but helped to spatiotemporally modulate them around the time of the saccade (“shifting receptive fields”). However, due to the presumed rarity of ipsilaterally-tuned visual and presaccadic information arriving at the FEF, it seems reasonable to speculate that SC input arriving through the crossed pathway may have a more causal role in governing the RF structure of recipient FEF neurons.

Our data suggest that signals from the opposite SC cross at the level of the diencephalon via the massa intermedia (Olszewski, 1952). The crossed projection would involve an MD neuron that sends its axon directly to the opposite FEF, providing a conduit for ipsilateral information and the means for generating a full field representation in a single FEF. This interpretation is consistent with anatomical reports of crossed thalamo-frontal cortical projections (Preuss and Goldman-Rakic, 1987).

Other sources of ipsilateral information may be present. A pioneering study showed that some ipsilateral information potentially arrives from the opposite FEF (Schlag et al., 1998). One possibility is that information from different sources subserves different functions. Interestingly, much of the ipsilateral information from the opposite FEF is accompanied by inhibition of the recipient neurons (Schlag et al., 1998). The function of this information may be to silence saccadic plans that would interfere with unity of purpose. In contrast, it appears that ipsilateral information from the opposite SC is accompanied by excitation of the recipient neurons. This provides a potential means of creating ipsilateral RFs.

The crossed projections also may provide an alternate route of interhemispheric communication. A host of lesion studies implicate subcortical structures as potential

sources of information that may provide for recovery of function in event of cerebral damage (Boire et al., 2001; Herter and Guitton, 2004; Poppel et al., 1973). It is well known that many V1-lesioned or cerebral hemispherectomy patients exhibit remarkably persistent visuomotor capabilities, i.e. blindsight. Our data demonstrate that information about the contralesional hemifield is available to cerebral cortex from the opposite SC via crossed projections. Visuomotor signals that may mediate blindsight could reach and influence intact cortical areas through this route.

2.4.3 Structure-function relationship in the SC-FEF circuit

We found that the RF laterality of FEF neurons connected with a single SC was largely predicted by the laterality of that SC. It is possible that we could have found a finer-scale relationship between direction tuning in the FEF and spatial location of stimulation in the SC. Direction tuning within a hemifield is likely correlated with electrode placement along the mediolateral dimension of the SC, just as amplitude tuning of SC-recipient FEF neurons is correlated with electrode placement in the rostrocaudal dimension of the SC (Sommer and Wurtz, 2004a). As predicted by our stimulation electrode placements on the SC's horizontal meridian, our FEF neurons showed average direction tunings that were close to horizontal (Fig. 8A left and right). We did not systematically vary stimulation along the mediolateral dimension of the SC because the experiment was technically daunting already, requiring stimulation within both SCs plus recording in the FEF.

Similar isomorphic mappings between RF lateralities and anatomical inputs exist elsewhere in the primate brain. Most primary sensory and motor centers, for example,

exhibit topographically preserved signaling (Canedo, 1997; Smith, 2000). Moreover, physiologically confirmed instances of structure-function relationships have been identified within the brainstem (Gandhi and Keller, 1997), between cortical and subcortical structures (Hoffmann et al., 2002; Nambu et al., 2002; Schlag-Rey et al., 1992), and within the cortical network itself (Movshon and Newsome, 1996; Schlag et al., 1998). The common finding of these studies is that the functionality of projection and recipient neurons is often highly correlated, and most parsimoniously explained by mutual connectivity.

We think the present results qualify as an additional example of a structure-function relationship. The SC-FEF pathway seems to mediate a “motor-to-sensory” rather than “sensory-to-motor” transformation that conveys corollary discharge (CD) from midbrain to cortex (Sommer and Wurtz, 2008b). A major implication of our results is to demonstrate for the first time that feedback from motor to sensory networks in the primate brain feature just as much structural organization in the mediation of functional purpose as feedforward pathways from sensory to motor networks. Clear topographical organization of CD transmission was predicted in the classic literature (Holst and Mittelstaedt, 1950b; Sperry, 1950), and had been identified in other animals (Crapse and Sommer, 2008a; Poulet and Hedwig, 2006), but had not been demonstrated previously in primates.

2.4.4 Special case of bilateral SC input

The structure-function relationship that we found for ConSC-only and IpsSC-only neurons was more complicated for BothSC neurons, those identified as receiving bilateral SC input. We expected that these neurons would feature RFs that were bilateral. We found instead that the RFs of BothSC neurons were lateralized and could point in any direction. Compared with the RF of neurons with unilateral SC input, the RFs of the BothSC neurons were broader, and the visuomovement class of BothSC neurons had visual and movement fields that were more misaligned. These two characteristics, greater breadth and relative misalignment, most likely do not provide the BothSC neurons with any functional advantage. More likely they are residual consequences of the FEF neuron having to process conflicting signals arriving from the two SCs. Analyses of the relationship between the weighting of SC inputs and the RF laterality of FEF neurons uncovered no correlations. Hence we found no discernable principle governing the RF directionality of the BothSC neurons. We speculate that the RF structure of BothSC neurons is established during development through a gain mechanism that acts on the two SC inputs to determine the overall laterality of the RFs, as well as breadth and visual-movement field alignment.

There seemed to be a categorical difference, therefore, between the BothSC neurons (RF laterality unrelated to SC input laterality) and the ConSC-only and IpsSC-only neurons (RF laterality predicted by SC input laterality). Further evidence for a categorical difference was the broader RF tuning of BothSC neurons and the relative misalignment of the visual and movement fields. These categorical differences have

an important implication for interpreting our stimulation results. One could argue that our ConSC-only and IpsSC-only terminology, although objective as a description of our ability to drive the neurons from a single SC, may be unreliable as a description of the true balance of SC inputs. The apparently unilaterally-driven neurons may have actually received a weak input from the other SC that we failed to detect due to inadequate stimulating electrode placement or current level. We think that the categorical differences between unilaterally activated neurons and known bilaterally connected (BothSC) neurons undermines this objection.

Furthermore, neurophysiological evidence in the literature supports the idea that ConSC-only and IpsSC-only FEF neurons receive input from only one SC. The evidence was documented in Figure 9 of Sommer & Wurtz (2004a). Without getting into the technical details, the take-home message was that if an FEF neuron is activated orthodromically from one place on the SC map, it can be activated from elsewhere on the map (although perhaps with a different current requirement). Hence, the yes-or-no question of whether an FEF neuron can be orthodromically activated from an SC should depend little on stimulation location within that SC. This is likely because the activated elements – initial segments of thalamic-projecting SC neurons – are highly sensitive. Therefore when we orthodromically activated an FEF neuron from one SC but not the other SC, the lack of activation from the other SC was probably not due to suboptimal stimulating electrode placement. We tried up to 1.5 mA, and if a connection had been present, we feel that we would have found it. Lack of activation may truly represent a lack of connection in this particular situation.

2.4.5 Conclusion

In sum, the results illustrate a means by which each FEF receives information about the entire visual field and all saccades. We think these findings supply an important piece of the puzzle for modeling how the FEF and interrelated regions perform perisaccadic omnidirectional functions such as shifting RFs and vector subtraction.

3.0 Frontal eye field neurons assess visual stability across saccades

3.1 Introduction

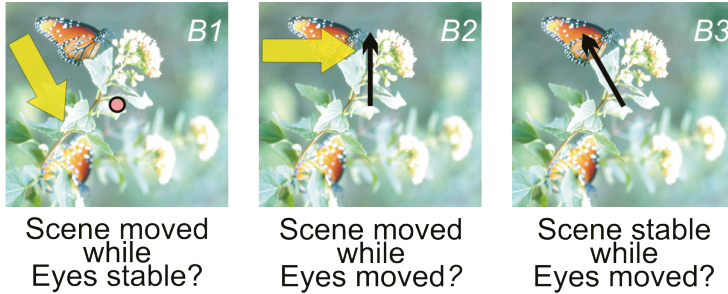
Movements are necessary to engage the world but are costly in that they may destabilize sensory inputs. Primates, for example, redirect their foveas to interesting objects in the environment by making rapid eye movements known as saccades. While beneficial in extending the range of visual analysis, saccades pose a problem to the visual system.

For example, a primate may observe a scene (Fig. 12A, left) that suddenly undergoes translation (Fig. 12A, right). Visual neurons throughout the animal's brain would suddenly detect something different in their receptive field (RF; Fig. 12A, ellipses). In our illustration, the RF stimulus changes from a blur to a flower, a change that is rife with ambiguity (Fig. 12B). Such a change may have occurred because the scene moved while the eyes were stable (Fig. 12B1), because the scene moved while the eyes moved (Fig. 12B2), or because the scene was stable while the eyes moved (Fig. 12B3). Visual signals alone, therefore, are insufficient to identify the nature of the scene change. The primate visual system, however, receives additional information that may help to resolve this ambiguity: internal signals about imminent saccades, i.e. corollary discharge (Sommer & Wurtz 2002, 2006). Visual neurons with access to corollary discharge may be in a position to disambiguate the cause of visual translations.

A Visual change



B Ambiguity



C Remapping



D Solution

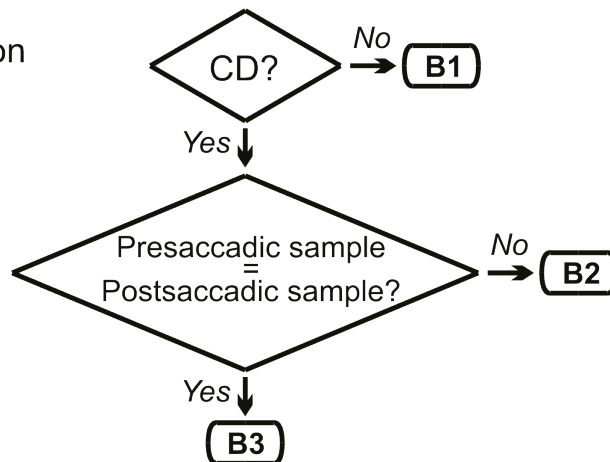


Figure 12. The ambiguity inherent in any visual change. A. A neuron suddenly finds a different spatial pattern within its RF. B. Potential causes of the sudden change. B1. The scene change could be due to a gust of wind that brought the flower and the perching butterfly down to the level of fixation. B2. A saccade to the flower plus a gust of wind from the left could also result in the very same scene change. B3. The scene change could also be due simply to a saccade to the butterfly. In sum, changes in sensory input are ill-posed problems for the visual system; they could arise from any number of equivalent factors. C.

Remapping as one constraint on the solution space. By comparing presaccadic samples with postsaccadic samples, neurons that remap can assess the degree to which world differs across a saccade. D. Together with corollary discharge, remapping provides the brain with a means to resolve the ambiguity of the scene change.

Some of the neurons that receive corollary discharge engage in an operation known as presaccadic remapping (Fig. 12C; Duhamel et al. 1992; Nakamura and Colby 1992; Sommer and Wurtz 2008). Just before a saccade, the neurons receive corollary discharge (CD in Fig. 12C left) that renders them visually sensitive at a future field (FF in Fig. 12C left) location, the portion of space that the RF will occupy after the saccade. Once the saccade is made (Fig. 1C middle), the future field becomes the RF. Critically, the future field and RF sample the same region of absolute visual space.

Neurons that remap offer a potential mechanism for resolving the ambiguities of Figure 12B. If a visual translation occurs in the absence of corollary discharge, it may be concluded that the scene moved while the eyes were stable (Fig. 12D, the B1 outcome). If visual translation *is* accompanied by corollary discharge, then neurons that remap could report whether the presaccadic sample in the future field matches the postsaccadic sample in the RF. If the samples differ, the scene must have moved in addition to the eyes (Fig. 12D, the B2 outcome). If the samples match, the scene must have remained stable while the eyes moved (Fig. 12D, the B3 outcome).

Figure 12D raises a fundamental question: Can single neurons compare the presaccadic and postsaccadic scene and report whether a stimulus remains stable, or moves, during a saccade? If neurons cannot detect transaccadic visual translation, then the algorithm of Figure 12D would be rejected outright. But if they can do it, the basic concept of Figure 12D would be supported.

We recorded from neurons in the FEF, a cortical area involved in cognitive aspects of eye movement control (Tehovnik et al., 2000). The FEF contains visual neurons that remap (Umeno and Goldberg, 1997, 2001) and is a known target of corollary discharge from the midbrain (Sommer and Wurtz 2006). We found that many FEF neurons are tuned for transsaccadic visual translations, i.e. they can tell the difference between a visual stimulus that remains stable, or moves, during a saccade. The effect was more ubiquitous than we expected, occurring both in neurons that remap and those that do not, and it was more visually general than we expected, occurring not only for translations but also for featural changes (e.g. stimuli that changed color during a saccade). The findings provide evidence at the single neuron level that the brain compares visual scenes before and after a saccade to judge whether they are stable.

3.2 Methods

3.2.1 Surgery and region identification

In two monkeys (*Macaca mulatta*) we implanted scleral search coils for measuring eye position, recording chambers for accessing FEF, and a post for immobilizing the head during recording experiments. Details are provided elsewhere (Sommer and Wurtz, 2000). The location of the FEF was determined stereotaxically and verified by physiological means: the recording of saccade related neurons and the evocation of saccades at $< 50 \mu\text{A}$ threshold (Bruce and Goldberg, 1985).

3.2.2 Behavioral tasks

During recording sessions each monkey sat in a primate chair facing a tangent screen onto which visual stimuli were back projected. Once a neuron was isolated, we characterized its activity with several oculomotor tasks (See Crapse and Sommer, 2009 for details). In all tasks the monkey was required to fixate a spot of light projected onto the center of the screen. Then, with timings that depended on task contingency, the monkey was required to execute an appropriate eye movement for a liquid reward. The critical task for screening neurons was the memory-guided saccade task. A monkey fixated a spot for 500-800 ms, a target flashed in the response field for 50 ms, and the monkey was required to maintain fixation. After a 500-1000 ms delay period, the fixation spot disappeared which was the cue to move. The monkey made a saccade to the remembered target location and received reward 500 ms later.

If the neuron exhibited visual activity in the memory-guided task (see Crapse and Sommer 2009 for analysis details), we had the monkey perform the central task for this study, the saccadic translation task. The monkey fixated a spot of light and after a delay of 200 ms a visual probe appeared on the screen. After an additional random delay (200-1000 ms) the fixation point stepped to a new location (typically 28-30 deg. away from initial fixation) signaling the monkey to make a saccade to its new location. During the saccade, the visual probe was translated by a specific amount (20%,40%, or 60% of saccade amplitude) or remained stable at its position (0%). In all cases, the postsaccadic probe was located at the center of the neuron's postsaccadic RF. Exact timings of visual events were determined with a photodiode on the screen that monitored the appearance of a visual spot (not visible to the monkey) that accompanied every visual event in the task.

The time of intrasaccadic probe translation varied as a function of saccadic amplitude (and therefore saccadic duration), but in general the probe translated at a time corresponding to when the saccade was $\sim 2/3$ toward completion (mean 68.9%, standard deviation 16.1%).

A subset of the neurons tested on the saccadic translation task were also tested on a fixation control task. The purpose of the task was to model probe change activity in the RF (i.e. “map” the RF) in the same way that we tested pre-to-postsaccadic probe changes relative to the FF in the saccadic translation task. For this control task, the monkey fixated a spot of light for 200 ms at which point a probe appeared on the screen. The probe’s initial position relative to the center of the RF (0 deg, 6 deg, 12 deg, or 18 deg) corresponded to the probe’s initial position relative to the center of the FF during the saccadic translation task (0%, 20%, 40% or 60% of typical, 30 deg, saccades). After an additional delay the probe stepped to a new location located at the center of the RF. Then after a final delay (500 ms), the monkey received a liquid reward.

We included a featural change version of the saccadic translation task designed to test whether FEF neurons are generalized change detectors. For this task, a visual probe appeared at the center of the neuron’s FF and could change along one of 2 featural dimensions: color, size or combined color-size change. The final probe at the end of the saccade was the same in all conditions; what varied from trial to trial was the initial presaccadic feature of the probe that was manipulated intrasaccadically. For color changes, the presaccadic probe was green and the postsaccadic probe was white. The green was created by maximizing the green output of the LCD projector and minimizing the red and blue outputs, while the white was created by maximizing all the outputs.

Hence there was a luminance difference as well. This did not matter for the experiment as we simply wanted a salient, nonspatial change. For size changes, the presaccadic probe was typically a 20 by 20 size probe that changed to the default 8 by 8 postsaccadic probe. The size change necessarily involved a spatial change at the edges of the stimulus, but this was spatially symmetric and the center of mass of the stimulus did not move.

3.2.3 Data Analysis

All neuronal data were converted from raw spike rasters to average firing rates during defined task epochs for off-line analysis. Our first goal was to determine if a neuron was significantly task modulated, that is, whether it fired differentially across the different translation conditions. To determine this, we employed two analytical approaches, one of which involved a coarse analysis in which we examined activity in an epoch ranging from -50 to 150 ms relative to saccade end, and a second, fine scale analysis, that involved looking at the precise time when the neurons exhibited significant task modulation.

First, we counted the number of spikes occurring for each translation condition in the 200ms epoch and ranked each condition in descending order from the condition with the maximum number of spikes, labeled rank 1, to the condition with the least number of spikes, labeled rank 4. This resulted in a total of 4 rank categories corresponding to the 4 trial conditions for each neuron. We then normalized the data to the rank 1 condition and pooled across neurons to generate a population result.

To analyze shape of tuning, we used a bootstrap procedure on shuffled trials to calculate the amount of tuning expected from random variations in firing rate. Specifically, for each neuron we pooled all trials from the 4 translation conditions and then randomly assigned each trial with replacement to one of 4 categories. The number of random assignments per category corresponded to the average number of collected data trials across the 4 original test conditions. Following random assignment, we computed the means for each category and then ranked the categories as described above. We repeated this procedure 1000 times to generate 4 rank bootstrapped means and standard errors. These were then compared to the 4 test means and standard errors.

To analyze the precise time of modulation onset and its duration, we performed a sliding ANOVA on the spike density functions across all 4 trial conditions for each neuron. The ANOVA was performed at a resolution of 1 ms, with a p value being generated at each ms time point. For a modulation onset time to be considered significant, we imposed the condition that significant modulation (that is, p values less than 0.05) had to persist for at least 20 ms.

3.2.4 Tuning curve analysis

We quantified the variety of translation tunings by generating two indices for each neuron that capture two dimensions of tuning curve shape: curvature and ramp. First, we found the average firing rate for each translation condition. Then we calculated the curvature and ramp indices. The curvature index is a contrast ratio of the average firing rates of the 4 translation conditions arranged in the following order: (20%+40%)-

$(0\%+60\%)/(20\%+40\%)+(0\%+60\%)$. The curvature index ranges from -1 (a tuning curve with completely concave shape, that is, firing maximally for the extreme translations and little for the intermediate translations) to +1 (completely convex shape, characterized by maximal firing for the intermediate translations and little for the extreme translations). The ramp index measures the degree of monotonic rise or fall in the firing rate as a function of translation using the contrast ratio: $(40\%+60\%)-(0\%+20\%)/(40\%+60\%)+(0\%+20\%)$. This index ranges from -1 (a tuning curve characterized by progressively decreasing firing rate as a function of translation) to 1 (characterized by progressively increasing firing rate as a function of translation).

3.2.5 Saccade endpoint analysis

We tested for differences in firing rate that may accompany differences in saccadic endpoint. For each neuron and translation condition (4 per neuron), we found the mean and variance of the saccade endpoints along the longest saccade dimension. We then defined a spatial window of inclusion defined relative to the mean with a total width equal to 2 times the variance. Spike counts for endpoints falling within the window were averaged and compared to the averages of those trials falling outside the window. We performed this process for both samples of neurons. Linear regressions were performed and tested against the null hypothesis that they were not significantly different from 1.

3.2.6 Statistics

All data were statistically analyzed using conventional parametric and nonparametric tests with $p < 0.05$ as the criterion for significance.

3.3 Results

3.3.1 FEF neurons detect transaccadic movement of a visual stimulus

We recorded from 157 visually responsive neurons in the FEF while monkeys performed the saccadic visual translation task (Fig. 13). The primary emphasis of the experiment

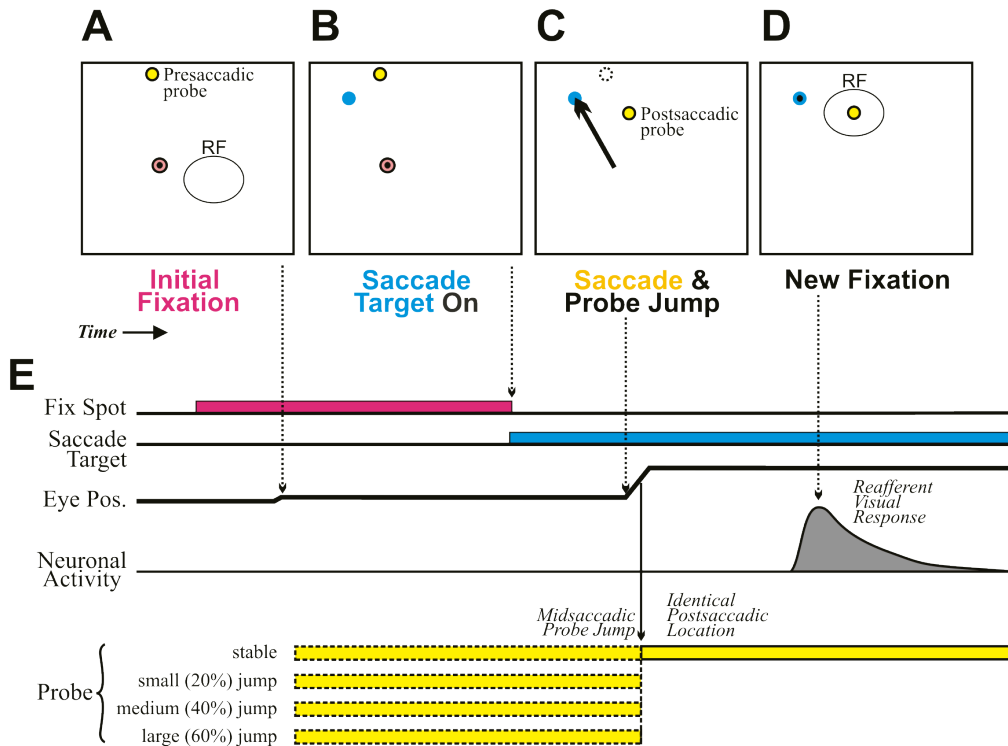


Figure 13. Saccadic translation task. A. Initial Fixation. The task begins with the monkey viewing a fixation point. After a delay of 200 ms a presaccadic visual probe appears on the screen. The probe can

appear at any 1 of 4 possible positions (e.g. 0%, 20%, 40%, or 60% of saccade amplitude where saccade amplitude is typically 30 deg) relative to the center of the RF. B. Saccade Target On. After an additional delay of 200-1000 ms the fixation point stepped to a new location signaling the monkey to make a saccade to its new location. C. Saccade and Probe Jump. During the saccade the visual probe jumped (20%, 40%, or 60% of saccade amplitude) or remained stable (0%). In all cases, the probe jumped to the center of the neuron's postsaccadic RF. D. New Fixation. The eye is at rest and the probe is in the center of the RF. E. Timeline of events.

was on neurons with shifting RFs, but we tested every visually responsive neuron that we encountered. Inspired by human psychophysics, we used two permutations of the task, one in which the probe jumped parallel to the saccade vector (for 111 neurons) and one in which the probe jumped perpendicular to the saccade (for 66 neurons; 20 of the neurons were tested in both conditions).

Data from three example neurons are shown in Figure 14. The rasters and spike density functions are aligned to the end of the saccade to emphasize the reafferent visual responses to the postsaccadic stimulus located at the center of the postsaccadic RF in every trial. The null hypothesis is that the reafferent visual response to this stimulus

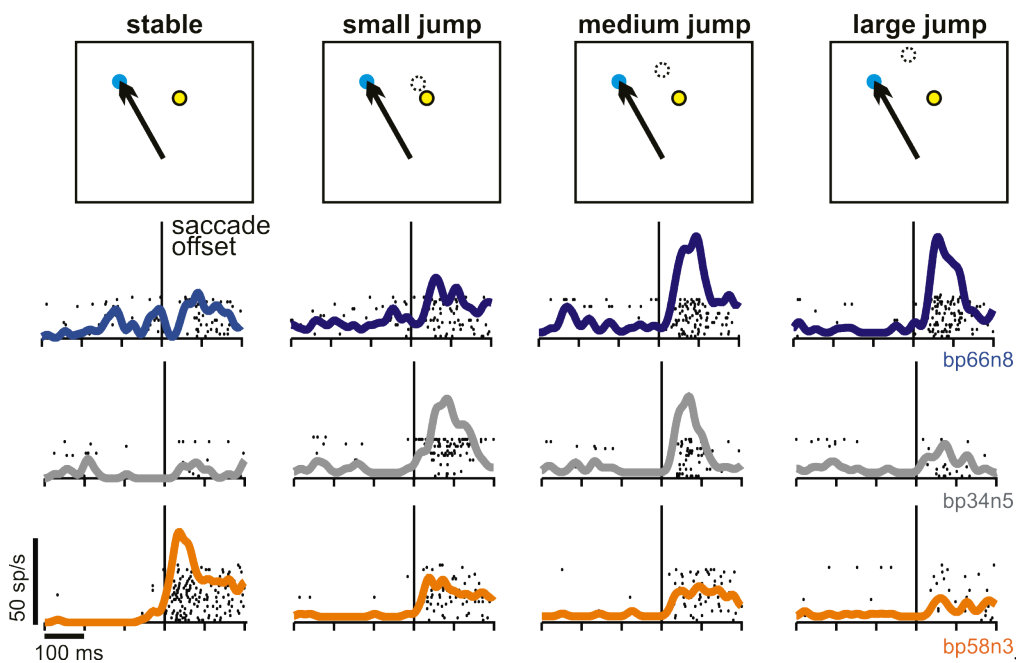


Figure 14. **Three example neurons tested on the saccadic translation task.** The blue example neuron showed modest activity for the 0% and 20% conditions yet exhibited a dramatic increase in firing rate for the 40% and 60% conditions. This neuron's tuning may be characterized as an increasing ramp. The neuron

in grey, fired very little for the extreme translation conditions (0% and 60%) yet fired maximally for the intermediate conditions (20% and 40%). Such a neuron exhibits an inverted U tuning profile. The neuron depicted in orange showed the polar opposite of the tuning featured by the blue neuron. It fired maximally for the 0% condition and exhibited a progressively decreasing modulation for the increasing translation amounts. This type of tuning may be characterized as ramp-down. Scales shown at bottom left.

should be invariant across the differing translations. The first neuron (top row, blue traces), however, varied its reafferent response as a function of how the postsaccadic stimulus attained its final position. The neuron fired little if the stimulus was stable, fired modestly if the stimulus attained its final position after a small (20%) translation, and fired vigorously after medium (40%) and large (60%) translations (the percentages refer to the extent of probe movement relative to total saccade amplitude). We refer to this type of translation tuning as “ramp up” because the activity increased monotonically with jump size. The second neuron (Fig. 14 middle row, grey traces) was tuned best for intermediate translations. It fired strongly for small and medium translations but weakly for the extreme conditions (stable stimulus or large translation). We refer to this sort of tuning as “curved up” because it fired maximally for the intermediate translations.

We also found neurons with inverted versions of the two tuning types, i.e. ramp down or curved down (i.e. U-shaped). As an example, a ramp down neuron is shown in the bottom row of Figure 14 (orange traces). Its reafferent visual response was strong for a stable stimulus but decreased for increasing translation size.

We quantified the nature of the translation tunings in our overall sample of visually-response FEF neurons by plotting, for each neuron, the degree to which its tuning showed ramp characteristics, curved characteristics, or both. Data were analyzed separately for the two translation geometries that we used: parallel (Fig. 15A) and perpendicular (Fig. 15B) to the saccade. The ramp index is positive for ramp-up tuning

(e.g. the neuron in Fig. 14, top row, is depicted in Fig. 15A with an “x” symbol) and is negative for ramp-down tuning (the neuron in Fig. 14, bottom row, is depicted in Fig. 15B with a triangle). The curvature index is positive for curved-up tunings (the neuron in Fig. 14, middle row, is shown in Fig. 15B with a square) and negative for curved-down tunings. Neurons generally had idiosyncratic tunings that could exhibit both ramped and curved attributes. For example, a neuron might have curved-up tuning that was slightly asymmetric so that the largest translation elicited more activity than the zero translation (such a neuron is noted with a cross in Fig. 15B). The considerable scatter of the plots indicates that the samples of neurons exhibited a myriad of tuning preferences.

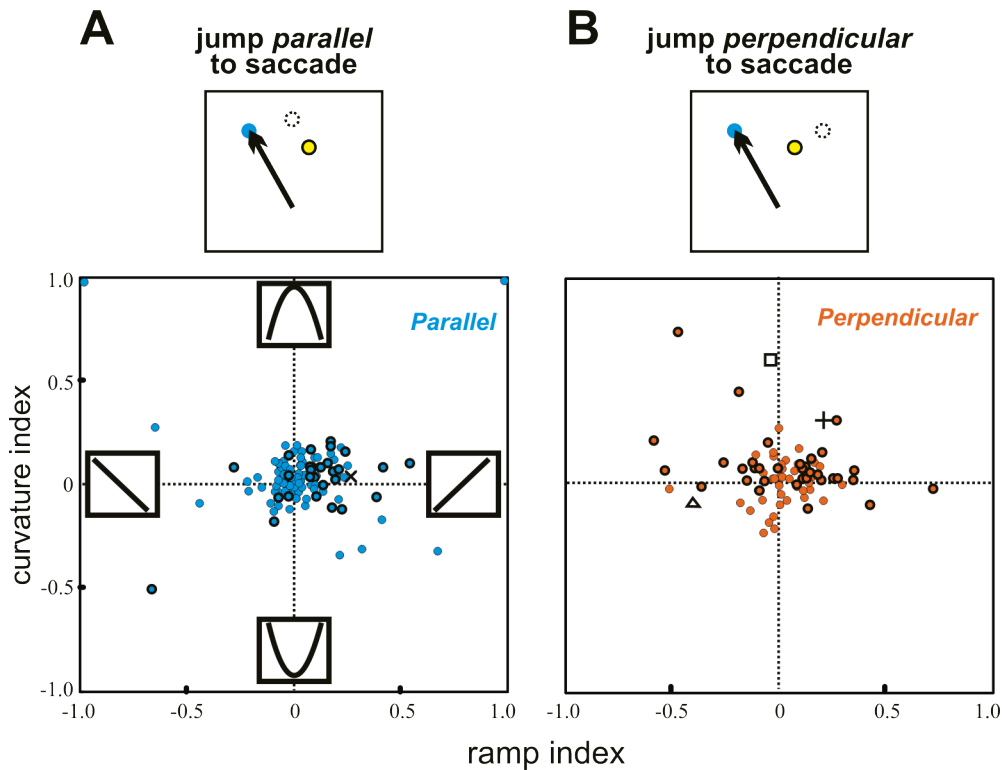


Figure 15. **Ramp/Curvature indices for the two populations of neurons tested on the parallel and perpendicular versions of the task.** The ramp index is positive for ramp-up tuning (e.g. the neuron in Fig. 14, top row, is depicted in Fig. 15 as an X) and negative for ramp-down tuning (the neuron in Fig. 14, bottom row, is depicted here with a triangle). The curvature index is positive for inverted-U shaped tunings (the neuron in Fig. 14, middle row, is shown with a square) and negative for U shaped tunings. All neurons with significant translation tuning as determined by the max-min index (see Figure 16) are shown with bold outlines.

In general, the neurons seemed to be less tuned for parallel jumps than for perpendicular jumps; the data appear more clustered near zero for the former than the latter (compare Fig. 15A with 15B). This is consistent with human psychophysics data that demonstrate less sensitivity for parallel than perpendicular transaccadic displacements of a stimulus (Niemeier et al., 2003). We calculated whether individual tunings were significant by comparing maximal and minimal firing across the translation conditions (t-tests at $p < 0.05$ criterion). For example, the neuron of Fig. 14, top row, had maximal activity (24 sp/s) for medium translation and minimal activity (15 sp/s) for no translation (stable stimulus). These firing rates were significantly different ($p = 0.002$, t-test), so the tuning was considered significant. All the individually significant

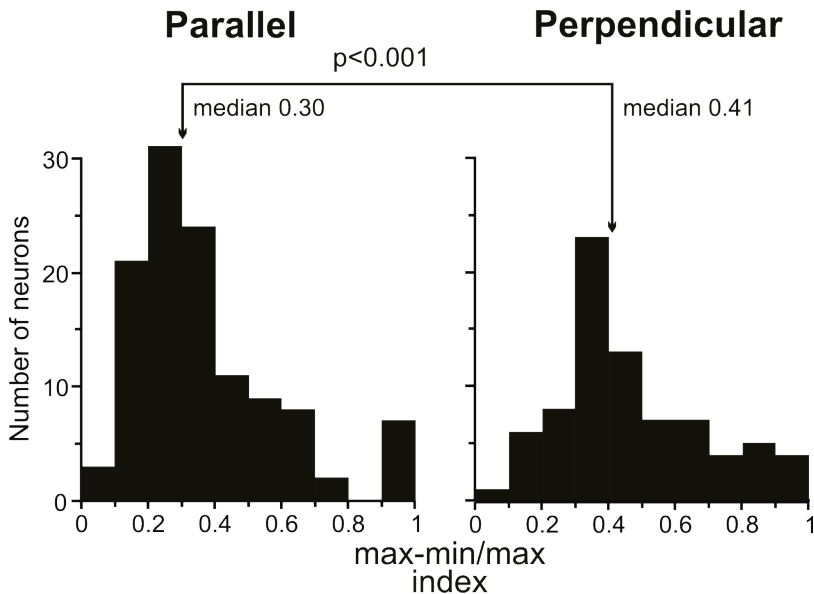


Figure 16. Max-Min indices for the parallel and perpendicular tested samples.

translation tunings are shown with bold outlines in Figure 15A and B. A greater proportion of tunings were significant in the perpendicular condition (59%, 39/66 neurons, Fig. 4B) than the parallel condition (29%, 32/111 neurons, Fig. 4A; Chi-Square, $p < 0.001$). To determine if the tuning was not only more prevalent, but also stronger, for

the perpendicular condition, we quantified the firing rate differences in Figure 16. Because the neurons showed a variety of maximal firing rates, we normalized the maximal-minimal differences accordingly, yielding an index that provided a fair comparison between the neurons $((\text{max}-\text{min})/\text{max})$. We found that the tuning was indeed stronger for perpendicular than for parallel translations (index difference of .11, $p < .001$). Finally, we found that maximal activity of neurons with significant tuning could represent any translation amount (Table 2), i.e. the tunings in the neuronal population covered the entire space of tested translation sizes.

Table 2.

	No jump	Small jump	Medium jump	Large jump
parallel	4	3	9	16
perpendicular	7	10	8	14

The above analyses only considered the maximal and minimal firing rates elicited from the range of translation sizes. To quantify the tuning in more detail, we next considered its overall shape – the profile of firing rate change from maximal to minimal levels. The analysis was restricted to those neurons with significant tuning according to the max-min test described above (39 neurons in perpendicular condition, 32 in parallel condition). We ranked the firing rates elicited by the translations from 1 (maximal) to 4 (minimal). Ranking a neuron’s responses yields its effective tuning curve regardless of peculiarities of whether the tuning was ramped, curved, or hybrid. We normalized each

rank-tuning curve to the maximal firing rate (set to 1.0) and averaged the results (Fig. 17). For comparison, we calculated the amount of spurious tuning expected from random firing variations by applying a bootstrap method to shuffled trials from the same neurons (squares in Fig. 17). The average tuning in both the parallel condition (black bars) and the perpendicular condition (white bars) was highly significant; the means and standard errors across all ranks were well below the bootstrapped means and standard errors. In both conditions of the task, average tunings dropped smoothly from maximal to minimal activity.

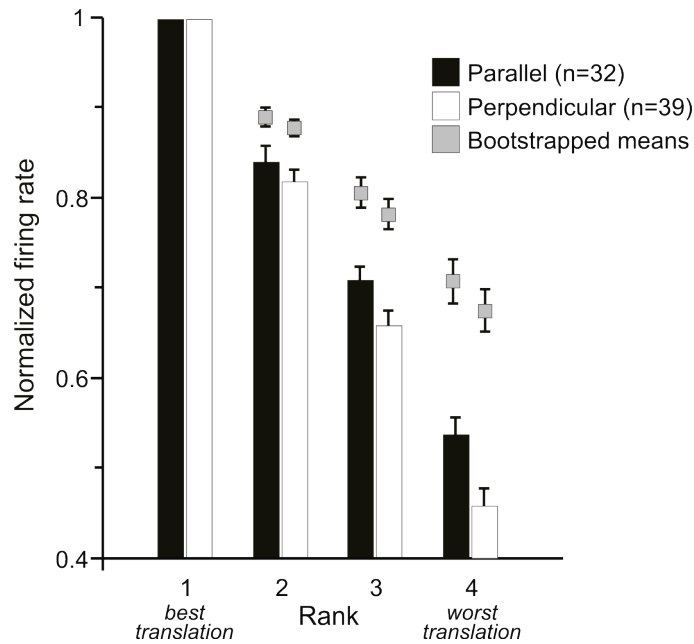


Figure 17. Ranked population of significant neurons. Each subset of the neurons exhibited a sharp decrease in normalized firing rate as a function of rank. These distributions were markedly different from the ranked bootstrapped distributions thus indicating significant tuning.

We next examined the exact timing of translation tuning modulation, that is, the precise moment when the neurons began to discriminate significantly amongst the different trial conditions. For this analysis, we performed a sliding ANOVA across the spike density functions for all translation amounts and looked for the time when the spike

density functions diverged from one another (see Methods). We found that the neurons began discriminating between the translation amounts right around the end of the saccade (Fig. 18A). The median timing of discrimination was 29 ms earlier for perpendicular than

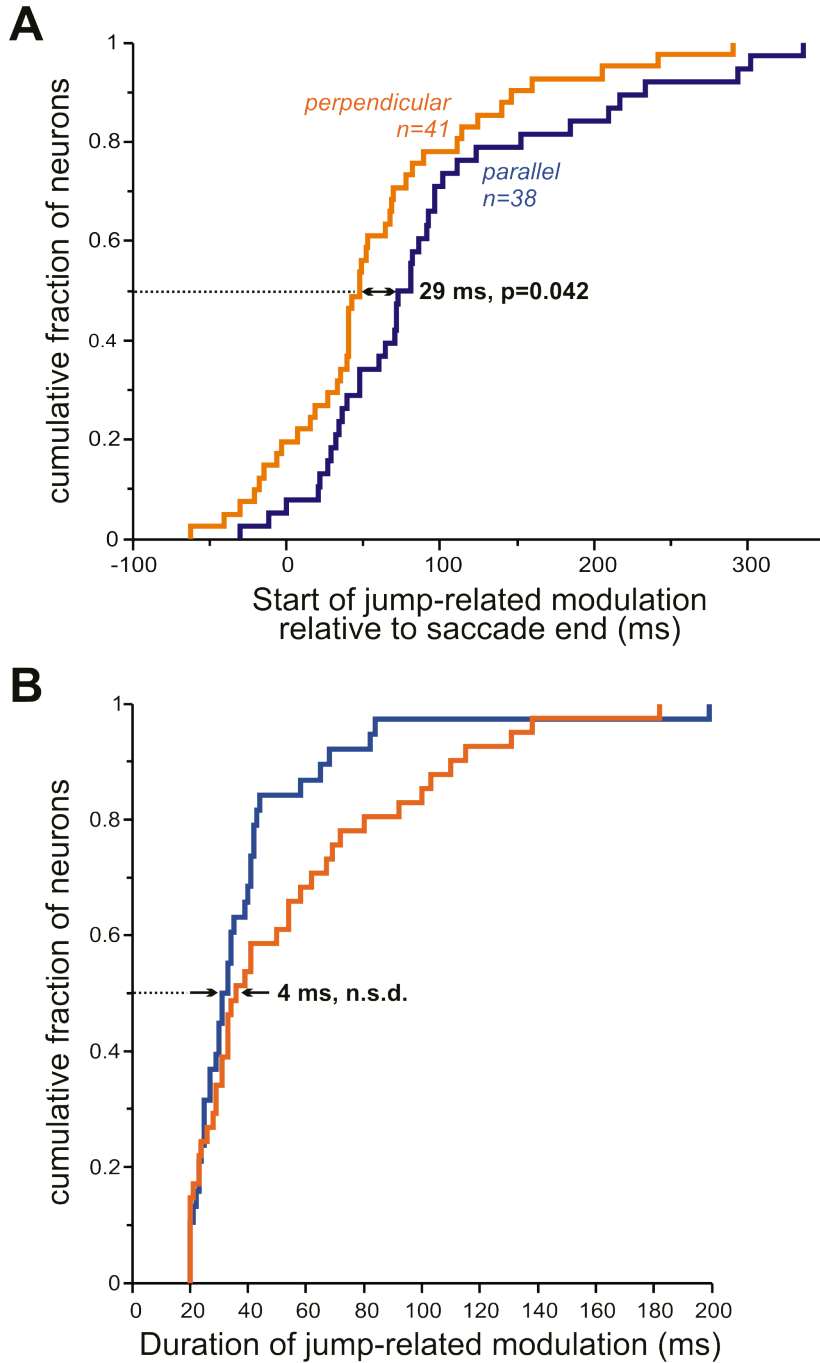


Figure 18. Temporal characteristics of translation tuning. A. Onset of significant tuning. The perpendicular subset of neurons began discriminating amongst the 4 translations some 29 ms earlier than

the parallel subset. This difference was significant. B. Duration of significant tuning. Once significant tuning began, the neurons remained modulated for about the same period of time (medians: 36 and 32 ms).

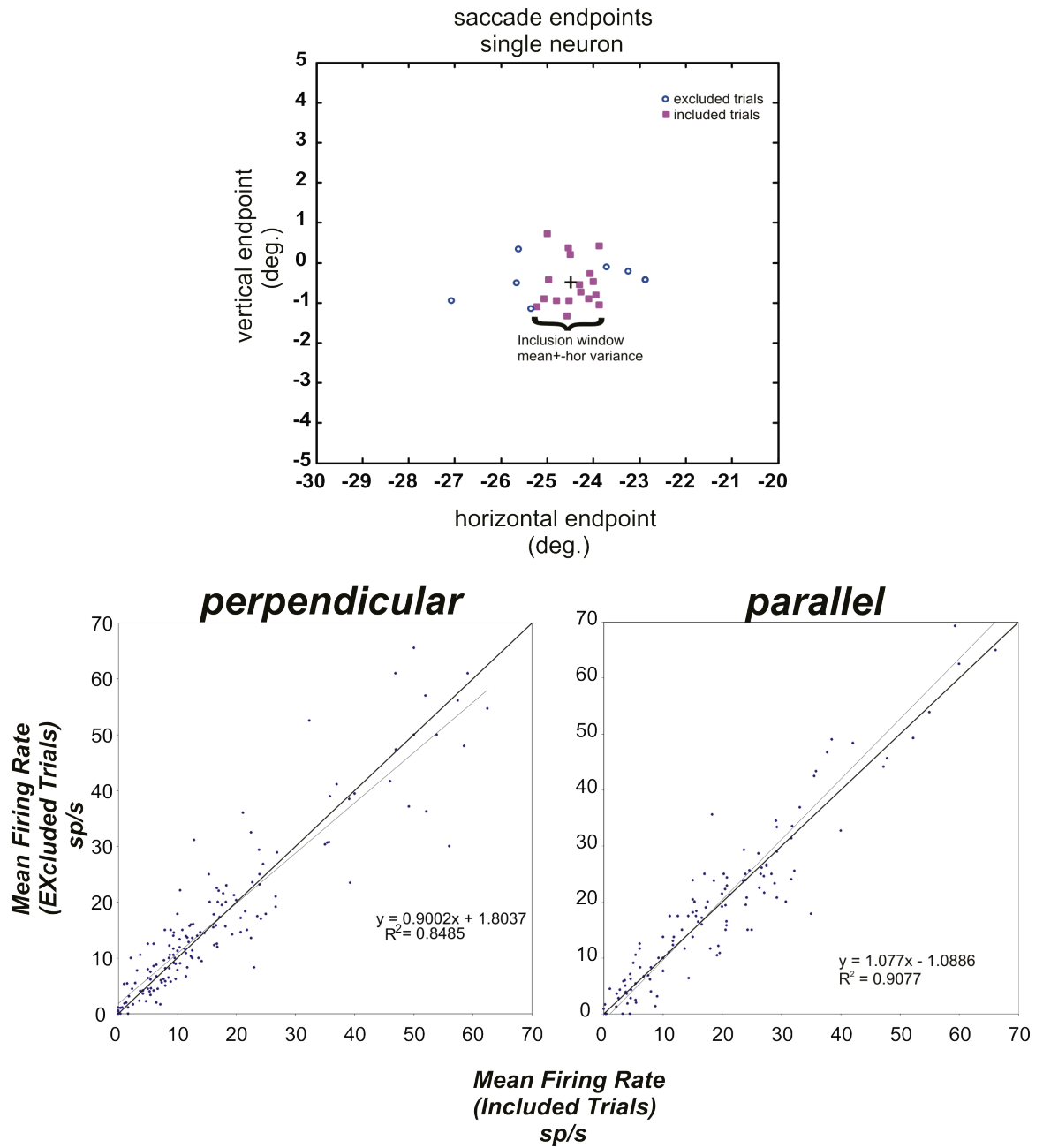


Figure 19. Saccadic endpoint analysis. Top: Single neuron example illustrating the procedure by which trials were separated into included and excluded trials. Bottom: Regressions performed on the perpendicular tested samples (left) and the parallel tested samples (right).

parallel translations (Mann-Whitney test, $p=0.042$). After the discriminations began, however, the length of time that they remained significant (Fig. 18B) was not significantly different between the two conditions (perpendicular, 36 ms; parallel, 32 ms; Mann-Whitney, $p=0.196$).

The general tuning differences found between parallel and perpendicular tested neurons could be due to the system's differing treatment of saccadic endpoint variability under the two conditions. Saccade endpoint variability tends to be greatest along the dimension of longest saccade amplitude. This variability has been suggested to interfere with the detection of parallel translating stimuli since failure of detection is often due to a deviation in the saccade landing point from the saccade target (Niemeier, et al. 2003). Does this account for the differences we observed? We tested this possibility by analyzing whether firing rate varies as a function of saccade endpoint. We parsed all saccade endpoints into two categories, corresponding to whether the saccade landed within a spatial window defined relative to the mean of the endpoints along the longest saccade dimension (Fig. 19). We then analyzed and compared the mean firing rates for trials included in this window and those excluded from this window. If saccade endpoint variability is causally involved in firing rate, then there should be a systematic difference in firing rate between those trials clustered around the center of mass and those distant from it. We found no difference between the two sets of firing rates, however. Linear regressions for both the parallel and perpendicular tested neurons were not significantly different from the unity line (Fig 19, bottom). This suggests that the system has an expectation of more noise in the parallel dimension, and it is this that affects the tuning, not the actual scatter of saccadic endpoints.

3.3.2 Translation tuning was not a passive mapping of the future field

An alternative hypothesis for the translation tunings might be that they represent an inadvertent mapping of the future field. That is, the tunings might reflect the various presaccadic locations of the probe, not their translations to the common postsaccadic location. We consider this highly unlikely because, as discussed below, translation tuning occurred whether or not a neuron was sensitive to stimuli in the future field (i.e. whether or not it remapped). But to test the alternative hypothesis directly, we recorded 28 neurons on a control version of the task that documented the RF tuning profile (Fig. 20 A,B), under the assumption that it is an adequate representation of the future field profile. For this task, the monkey simply fixated while the probe either appeared and remained stable in the center of the RF, or jumped into the center of the receptive field from 1 of 3 initial locations (6 deg, 12 deg, or 18 deg from RF center) that corresponded to typical jump distances in the future field during the saccade translation task. If the effect was an artifact of mapping the future field, then one would expect tuning in this control task to match that in the regular task. We saw little evidence of such a match. An example neuron had broad tuning in the control, fixation condition (Fig. 20C top), showing that the range of stimulus locations were well within the RF. In the regular task, it showed ramp-up tuning (Fig. 20C). For every neuron, we examined activity in a 100 ms epoch after the probe appeared in the fixation task and compared this to the reafferent activity found in the regular task. Curvature (Fig. 20D) and ramp (Fig. 20E) indices of the tunings

were calculated and compared between the two experimental conditions. There was no

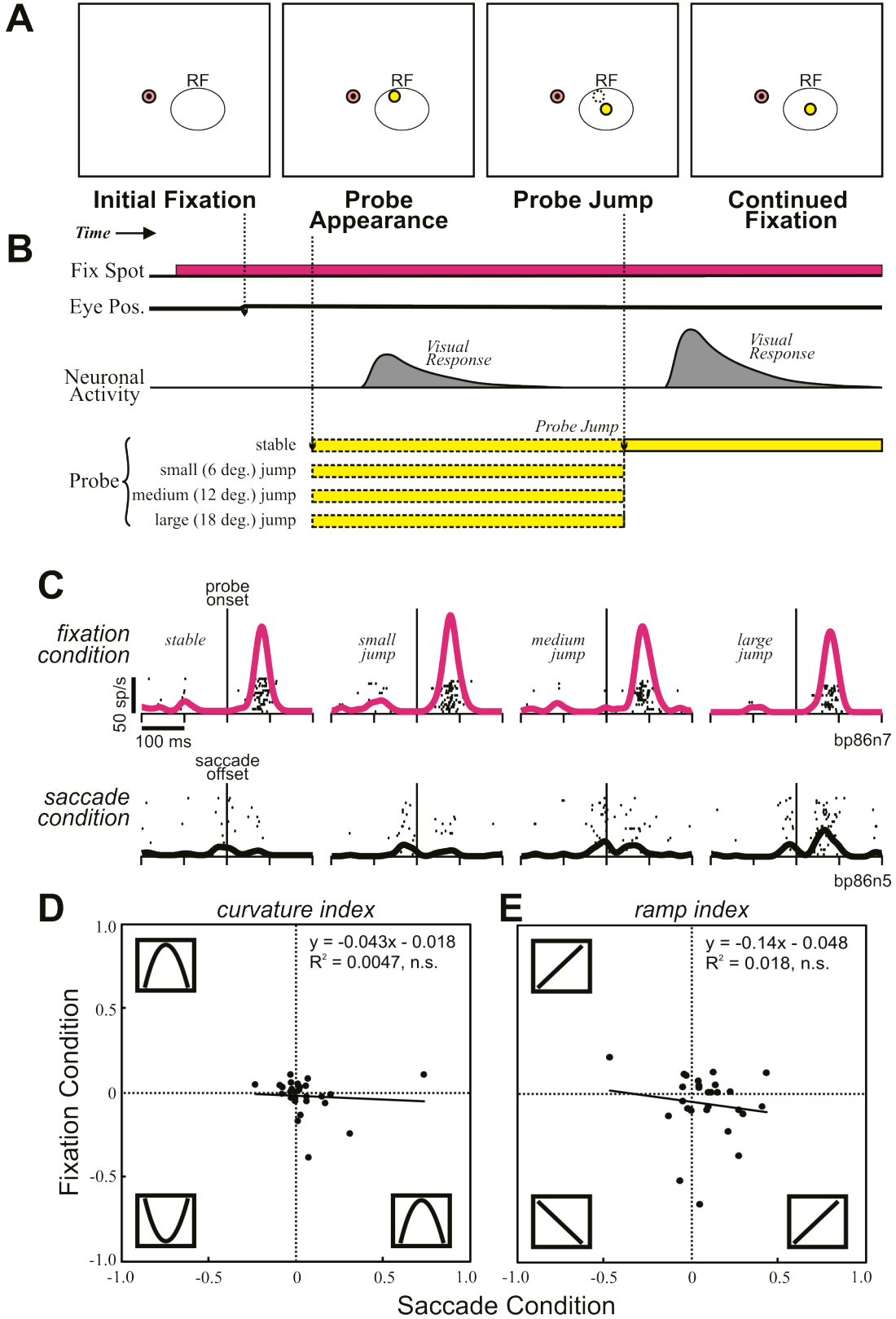


Figure 20. The RF mapping hypothesis. A. Fixation control task. The monkey began by fixating a spot of light. After a delay a probe appeared at one of 4 locations relative to the center of the neuron's RF. After a random period of time, the probe jumped to the center of the neuron's RF. B. Example neuron recorded during the fixation control task. This neuron fired robustly for each pre-jump probe placement and did not discriminate amongst the different probe positions. Data are aligned to pre-jump probe onset. C. Same example neuron as B tested on the saccadic version of the task. This neuron exhibited ramp-up tuning and was clearly able to discriminate amongst the 4 translation conditions. D. Fixation task curvature tuning as a function of saccadic task curvature. No correlation was found between the two conditions. E. Fixation task ramp tuning as a function of saccadic task ramp tuning. Again, similar to the curvature tuning, no relationship was found between the two test conditions.

significant correlation between the RF map and the transaccadic tuning map with respect to either the curvature index ($p = 0.73$) or the ramp index ($p=0.541$). These data suggest, therefore, that our translation tunings were not just static maps of future field geometry.

3.3.3 Translation tuning is not exclusive to neurons that remap

We examined whether translation tuning was a feature particular to neurons that engage in presaccadic remapping or, instead, a property common to all visually-responsive FEF neurons. We parsed our neurons into those that remap and those that do not using a conventional remapping task (Nakamura and Colby, 2002). Of 82 neurons tested, 31 remapped and 51 did not. Thirteen of the 31 remapping neurons (42%) were tuned for translations, but so were 15/51 (29%) of the more "normal", non-remapping neurons. While there was a trend for translation tuning to be associated with remapping, this was not significant (Chi-square, $p=0.358$). Hence translation tuning is not an exclusive property of neurons that show presaccadic remapping.

3.3.4 The neurons detect other transaccadic changes as well

So far we have shown that FEF neurons are sensitive to translations of a visual stimulus during a saccade. Are FEF neurons also sensitive to non-spatial changes that occur during a saccade? To answer this question we implemented a modified version of the saccadic translation task in which the probe remained in place yet underwent a featural change (in color, size, or both). As in our original task, the postsaccadic stimulus was the same in all conditions and should, in principle, elicit the same reafferent response; what varied was the presaccadic feature of the probe.

We tested 23 FEF neurons on the task and found that some were indeed sensitive to transaccadic featural changes. Two example neurons (Fig. 21A and B) showed a range of weak activity for the no-change, color change, and size change conditions. But both fired vigorously for the color +size change condition. We analyzed the data the same as for translation tuning, except that here the ranks were across types of feature change, not translation sizes. Of the 23 neurons, 16 showed a significant max-min difference when ranked from best to worst feature changes for eliciting a response. By far the best condition for evoking peak firing was the combined, color+size change (10/16 neurons). Ranked population data are illustrated in Fig. 21C. The data exhibited a tuning profile that dropped steadily with rank and was statistically different from the bootstrapped means and standard errors at all the non-optimal ranks. Therefore, while FEF neurons are sensitive to transaccadic spatial change, the effect may be a special case of a more

generalized capacity to detect any prominent change in a visual stimulus during a saccade.

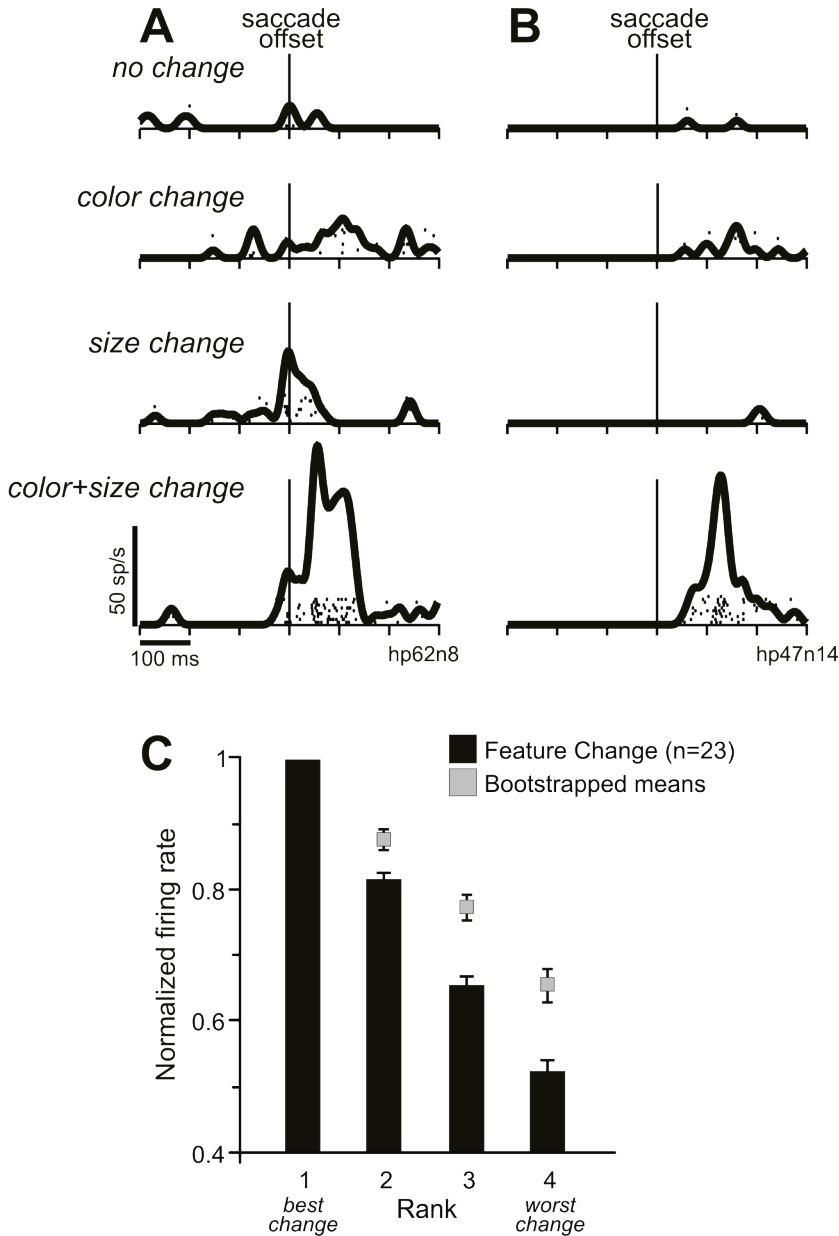


Figure 21. FEF responses to transaccadic featural changes. A. Example neurons. Each of these neurons fired very little for the control, color, and size changes, yet fired vigorously for the combined color/size changes. B. Ranked population. Similar to the translation data, the neurons were tuned for featural changes as evidenced by the steep decline in firing rate as a function of rank. These distributions were significantly different from the bootstrapped means.

3.4 Discussion

3.4.1 Overview

In this study we tested the hypothesis that FEF neurons perform a transaccadic comparison of the visual scene. Our major prediction was that neurons would report whether a visual stimulus moved during a saccade. We found that many FEF neurons were tuned for transaccadic translations of a visual stimulus, and that the tuning was more prevalent, stronger, and quicker for perpendicular than parallel translations. Surprisingly, translation tuning was found both in neurons that remapped and those that did not, and transaccadic change detection was not exclusive to translations, as the neurons could also report prominent featural changes.

3.4.2 The variety of translation tuning curves

We found that FEF neurons exhibit a wide range of translation tunings. Some had monotonically changing tuning curves, firing steadily more as translations increased or decreased (ramp tuning). Others were tuned for midrange jumps (curved tuning), or had tuning that was a hybrid of these two main tuning types. As a population, the neurons provided comprehensive information about spatial translations. Similarly diverse, thorough tuning profiles have been found in other areas of the primate visual system. Neurons in visual area MT, for example, may be tuned for low velocities, medium velocities, or high velocities of smooth motion (Liu and Newsome, 2003; Maunsell and

Van Essen, 1983; Perrone and Thiele, 2001). In short, all possible values of the sensory variable of interest – in the case of FEF, discontinuous movement during a saccade – are represented by the network as a whole. On a trial-by-trial basis, how information about a specific visual change is read out from the population response by downstream neurons is an area of active research and modeling (Pouget et al., 2000; Sanger, 2003)

3.4.3 A perpendicular translation tuning advantage

As a population, FEF neurons are better at detecting translations occurring perpendicular to the saccade vector than to those occurring parallel to it. This matches the perceptual finding that human subjects are better at detecting perpendicular than parallel stimulus translations relative to their saccades. A potential explanation for this perpendicular-preference effect at both the neuronal and psychophysical levels has been offered by a recent computational study (Niemeier et al., 2003). Using a Bayesian approach, Niemeier and colleagues found evidence that the oculomotor system seems to place varying weights on such variables as internal monitoring signals (i.e. corollary discharges) and visual input depending on the noise intrinsic to these two signals. For example, in the case of completely horizontal saccades, more variability or noise is found in the scatter of the saccadic endpoints along the horizontal than the vertical dimension. As such, the system attributes any discrepancy between the presaccadic and postsaccadic location of a stimulus that moves parallel to the saccade as due to motor noise, rather than to an actual change in the location of the visual stimulus. Accordingly, the actually translated stimulus is perceived as stable during the saccade. Stimuli that move perpendicular to the

saccade vector are more clearly perceived as moving; motor noise along that dimension is less, so an accordingly greater weight is placed on the visual discrepancy between the presaccadic and postsaccadic stimulus locations. Such computations could reasonably be occurring at the level of FEF neurons and may explain the perpendicular tuning bias we uncovered. Note that it is the expectation of less noise in the perpendicular direction that affects the tuning, not the actual scatter of the saccadic endpoints; when we controlled for differing scatter in the parallel and perpendicular directions, the tunings were still present, i.e. there was no difference in firing rate between included trials and excluded trials.

3.4.4 The future field mapping hypothesis

We interpret the translation tunings as being a transaccadic report of the translation vector, but we investigated the alternative hypothesis that they were a purely visual phenomenon. Varying the presaccadic location of a visual stimulus within the future field of a neuron was an essential feature of our task, so that the postsaccadic locations would all be identical, and we were careful to place all of the varying presaccadic locations entirely out of each neuron's RF. But conceivably, the varying locations could inadvertently "map" the future field. We see three lines of evidence against this alternative explanation. First, our fixation control task showed that translation tuning had little in common with the fundamental spatial profile of the individual neurons' RFs. Second, neurons with no explicit sensitivity to stimuli at the future field – i.e. those that failed to remap – still showed translation tuning. Third, a trivial mapping of the future field should result in exclusively ramp-down tuning, with highest activity for 0%

translation (stimulus at the future field center) and lower activity for larger translations (presaccadic locations further from the future field center). Yet we found myriad tuning shapes. The essential point is that FEF neurons generate a reafferent response to a postsaccadic stimulus that is a clear function of its immediate spatial history – whether it moved during the saccade, and by what amount and direction it did so.

3.4.5 A generalized change detection capability

We do not claim, however, that FEF neurons are specialized translation detectors. We found that they are also sensitive to featural changes across saccades. This part of the experiment was not exhaustive; further work is needed to elucidate the transaccadic featural tuning of FEF neurons. But our data do provide proof-of-principle. With spatial location held constant, the neurons reported changes in color or size, and especially the highly salient combined change, color + size. We think, therefore, that it is best to consider FEF neurons as performing a generalized comparison computation that determines if any aspect of the visual world, be it spatial or featural, changes during a saccade. Overall, the results are consistent with a notion that the neurons compute a type of prediction error (Crapse and Sommer, 2008c). Presaccadically, a prediction of the postsaccadic configuration of the scene is generated (presumably by neurons with shifting RFs) and then this signal is compared postsaccadically with the actual configuration (by the same neurons, or by non-shifting, downstream neurons that compare the pre- and postsaccadic signals). Any deviation from the predicted visual input is signaled as an error. The outcome of the comparison could be used widely in the visual

system for judging if the world is stable across saccades, for performing featural change detection across saccades (Irwin, 1991; Rensink, 2002), for maintaining calibration of the visual and oculomotor systems as required during development and following oculomotor trauma (Hopp and Fuchs, 2004), or for all these purposes.

Transsaccadic comparisons are necessarily limited by the biology of the visual system (Banks et al., 1991; Virsu and Rovamo, 1979). The future field is expected to have lower acuity than the RF, because it represents a more eccentric retinal location (the fovea-future field vector is the sum of the fovea-RF vector and the saccade vector) (Merigan and Katz, 1990). Models of comparison operations must take into account the fact that the future field and RF samples will never exactly match, even for an identical visual stimulus. But this caveat is not a limitation for detecting if a stimulus remains stable, or translates, during a saccade. The location of a stimulus can be reduced to its center of mass, which is the same whether viewed at low or high acuity. If a stimulus's center of mass differs in the presaccadic and postsaccadic samples, the stimulus translated; if it remains the same, the stimulus was stable. Detection of transsaccadic featural changes, though, would suffer. Color discrimination degrades rapidly with eccentricity (Nagy and Wolf, 1993), and size discrimination is aided by edge detection which degrades at lower acuity (Anstis, 1974). These factors may explain why neurons were poor at reporting color or size changes alone and responded vigorously only to highly salient, color + size changes in featural attributes.

3.4.6 Change detection is performed even by neurons without shifting RFs

To expand on a point mentioned above, we expected translation tuning to occur only in neurons that engage in presaccadic remapping. This was not the case: tuning was found as well in neurons that showed no evidence of remapping. It is clear how remapping neurons could compare the pre- and postsaccadic visual scene, since those individual neurons sample the same location in space before and after a saccade (Fig. 12). But how non-remappers detect transaccadic visual translation neurons is more mysterious. The presaccadic probe location is well beyond their classical RF and they never respond to its presence. A simple explanation would be that they use information that is provided by the remapping neurons. The shape of the tuning curve in non-remappers could be determined by the respective weights of the incoming synapses from upstream neurons that do remap. Another possibility is that tuning for transaccadic visual translation is not achieved by individual neurons, but is more of a network property. Proper modeling will be needed to study this, but a brief explanation could be as follows. Any stimulus is always at the center of the RF for some FEF neuron. During the saccade, a neuron with an RF that will encompass the stimulus's location postsaccadically could receive information from an FEF neuron that encompasses the presaccadic location of the stimulus. The recipient neuron could compute the error and, through its reafferent visual response, signal the difference. In general, we think that reafferent responses should not be considered an absolute representation of the stimulus in the postsaccadic RF. They are a differential representation of the stimulus relative to the presaccadic state of the same

stimulus. This concept predicts that FEF inhibitory neurons, which could prevent the two neurons from normally communicating, should pause at the time of a saccade to permit the presaccadic visual information to reach the recipient FEF neuron. Unpublished data from our laboratory has found evidence of such a pause in identified inhibitory interneurons of the FEF (Shin and Sommer, personal communication). More generally, all of these ideas are testable with computational and physiological methods.

3.4.7 Conclusion

Our overall hypothesis was that cerebral cortical neurons might help to disambiguate sudden translations of a visual image by taking into account both visual and corollary discharge information. We tested this by examining if single cortical neurons are indeed capable of reporting transaccadic visual jumps. FEF neurons clearly provide such a report with a myriad of translation tunings. The result supports our hypothesis, but is not exclusive to it; the tuning could be useful for many purposes including calibration of the visual and oculomotor systems. And more broadly, FEF neurons detect changes in features as well as spatial location. FEF neurons are remarkably sensitive to the relationship between visual arrangements of objects and the eye movements that threaten to disrupt the accurate perception of those objects.

4.0 Frontal eye field activity predicts performance in a visual stability judgment task

4.1 Introduction

A long-standing question of cognitive neuroscience is how the brain generates a cohesive representation of the world. The problem is difficult because sensory processing itself is a non-trivial process given the welter of sensory inputs with which the brain must contend. Movements of sensory organs compound this problem further. Vision, for example, is disrupted some 2-3 times per second by rapid saccadic eye movements. These movements cause a wholesale displacement of the visual image to occur across the retina. Such artifactual motion is not perceived, however. Yet under some circumstances, actual movements of objects occurring during saccades are detected (Deubel et al., 1996; Li and Matin, 1990). This implies that the brain possesses a mechanism for disambiguating real retinal motion from artifactual retinal motion due to the saccade itself. According to some theories, the brain maintains a transaccadic record of the visual scene that it assesses upon completion of the saccade. If the presaccadic record matches the postsaccadic scene, then the world is perceived as stable; if they differ, something must have changed during the saccade (Deubel et al., 1998; Sommer and Wurtz, 2008a; Wurtz, 2008).

Evidence for such a comparison operation has recently been uncovered in the frontal eye field (FEF), a cortical area involved in cognitive aspects of visual perception and eye movement control (Crapse and Sommer, in preparation). FEF neurons were found to be responsive to translations as well as featural changes to visual probes that

occurred during saccades. Such signals could be utilized by the animal for judging whether the world is stable across saccades. In that study, however, the probes were task-irrelevant, so it remained unknown whether the error “change” signals had any influence on the monkey’s perception.

In the present study, therefore, we recorded from FEF neurons in monkeys trained to report whether the visual scene stayed stable, or moved, during saccades. Our hypothesis, motivated by the previous work, was that FEF neuronal activity would signal changes occurring to a visual scene and predict the animal’s perceptual judgment of visual stability. Our first goal was to verify whether monkeys, while making saccades, are able to distinguish true displacement of an external visual stimulus from saccade-induced apparent displacement. We found that the animals were adept at this judgment, so our second goal was to see if the performance was predicted by visual responses of FEF neurons. The results demonstrated a striking attention-like effect in which visual responses were strongly modulated in trials when the animal reported movement of the stimulus. The effect occurred not only at the time of a behavioral report, but also during earlier saccades of the same trial. These results show that neuronal mechanisms are in place within the FEF for detecting if the visual scene moves during saccades, and that monkeys seem to access and use this information.

4.2 Methods

4.2.1 Surgery and region identification

In two monkeys (*Macaca mulatta*) we implanted scleral search coils for measuring eye position, recording chambers for accessing FEF, and a post for immobilizing the head during recording experiments. Details may be found in prior reports (Sommer and Wurtz, 2000). All procedures were approved by the University of Pittsburgh Institutional Animal Care and Use Committee. The location of the left FEF was determined stereotaxically in each monkey (25A, 20L) and verified by physiological means: the recording of saccade related neurons and the evocation of saccades at $< 50 \mu\text{A}$ threshold (Bruce and Goldberg, 1985).

4.2.2 Behavior

4.2.2.1 Visual stability judgment task

The central task of the study was a visual stability judgment paradigm (Fig. 22), the purpose of which was to determine whether monkeys can discriminate whether a peripheral visual stimulus remains stable, or intrasaccadically jumps to a new location, as they make scanning saccades. The monkey faced a tangent screen onto which visual stimuli were projected by an LCD projector (ViewSonic PJ550) and in some experiments, lasers (LDM115, Global Laser Technology). A trial began with the

appearance of two spots, always provided by the LCD projector, positioned near the center of the screen but 28 deg. apart (shown as white spots in Fig. 22A, left). These stimuli were white 10 x 10 pixel squares. The monkey fixated either of the spots (black dot in Fig. 22A, left) and began making scanning saccades between them (Fig. 22A, second from left). Little training was involved for this aspect of the task, as monkeys scan between spots readily (Sommer 1994; Sommer 1997). During recording sessions, the arrangement of the two fixation spots was adjusted if necessary to always keep both spots out of a neuron's receptive field. Also presented at the start of a trial was a peripheral visual probe, provided either by the LCD projector or a laser (shown as a yellow spot, Fig. 22A left). The probe was a green 20 x 20 pixel square if provided by the projector or a red ~ 1 deg. dot if provided by the laser. The probe remained stationary on the screen at one of several possible "pre-jump" locations: 0.5, 1.0, 2.0, 3.0, 5.0, or 10.0 deg. from a constant, final "post-jump" location. During purely behavioral sessions the post-jump location was typically 15 deg. above or below the left fixation spot; during recording sessions it was at the center of the receptive field relative to one of the fixation spots. Two permutations of probe jump direction were used: either perpendicular or parallel to the saccade vector (Fig. 22A shows a parallel jump).

As the monkeys scanned between the fixation spots in the presence of the pre-jump probe, one of the scanning saccades triggered the probe to step to its post-jump location (Fig. 22A, second from right). For a given recording session, the trigger saccade was chosen randomly (uniform distribution) as the 3rd to 9th leftward or rightward scanning saccade. Whether it was selected from the sequence of leftward or rightward

directed saccades was based on RF geometry; once selected, the direction of trigger saccade (leftward or rightward) remained fixed for the entire session.

The crucial task of the monkey was to report when the probe moved. It did this by ceasing its scan and making an immediate saccade to the probe within 500 ms after termination of the trigger saccade (Fig. 22A, right). Such a response was a “hit”, for which it was rewarded with two drops of water. If it continued scanning (a “miss”) or if it made a saccade to the probe before it moved (a “false alarm”), the trial ended with no reward delivery. Furthermore, for false alarms the monkey was penalized with a 2 second time-out.

4.2.2.2 Other tasks

In recording sessions, we first mapped the center of the receptive field and characterized the fundamental properties of single neuron activity (e.g. presence of visual responses) using several oculomotor tasks as described in detail elsewhere (Crapse and Sommer, 2009). In all tasks the monkey was required to fixate a spot projected onto the center of the screen. Then, with timings that depended on task contingency, the monkey was required to execute an appropriate saccade for a liquid reward. The critical task for screening neurons was the memory-guided saccade task. A monkey fixated a spot for 500-800 ms, a target flashed in the response field for 50 ms, and the monkey was required to maintain fixation. After a 500-1000 ms delay period, the fixation spot disappeared which was the cue to move. The monkey made a saccade to the remembered target location and received reward 500 ms later. If the neuron exhibited visual activity in

the memory-guided task (see Crapse and Sommer 2009 for analysis details) we had the monkey perform the visual stability judgment task.

4.2.3 Physiology

We recorded only well-isolated FEF units with tungsten microelectrodes (FHC; typical impedances: 1000-2000 k Ω). Electrodes were inserted through a guide tube positioned by a grid system (Crist et al., 1988). All behavioral and neural events were monitored in real-time by a personal computer running a QNX-based real time experimentation data acquisition system (REX, developed at the Laboratory of Sensorimotor Research at the NEI, NIH; Hays et al., 1982). A second computer ran custom software that permitted separation of action potential waveforms with use of spatial windowing (MEX system, also developed at the LSR

4.2.4 Data Analysis

4.2.4.1 Behavior

To quantify performance we computed d' , where $d' = z(\text{Hit Rate}) - z(\text{False Alarm Rate})$. The parameter $z()$ refers to the calculation of a z score. Psychometric functions were fit to the behavioral data with use of the `nlinfit` function in Matlab. Other analyses involved standard parametric and non-parametric statistical tests, described as the data are presented, using a criterion of $p < 0.05$.

4.2.4.2 Neurons

We had several goals for analysis. Primarily we studied the reafferent visual response, i.e. the neuronal activity elicited when a saccade moves a receptive field onto a visual stimulus. First we wanted to determine if a neuron's reafferent response following probe translation was tuned for degree of probe translation and also if it differed depending on whether the monkey correctly detected the change with a report saccade. For this analysis, we analyzed the mean firing rates occurring in a 125 ms epoch spanning from 75 ms to 200 ms relative to the end of the trigger saccade; this epoch was deemed optimal based on inspection of the trigger saccade-aligned population spike density functions.

Our second goal was to determine if neuronal activity occurring earlier in the trial, prior to the trigger saccade, predicted the outcome of the trial (i.e. commission of a hit, miss, or false alarm). To determine this, we analyzed neuronal activity in a 200 ms epoch time locked to the end of the t-2 saccade, i.e. the saccade 2 saccades prior to trigger saccade "t". This epoch was chosen based on inspection of the t-2 saccade aligned population spike density functions. For those trials in which the monkey ultimately committed a false alarm, t represents the scanning saccade immediately preceding the saccade launched to the probe in error. In terms of the visual stimulation and motor acts, all the t-2 data were the same (for a given pre-jump probe location); specifically, all the reafferent responses should be identical.

Our final goal was to assess for correlations between visual activity and saccadic reaction time. We limited this analysis to significant, purely visual neurons, since the

motor-related responses of visuomovement neurons can obscure signals related to purely visual activity. To ascertain reafferent response latency, we performed a poisson burst analysis on single hit trials aligned to the end of the trigger saccade (Hanes et al., 1995). To minimize noise in the measurements, each neuron had to possess at least 10 trials per translation condition that exhibited a burst of activity. This selective criterion resulted in the subsequent analysis of only the 3 deg, 5 deg, and 10 deg translation conditions, since the monkeys typically achieve more hits for these conditions. To test for a within-condition correlation between latency and reaction time, we chose the 10 deg condition as an example and separated all trials for a given neuron into two categories corresponding to short and long reaction times (similar to Hanes and Schall, 1996). We then performed a t-test on the distribution of means to assess whether the two distributions were significantly different. To test for an across condition correlation between latency and reaction time we pooled the two categories for each translation condition and performed an ANOVA across the translation conditions. A similar procedure was performed for assessing the differences between reaction time and time of peak response.

4.3 Results

4.3.1 Behavior

To test if monkeys can discriminate artifactual motion of a visual stimulus from real stimulus motion we had them perform the visual stability judgment task (Figure 22A). For this task, the monkey made alternating saccades between two stationary visual stimuli. After a random number of scanning saccades, on the “trigger saccade”, a stimulus present on the screen throughout the trial translated to a new position. The

animal was tasked to report its percept of the change by quickly making a saccade to the stimulus, in which case a “hit” occurred (Fig.22B&C, left). The trial would otherwise end as a “miss” if the monkey failed to saccade to the stimulus (Fig 22 B&C, right). If they looked at the stimulus before it moved, the trial was a “false alarm”.

Both monkeys were adept at the task. An example trial is shown in Figure 22B,C, and pooled behavioral data are illustrated in Figure 23. The figure relates two salient findings, using measures of Percent Correct (above) and d' (below). First, performance improved as a function of probe translation amount. The monkeys performed near threshold (d' near zero) for the smallest intrasaccadic movement of the probe (0.5 deg translation) but did very well (~90% correct, $\sim d' = 4.5$) for the largest (10 deg.) translation, and their behavior improved smoothly between those points. Second, the monkeys detected perpendicular translations better than parallel translations. For the majority of the data points shown in Figure 23 (8/12 points), performance for the perpendicular condition was significantly better than for the parallel condition (t-tests, $p < .05$). A detection advantage for perpendicular visual displacement is consistent with findings from human psychophysical studies (Niemeier, Crawford et al. 2003) and with the transaccadic translation tuning of FEF neurons (Crapse and Sommer, submitted).

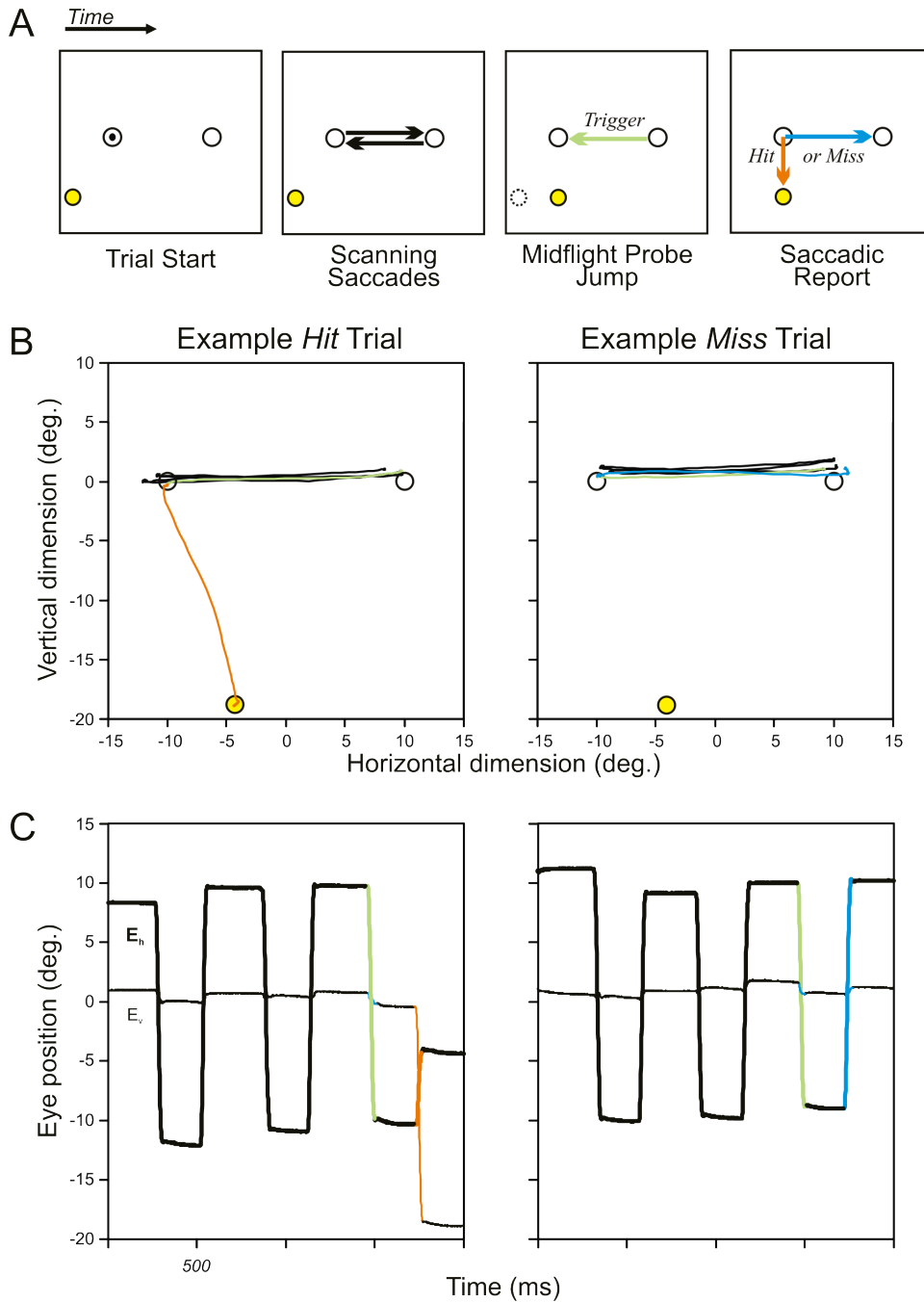


Figure 22. The visual stability judgment task. A. The monkey is tasked to make spontaneous scanning saccades between two constantly illuminated targets. After a random number of saccades, a visual probe (yellow) present in the periphery translates by a particular amount. To obtain a liquid reward, the monkey must quickly make a saccade to the translated probe to indicate its percept of the translation. B & C Eye traces depicting performance in the task. Left column: A successful trial in which the monkey correctly detected the translation. Right column: An unsuccessful trial in which the probe was undetected.

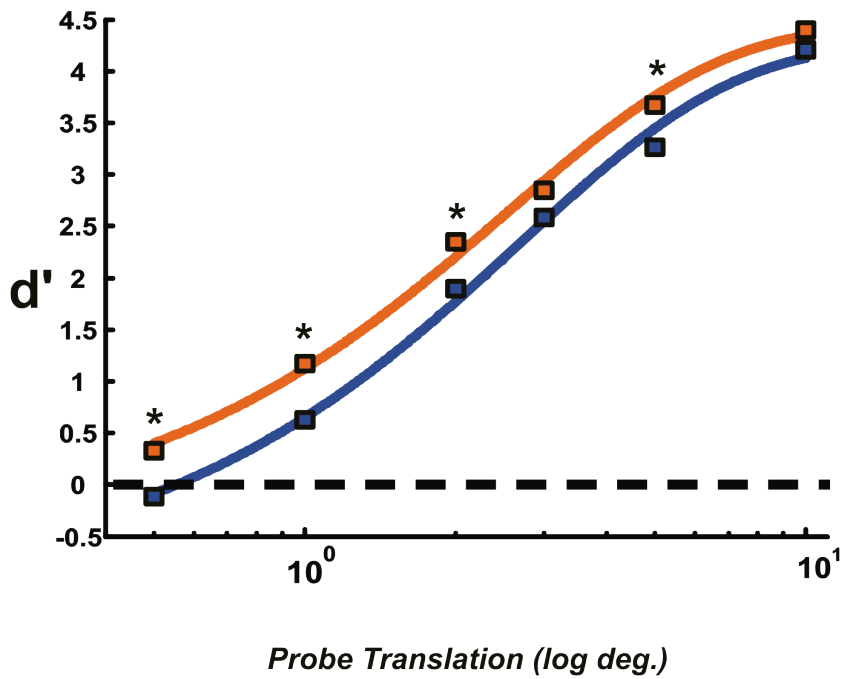
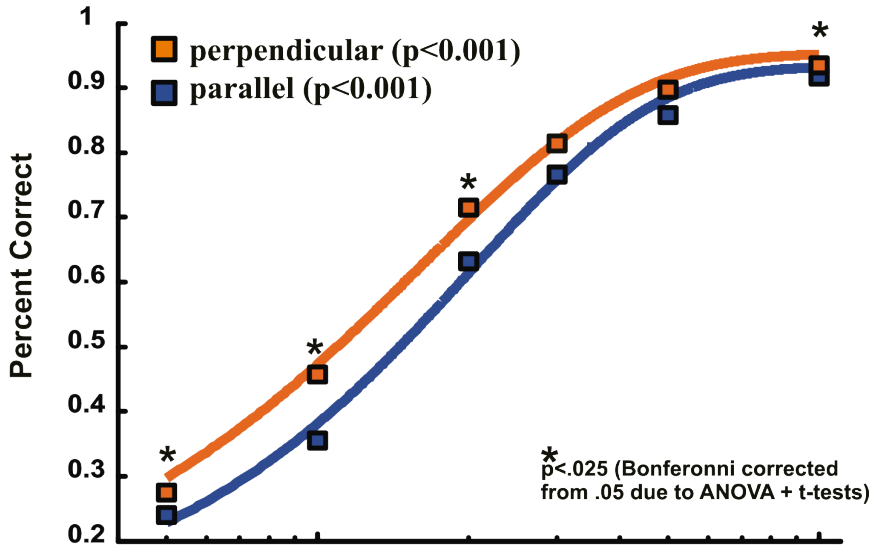


Figure 23. Behavioral Performance. Top: Percent correct for both the perpendicular and parallel conditions is depicted as a function of probe translation amount. Bottom: Psychometric functions representing d' as a function of probe translation.

Hit reaction times

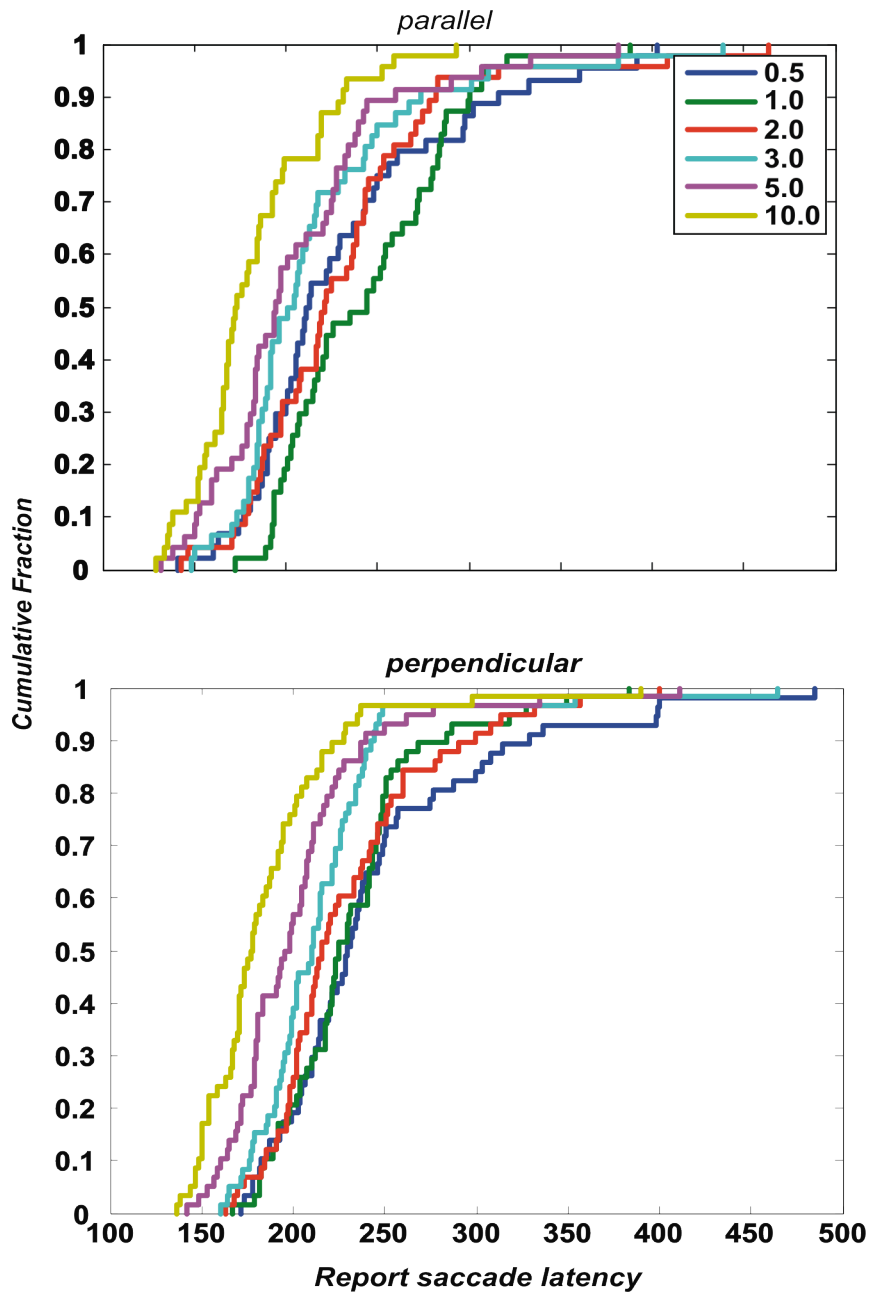


Figure 24. Reaction time distributions. Top: Parallel condition. Generally, reaction times were inversely correlated with translation amount, the larger the translation, the shorter the reaction time. Bottom: Perpendicular condition. Same general trend.

We next examined the distribution of reaction times for hit saccades. The hit reaction time is defined as the time following completion of the trigger saccade (i.e. the saccade during which the probe changed locations) to the initiation of the report saccade to the probe. Results are depicted in Figure 24: the larger the translation, the shorter the reaction time (Kruskal-Wallis, $p < 0.001$). The results were similar for both the perpendicular (Fig. 24A) and parallel conditions (Fig. 24B). We also compared the perpendicular and parallel reaction times for each individual probe translation to see if the perpendicular translation detection advantage was accompanied by a reaction time advantage, but no differences were found.

As might be noticeable in the example scanning patterns of Fig. 22B, the endpoints of scanning saccades could differ slightly in hit and miss trials. We quantitatively analyzed the scanning saccade endpoints for hit, miss, and false alarm trials, and found that scanning saccades were slightly but significantly hypometric on miss trials relative to hit and false alarm trials (by an average of 0.3 deg., not shown, $p = 0.002$, Kruskal-Wallis). No differences were found between the saccade endpoints for hits and false alarms. As addressed in the Discussion, we think the slight hypometricity on miss trials was related to premature planning of the next (oppositely directed) scanning saccade, causing foreshortening due to collision (Becker and Jurgens, 1979; McPeck and Keller, 2001).

4.3.2 Neurons

4.3.2.1 On hit trials, frontal eye field neurons are tuned for translations

To test if FEF neural activity is correlated with behavioral performance we recorded from 70 visual and visuomovement neurons while monkeys performed the visual stability task. In previous work we found that FEF visual reafferent responses were tuned for translations. We were interested therefore in examining whether reafferent visual responses generated within the context of the scanning task were similarly tuned. An ANOVA analysis on correct (hit) trials found that 34 of the 70 neurons (49%) were significantly tuned for translations. Activity for an example neuron with significant tuning is depicted in Figure 25. This particular neuron, representative of the larger population, exhibited a monotonic increase in firing rate as a function of translation amount, firing modestly for the smallest translation (0.5 deg, top) and vigorously for the 10 deg translation (bottom). Population results for the tuned subset is represented in Figure 26. For hit trials, the population shows a monotonic increase in firing rate as a function of translation tuning (Fig. 26A). For miss trials, no tuning was apparent (Fig 26B). As a population therefore, the neurons can discriminate amongst the translations on hit trials, and report the degree of error between the presaccadic and postsaccadic stimulus positions. A significant difference was also present between the hit and miss conditions across each translation condition, indicating that the neurons are also correlated with the monkeys' choice (Fig. 26C). The results reveal that FEF activity is modulated as a function of translation amount, and further is correlated with whether a moving probe is detected at the behavioral level.

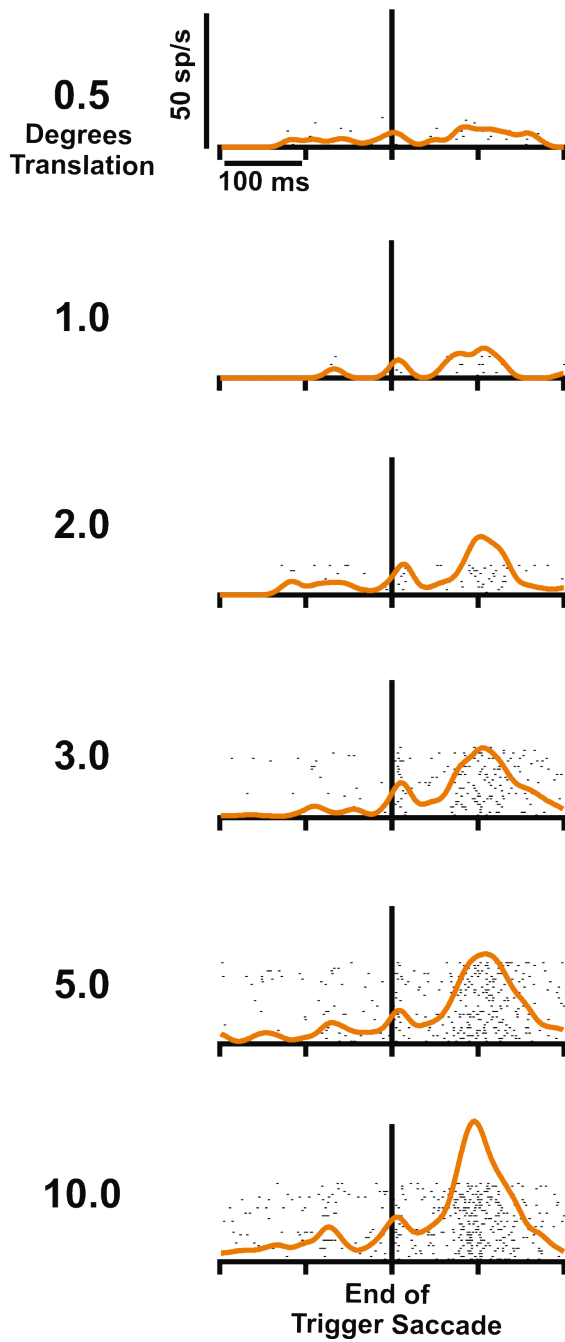


Figure 25. Spike density functions for an example neuron. This particular neuron exhibited pronounced tuning for translations.

A subset of the neurons in the significant population (16/34) had saccade-related activity, i.e. visuomovement neurons in the terminology of Bruce and Goldberg (1985). Hence the observed differences between the hit and miss trials may have been caused by

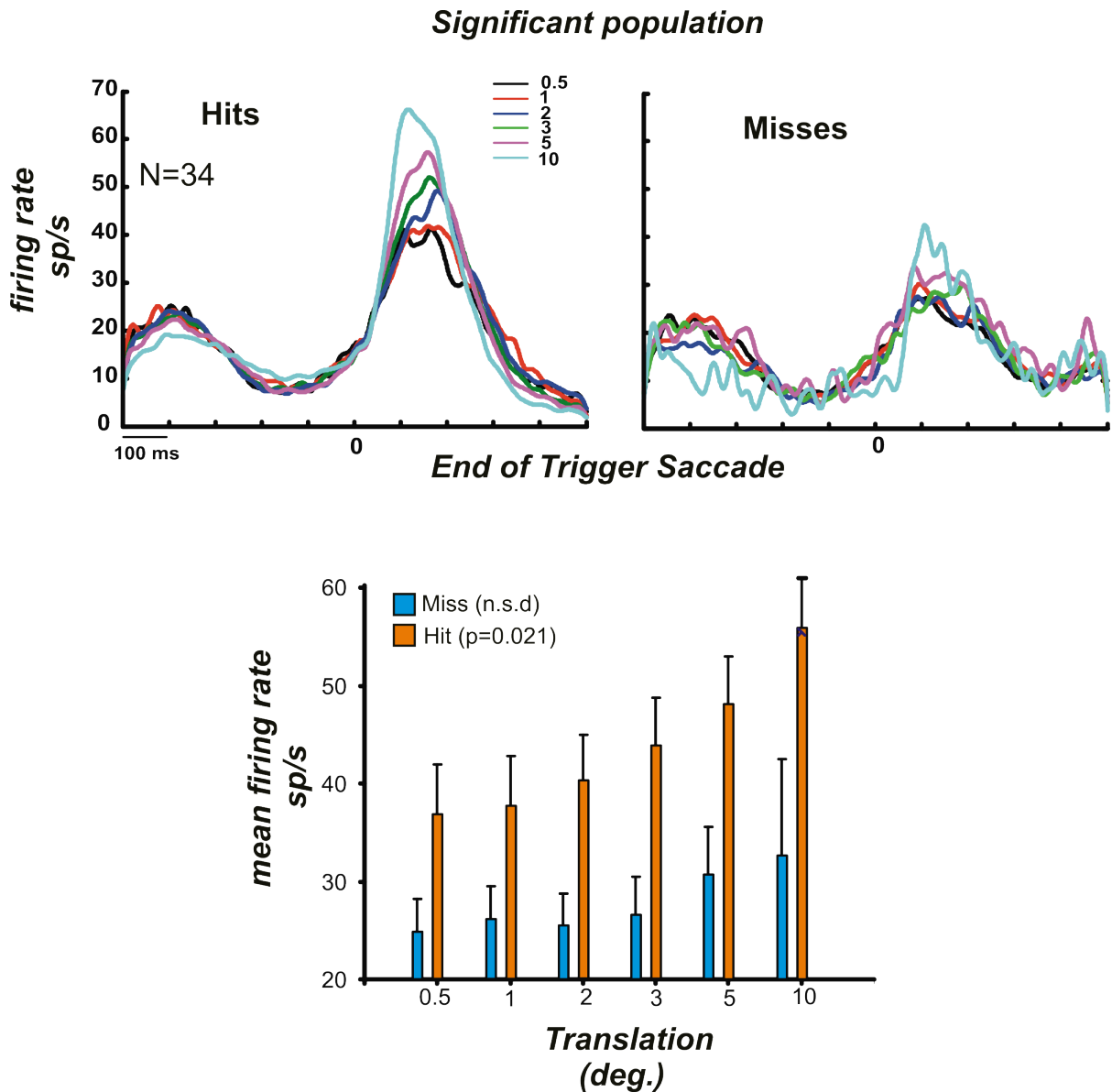


Figure 26. Neuronal Population. Top, left: Population sdfs for all hit trials from the significant subset of neurons. Top, right: Population sdfs for all miss trials from the significant subset. Bottom: Summary of firing rate differences between Hit and Miss trials.

activity associated with the report saccade launched into the movement field. We examined this issue in two ways. First, we performed the same analyses on the subset of neurons that lacked saccade-related activity (“visual” neurons of Bruce and Goldberg, 1985). An example of one such neuron in the memory-guided task is shown in Fig. 27B; it had a visual response but no saccade-related activity. In the visual stability task (Fig.

27A), it had a larger reafferent visual response on hit than miss trials (2 deg. translation condition shown). Figure 27 C&D shows the population data for the entire subset of 18 significantly tuned, visual neurons. The result was similar to that in the entire significant population (cf. Fig. 26A&B).

4.3.2.2 Early trial activity is predictive of psychophysical performance

The second analysis involved circumventing the issue by examining reafferent responses when the subsequent saccade was exactly the same – a scanning saccade back to the fixation spot. We studied the activity two saccades prior to final saccade of the trial, t (i.e. the trigger saccade on hit and miss trials, or in the case of false alarms, the last scanning saccade before the premature saccade to the probe; see methods). Early trial data from the same neuron and trial condition depicted in Figure 27A is represented in Figure 28A (2 deg. translation condition shown). This neuron’s reafferent visual response on the $t-2$ saccade clearly predicted whether the monkey, two saccades later, would commit a miss or make a saccade to the probe, either correctly (hit) or incorrectly (false alarm). Similar results were found for many of the translation conditions in the population (Figure 28B).

The shape of the tunings across hits, false alarms, and misses as a function of translation amount was remarkable (Fig. 28B). Because these data were collected two saccades before the probe jump, “translation amount” here actually means “pre-jump

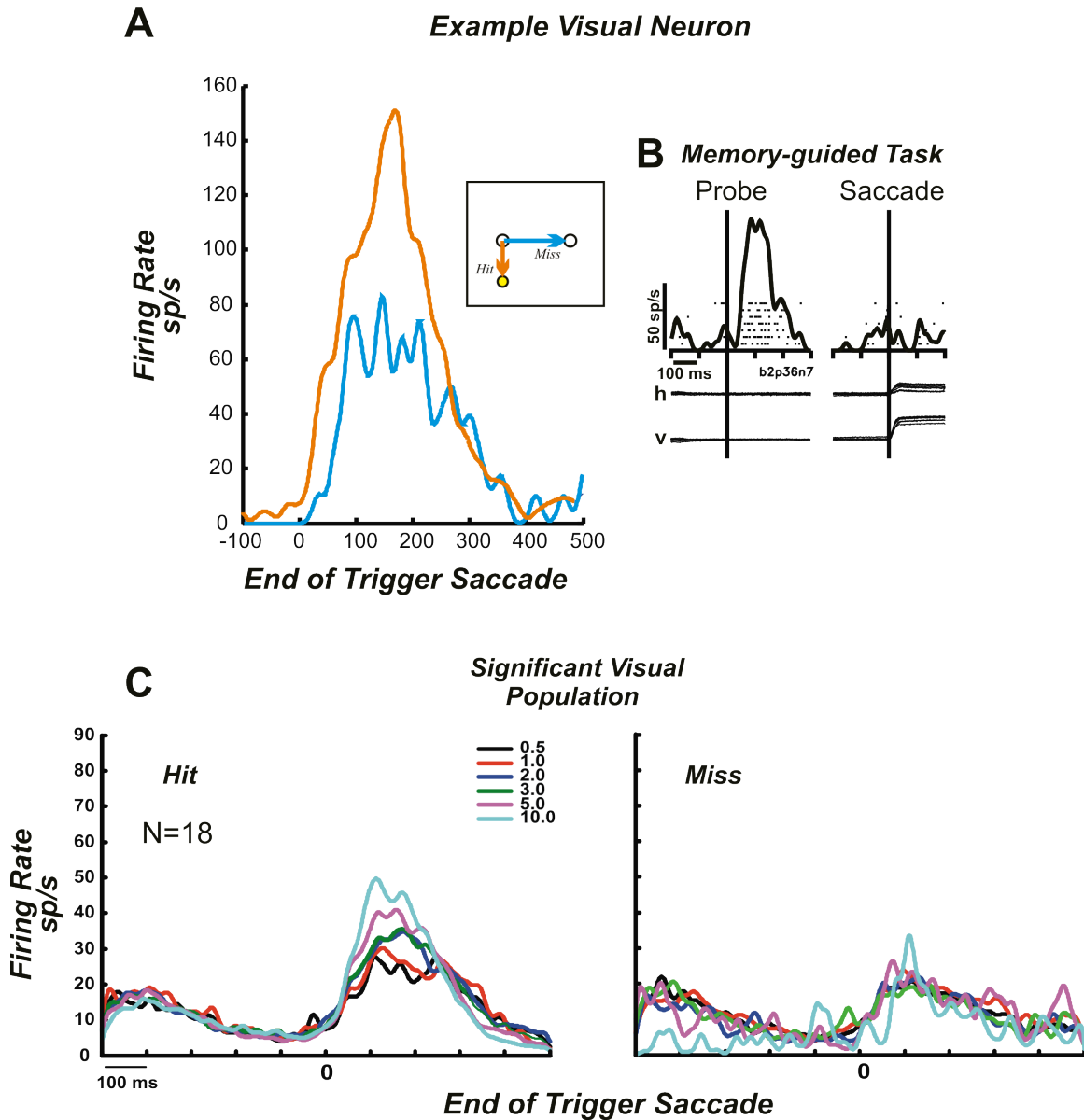


Figure 27. Visual neuron response profiles. A. Example visual neuron responses on 2 deg. hit (orange) and 2 deg. miss trials (blue). B. Demonstration of purely visual nature of the neuron depicted in panel A. C. Significant visual population. Left, Population sdfs for all hit trials. Right, Same but for Miss trials.

probe location” relative to the receptive field center. If monkeys eventually made a hit or false alarm, the reafferent activities were strong and flat across the range of pre-jump probe locations, dropping off only for probes around 10 deg. from the receptive field

center. The simplest explanation is that, as monkeys scanned, they attended to the probe much more in trials that culminated in hits and false alarms. For trials that eventually

Early Trial Activity

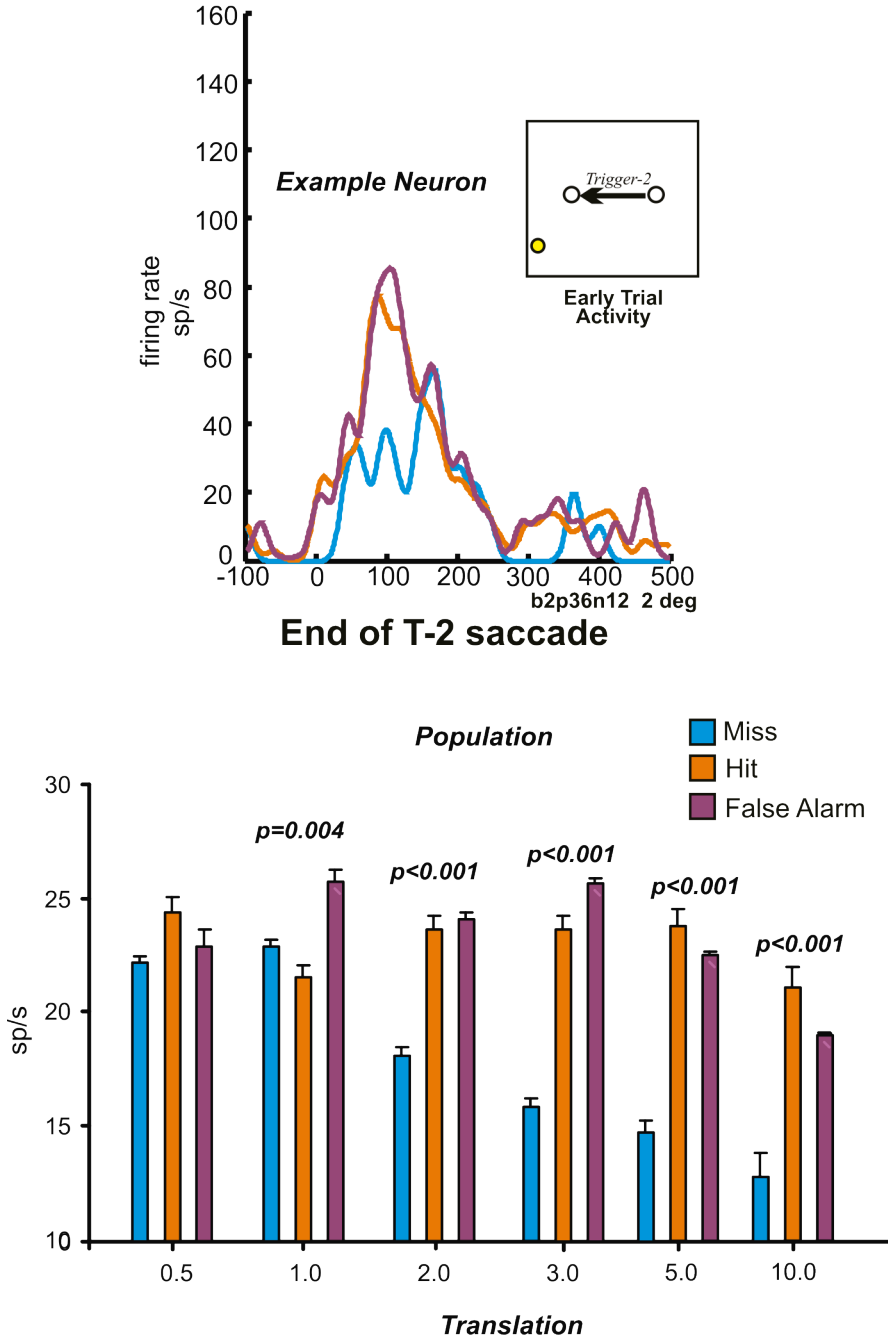


Figure 28. Early trial activity is predictive of monkey psychophysical performance. Top: Activity profiles for an example neuron during the 2 deg translation condition. Shown are spike density functions aligned to the end of the trigger-2 saccade, i.e. two saccades prior to a miss (blue), hit (orange), or false alarm (purple). Bottom: Population results as a function of translation condition.

ended in a miss, activity progressively declined as a function of pre-jump probe location, with the 0.5 probe position (nearly at receptive field center) eliciting maximum activity, and the 10 deg probe position (far from receptive field center) eliciting the least activity. In other words, on miss trials, the varying pre-jump locations simply mapped the radial profile of the receptive field.

Our final reafferent response analysis searched for relationships between visual neuronal activity and behavioral reaction time. Specifically, we focused on reafferent visual response latency and peak reafferent response time, and asked if either of these parameters were correlated with the reaction time distributions of the report saccades. We found first that the neurons all began signaling the different translations at about the same time (~95 ms). Next, we assessed the degree to which time of peak correlated with reaction time. An example neuron with a session's worth of 10 deg translation trials sorted according to short and long reaction times is depicted in Figure 29A. Despite equivalent onset latencies (green and blue arrows), the shorter reaction time average (blue sdfs) reached peak magnitude significantly earlier than the longer reaction time average (green sdfs), a finding reflected in the 10 deg. translation population (Figure 29B). This result also extended across translation conditions (Fig 29C). Despite equivalent latencies, the neurons reached peak magnitude at times that were correlated with reaction time; the earlier the peak, the faster the reaction time.

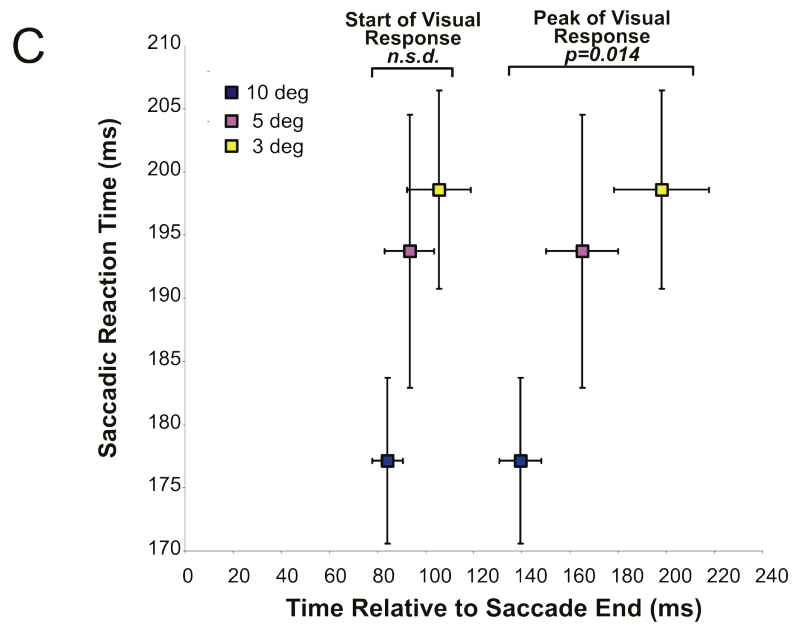
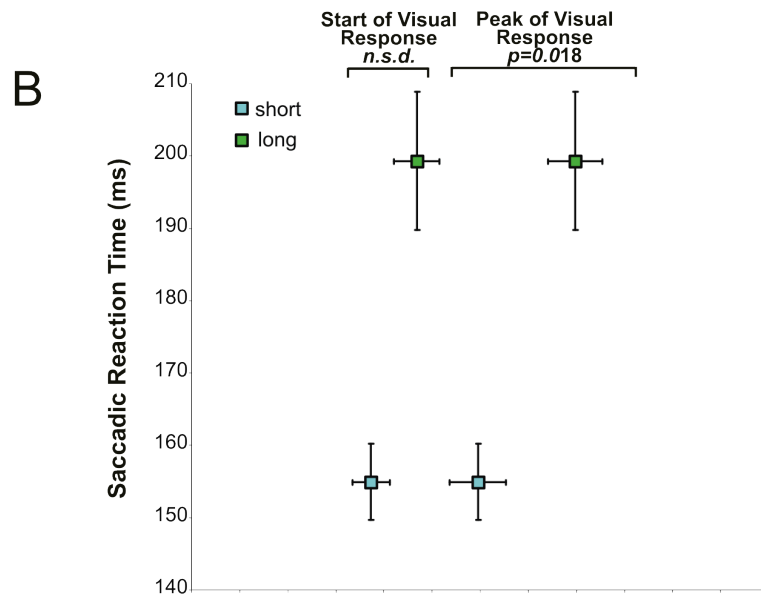
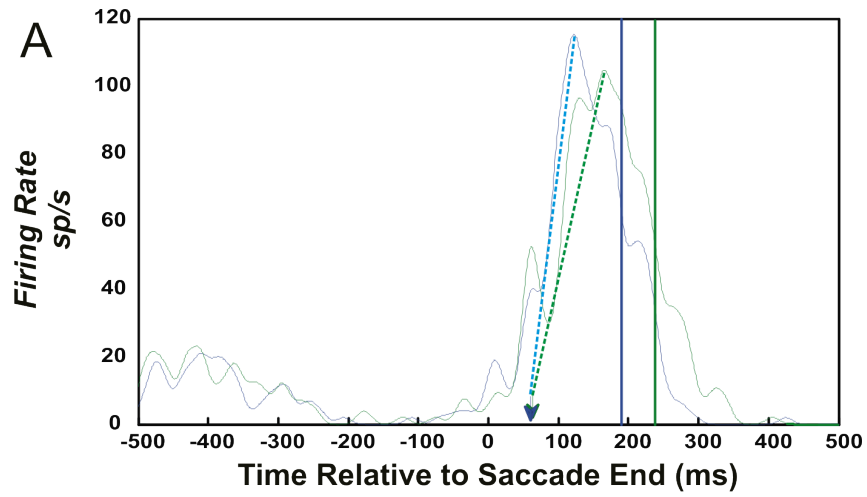


Figure 29. Reaction time is correlated with time of peak firing rate. A. Trials sorted according to reaction time (blue=short; green=long) for an example neuron during the 10 deg translation condition. Arrows represent mean latency per subset; vertical bars represent mean time of saccadic report for each subset. B. Ten degree translation condition data for the entire population sorted according to short and long reaction times. Shown are mean visual response latencies as a function of mean reaction time, and mean peak visual response times as a function of mean reaction time. C. Population results for the 3 deg (yellow), 5 deg (red), and 10 deg (blue) translation conditions. Same conventions as panel B, save the short and long reaction time trials for each condition have been pooled for cross condition comparison. Error bars represent standard error of the mean.

4.4 Discussion

4.4.1 Overview

Our previous work showed that FEF neurons are able to detect whether a stimulus remains stable, or moves, across saccades (Crapse and Sommer, in preparation). Two questions remained open: whether monkeys, similar to their neurons, could make accurate judgments about the stability of the world, and whether FEF activity predicts a monkey's ability to report whether a scene is stable across saccades. The data reported here answered both questions in the affirmative, supporting our overall hypothesis that FEF neurons contribute to disambiguating visual movement from visual stability during saccades.

4.4.2 Monkeys distinguish true displacement of a visual stimulus from illusory, saccade-induced displacement.

Behaviorally, we found that monkeys are clearly able to make accurate perceptual judgments about the transaccadic stability of the world. This implies that monkeys enjoy

a stable visual world not unlike that experienced by humans. This had been assumed, of course, but to our knowledge had not been explicitly demonstrated. Our data indicate that the ability of monkeys to distinguish stable scenes from intrasaccadically displaced scenes is similar to the ability in humans. Early human psychophysical work had suggested that subjects are largely blind to translations that occur to visual stimuli during saccades, a phenomenon known as saccadic suppression of stimulus displacement (SSD). Bridgeman and colleagues found, for example, that for a translation to be perceptible, the translation had to be at least 30% of the total saccade amplitude (Bridgeman et al., 1975). A later study examining SSD, however, found that thresholds for detecting probe displacements were on the order of $1/10^{\text{th}}$ of saccade amplitude (Li and Matin, 1997; Li and Matin, 1990). Trained monkeys seem to do even better; we found thresholds around 1 deg., which is about $1/20^{\text{th}}$ of the (trigger) saccade amplitude. We do not know why the sensitivity of our monkeys is better than the reported results for humans. The monkeys were probably more motivated and were definitely better trained than any human subjects, but there could be phylogenetic reasons as well.

4.4.3 Perpendicular translations are more salient than parallel translations

We found that translations occurring perpendicular to the saccade vector were more salient to the monkeys than parallel translations as evidenced by the greater performance on this configuration. These results are consistent with and were predicted by our earlier physiological work. In that study, we found that FEF neurons that reported stimulus translations were most sensitive to translations that occurred perpendicular to the saccade

vector. The result is also consistent with data from human psychophysics. Crawford and colleagues found that human subjects are better at detecting translations that occur perpendicular to the saccade vector than those that occur parallel to the saccade vector. The difference may be due to the fact that there is more saccadic endpoint variability along the dimension parallel to the saccade vector. As such, the system may ascribe any jitter in a probe's position to motor noise rather than to a discrepancy in the probe's physical location. Probes that move perpendicular to the saccade vector, on the other hand, are more perceptible due to the minimal motor noise along this dimension. Consequently, the system correctly assigns any discrepancy in the presaccadic and postsaccadic positions to genuine differences in physical location.

4.4.4 Reaction times are inversely proportional to translation amount

A reaction time advantage was observed for larger probe translations across both parallel and perpendicular conditions. The median reaction time for reporting 10.0 degree translations was about 170 ms, while the median reaction time for 0.5 degree translations was around 220 ms, a drastic difference of some 50 ms. These differences were mirrored by differences in neuronal peak response time. The neurons peaked earlier for earlier reaction times within a condition and showed a similar pattern across conditions. These results suggest that time of peak activation plays a causal role in the timing of saccade onset.

These reaction time effects may be interpreted with an evidence accumulation model (e.g. Gold and Shadlen, 2007). For larger translations, the probe jump is most

salient and the evidence accordingly stronger than for smaller translations where the jump is less salient and the evidence weaker. These differences translate into rates of accumulation that vary as a function of evidential strength and are ultimately expressed as differences in reaction time. Similar reaction time differences as a function of task difficulty have been noted across a variety of psychophysical tasks e.g. (Roitman and Shadlen, 2002).

4.4.5 FEF reafferent responses represent prediction error

At the neuronal level, we found that FEF reafferent responses were monotonically tuned for translation amount: the greater the presaccadic-postsaccadic mismatch, the larger the reafferent response. This suggests that the system sets up an expectation at the time of a saccade and evaluates at the end of the saccade how well the expectation was met. These responses are therefore similar to the prediction error signals that have been uncovered throughout the primate reward system (Schultz and Dickinson, 2000). Theoretical studies had long postulated that predictive signaling occurs throughout the brain in a range of different contexts (Friston and Price, 2001; Mumford, 1992; Rao and Ballard, 1999). Here we show evidence for predictive computations at the single neuronal level in the context of a task that integrates action with vision.

We found similar error signals in an earlier study. There, we tested the basic hypothesis that FEF neurons were sensitive to intrasaccadic alterations of visual stimuli. In that study, we manipulated probes while monkeys made single saccades. Similar to this study, the neurons were found to be tuned for translations, but with one poignant

exception: the neurons together exhibited a range of different tuning curve shapes, not just the monotonically increasing functions we observe here. For example, some of the neurons fired maximally for intermediate translations, while others fired most for the smallest translations. The cause of the discrepancy is likely to reside in the fact that in that study the probe was task-irrelevant; the monkey did not have to regard to probe for proper task performance. As such, the monkeys allocated little, if any, attention to the probe. As our current results demonstrate, attentional allocation can have remarkable effects on the reafferent responses of FEF neurons. Attention, therefore, is the most likely reason for the discrepancy.

4.4.6 Monkey performance is predicted by an attention-like elevation of reafferent visual responses

In addition to translation tuning, we found generally that trigger saccade-aligned neuronal activity was significantly greater on hit trials compared to miss trials, despite identical retinal stimulation. The principal difference between the two outcomes is that for hit trials a saccade is immediately launched into the neuron's visual receptive field. On miss trials such a saccade does not occur, instead the monkey continues saccading between the two scan targets, apparently oblivious to the probe change. It is a well known fact of visual neuron physiology that responses to visual stimulation are enhanced if attention is directed to the region, or if a saccade is launched into the response field (Burman and Segraves, 1994; Bushnell et al., 1981; Goldberg and Bushnell, 1981; Goldberg and

Wurtz, 1972). Overt ignoring of the stimulus, or failure of detection results in minimal activity. Such an explanation is the likely cause of the difference we observe.

Surprisingly, we found that early activity in each trial betrayed whether the monkey would eventually make a miss or a hit/false alarm. The early (t-2 saccade) reafferent responses for hits and false alarms trials strong and flat across the pre-translation probe positions despite the fact that retinal stimulation differed dramatically for those different positions. This contrasts with the early reafferent responses in miss trials. Those reafferent responses appeared to represent simple, passive stimulation, resulting in a straightforward "mapping" of the RF radius with the differing pre-jump probe locations. This implication is that the monkeys were not attending well to the probe during miss trials, a finding further supported by our saccade endpoint data. Saccades were generally hypometric for miss trials, suggesting that the monkeys were more involved in planning the next scanning saccade than keeping track of the translation probe. In contrast, on hit and false alarm trials, the monkeys seem to have been attending to the probe quite intensively, which would explain the "flat" tuning profiles for early reafferent responses. Attentional allocation seemed to either move or expand to keep track of the pre-translation probe location over its wide range.

Most cases of attentional modulation result in an elevation of a neuron's firing rate with little to no change in RF width or location. Such responses are said to be multiplicative since they involve a simple change in gain that results only in a scaled alteration of tuning curve height. Our data reveal the workings of non-multiplicative modulation since the spatial structure of the neurons' RFs seems to be altered. Similar instances of non-multiplicative modulation have been documented in areas V4 and MT

(Connor et al., 1996; Womelsdorf et al., 2006; Womelsdorf et al., 2008). These studies found that attention shifts the RF toward the attended location and narrows the width of the spatial tuning curve. In MT, Womelsdorf et al found that the RFs typically shift by 3.0 degrees of visual angle, or 22% of the neuron's RF diameter. Our data suggest that during attentional allocation of the pre-translation probe FEF RFs are shifting or expanding by as much as 5-10 degrees of visual angle. Given the typical width of FEF RFs, the relative shift of the RF is consistent with the values found in area MT during attentional allocation.

4.4.7 Conclusion

These results support the hypothesis that monkeys can reliably discriminate between artifactual motion of a stimulus, the default scenario occurring with each saccade, and actual motion of a stimulus. FEF activity encodes the dimensions of the stimulus motion and is predictive of monkey performance. The data support our general hypothesis that behaving monkeys rely on FEF activity for judging the stability of visual images across saccades.

5.0 General Discussion

5.1 Overview

The purpose of the experiments described in the previous chapters was to achieve a better understanding of FEF perisaccadic computations by testing various hypotheses as to how they mediate a percept of visual stability. Chapter 2 was an attempt to identify a pathway by which FEF shifting RFs gain access to ipsilateral visual signals and ipsiversive eye movement signals, prerequisites for omni-directional shift capability. To address this question we implanted stimulating electrodes in each SC and searched the FEF for neurons we could drive orthodromically from the SC. We found populations of neurons that were drivable from the opposite-SC, same-side SC, or both, and uncovered a striking structure-function relationship: the laterality of an FEF response field was largely predicted by the laterality of the SC from which it received input. Each FEF therefore receives information about all of visual space, and saccades made to points within it, a prerequisite for omni-directional shifting RFs. Such subcortically derived pathways may mediate also the remarkable visuomotor capabilities that survive transection of the corpus callosum.

In chapter 3 we set out to test a long-standing hypothesis regarding the mechanism by which receptive field shifting contributes to visual stability. This hypothesis posits that shifters perform a comparison operation whereby the similarities between presaccadic and postsaccadic data samples are measured. According to the theory, the presaccadic sample serves as a prediction and may set in motion various

corrective processes throughout the rest of the brain. The postsaccadic sample serves as confirmation, an indication as to whether the prediction was correct. We tested this hypothesis by recording from FEF neurons while monkeys performed a task in which a behaviorally-irrelevant probe changed along some spatio-featural dimension during a saccade. For the comparison hypothesis to be true, the neurons should signal these changes, as it would indicate a discrepancy between presaccadic prediction and postsaccadic confirmation. We found that FEF neurons are sensitive to spatial as well as featural changes that occur to stimuli during saccades. Surprisingly, change detection capabilities were found even in neurons without measurable shifting RFs. These results indicate that the FEF is a generalized change detector and contains signals that may be used by the visuosaccadic system for oculomotor calibration and for generating a stable visual percept. Whether these signals are used by the behaving animal was the question addressed by the third and final study (chapter 4).

In chapter 4 we attempted to bridge the neuron-behavior gap by recording from FEF visual neurons while monkeys performed a visual-stability judgment task that required them to explicitly report their percept. The monkeys were tasked to identify an intrasaccadic probe change as they made scanning saccades between two targets. Given the chapter 3 results, we predicted that FEF activity would be correlated with monkey psychophysical performance. We found just that. The visual reafferent responses matched psychophysical performance, and early trial activity was often predictive of whether the animal would ultimately commit a miss, hit, or false alarm. These data suggest that monkeys rely on FEF activity for judging whether the visual world is stable across saccades.

Together, these results provide a window into the neural events that occur in the FEF around the time of a saccade: (1) Just before a saccade of any direction or amplitude, the appropriate corollary discharge arrives from either the left or right SC and impinges upon a network of FEF visual neurons, thereby apprising them of an imminent change in gaze. (2) Some of these neurons shift and collect data about what will fall in their RFs after the saccade. Other neurons, without shifting RFs, may communicate this same information to one another via horizontal connections. (3) Once the saccade is completed, a measurement is made between the predicted sample and the actual sample. (4) The outcome of the comparison is encoded in the strength of the reafferent visual response. (5) Mismatch signals are useful to the animal, and alert it to the change; the animal responds with an action after a reaction time directly proportional to the latency of the peak of the mismatch signal.

Many intriguing questions remain. We have yet to conclusively establish how shift signals actually influence the rest of the brain and assist in the construction of a stable visual world. What we know is that FEF neurons are sensitive to changes that occur to a scene during saccades, the outcome of a putative comparison process between presaccadic predictions and postsaccadic tests. But what role does the initial presaccadic prediction play in visual stability? To be of any functional utility it must be exported in some form or another to other brain areas, particularly to those extrastriate areas that directly mediate visual perception. Currently, we possess no data or theory to account for predictive shifting-FEF-interareal interactions. In this final chapter I will propose a theoretical account of perisaccadic FEF signaling, speculate about the computations that are being performed around the time of a saccade, and describe a role that they might

play in guiding the actions of posterior visual areas. Spatial visual perception seems to be mediated by these posterior areas, so it would seem that a pre-emptive interaction between the FEF and the posterior areas is necessitated for spatially-corrective vision. I will cast this discussion in terms of prediction, as it is my contention that predictive processes, enabled by shifting RFs, are implemented in the FEF and play a critical role in constructing a stable percept despite saccadic eye movements. I will begin by making the case that predictive processes are important for proper neural function generally and are a ubiquitous phenomenon found throughout the nervous system. I will then follow with a detailed description of my visual stabilization theory.

5.2 A large-scale theory of visual stability

5.2.1 Prediction and the brain

A host of computational and recording studies suggest that the brain engages in predictive computations, both in the motor and sensory systems (Bar, 2007; Bullier, 2001; Engel et al., 2001; Friston, 2005; Gilbert and Sigman, 2007; Hamker, 2005; Hwang and Shadmehr, 2005; Lee, 2002; Miall and Wolpert, 1996; Mumford, 1992; Roelfsema et al., 2000). Hierarchical models of the visual system, for example, suggest that visual cortical neurons fire predominately to signal deviations from predicted inputs (Lee and Mumford, 2003; Rao and Ballard, 1999). The predicted inputs are imposed upon lower levels of the hierarchy by feedback projections from higher levels. The lower areas spike only when the predicted input differs from the actual input. This residual or prediction

error is then forwarded to the next level. Recurrent iterative cycles continue until prediction error is minimized and the image is sufficiently determined. Predictive coding of this sort is thought to mediate functional purposes such as figure/ground segmentation, extraclassical RF effects, and the resolution of ambiguous stimuli (Fenske et al., 2006; Hupe et al., 1998; Kleinschmidt et al., 1998).

Studies in the motor realm suggest that predictions are also utilized for the purpose of adaptive control of the skeletomotor system (Hwang and Shadmehr, 2005; Miall and Wolpert, 1996). Skeletomotor movements can be amazingly fast and complex. They require feedback control. But often feedback is too slow to be of any use. Psychophysical and computational studies indicate that the motor system implements forward and internal models of the mechanics of the skeletomotor system and the dynamics of its interaction with the surrounding workspace. Such implementations escape the problem of delay and noise and provide fast motor solutions through predictive control processes. In short, predictive processes pervade the brain. Here I propose that predictive operations for both the sensory and motor domains find unification in the primate visuosaccadic system for the purpose of constructing a stable transaccadic percept.

5.2.2 A prediction map in primate FEF

I propose that shifting neurons of the FEF are components of a larger FEF inferential architecture that engages in predictive coding, that is, the FEF is a prediction map. This scheme assigns a causal role to the FEF in the construction of a stable visual percept

despite saccadic interruptions. According to this conception, predictions of the future (postsaccadic) scene are generated based upon predictive extrapolations from the current (presaccadic) scene. Neurons with shifting RFs, apprised spatiotemporally of the imminent change in gaze by CD, collect data about what will fall in their RF after the saccade. These data are then convolved with causal estimates of an internal model of the visual world. What follows is a prediction of the visual structure of the postsaccadic scene. These predictions are proposed to be exported perisaccadically from the FEF to the posterior lobes via feedback projections. The visual lobes are primed with activity-constraining expectations. Deviations from the predicted inputs (prediction errors) are calculated by the FEF (and potentially other areas) from information about the actual postsaccadic outcome. The prediction errors therefore are ultimately manifest in the visual responses of FEF neurons. This is consistent with the error signals uncovered in the experiments of chapter 3. These residuals alert the FEF to unpredicted events. This may entail calibration/updating if the error is related to a miscalculation/noise or it may provide useful information about the environment that was unexpected, i.e. perhaps something moved or suddenly appeared. Either way, it is hypothesized that a result of the iterative signaling is the perception of a stable world despite the change in gaze. There are certain conditions that must be satisfied for the FEF to plausibly assume this computational role. I will review them now.

First, to generate predictions the FEF would need information about the entire visual field. The FEF has this information. As the experiments in chapter 2 revealed, it receives information about all of visual space, not just the contralateral hemifield. In addition to this subcortically-derived route, the FEF receives dense topographically

organized projections from both the dorsal and ventral visual streams (Schall et al., 1995b). Second, the FEF would need to sample across the map with great speed. This is especially important for both the quick generation of postsaccadic predictions and for their rapid assessment. The presence of neurons with shifting RFs as well as the small size of the FEF map (~100 mm²) should facilitate single FEF neurons to sample across the map and acquire information about any part of the visual scene with relative ease. Another important element is that the RFs of FEF neurons are relatively large. They can occupy ranges from 20 to 30 deg. (Bruce and Goldberg, 1985). This grants single FEF neurons access to a large portion of the visual image. Moreover, the visual responses of FEF neurons are also generally insensitive to primary visual attributes such as orientation (Mohler et al., 1973). This should help FEF neurons to serve as general-purpose analyzers of the visual scene and speak in a featureless language that can be imposed back upon the more specifically tuned compartments of the various visual areas. Finally, the FEF has access to precisely timed saccadic information in the form of corollary discharges (Sommer and Wurtz, 2004a, b). The corollary discharges provide motor context that assist spatiotemporally in the perisaccadic predictive computations of the FEF network.

FEF neurons also possess more sophisticated functions that could assist in the operations of a perisaccadic prediction map, namely, they have the capacity for visual inference. The work of Schall and colleagues reveals the inferential powers of FEF neurons, particularly in the context of a salience map (Schall, 2002; Thompson and Bichot, 2005). As demonstrated through target selection tasks, the FEF neurons come to selectively represent the most salient objects in the visual scene. They do so after an

initial inferential process by which the identity and salience of the object is determined. This inferential process undoubtedly involves processing with the posterior lobes via reciprocal connections, an important feature exploited by the postulated prediction map. The Schallian salience map applies to a single scene or fixation. It, in other words, applies only to the salient contents of the presaccadic scene. The prediction map builds a bridge between the presaccadic and postsaccadic scenes by updating in a predictable and stable manner the postsaccadic locations of salient objects.

5.2.3 Computational basis of the prediction map

Computationally, the prediction map could be grounded in an inferential process based on empirical Bayes. Numerous studies indicate that neurons throughout the brain from the SC to the prefrontal cortex engage in probabilistic and inferential computations (Gold and Shadlen, 2007). Much of what the brain does has to be probabilistic given the noise and ambiguity intrinsic to neural computation (Barlow, 2001; Knill and Pouget, 2004). With Bayesian inference, prior and conditional probability distributions are utilized to generate a posterior distribution, i.e. the outcome expected on the balance of known probabilities and other inputs (in other words, a prediction). For the case of a single saccade, the proposed Bayesian computation would express the conditional expectation or probability of observing the postsaccadic scene (p) given the relative probability of two independent pieces of evidence: the visual structure of the current scene (c), and various saccadic parameters (s), written:

$$P(p|c,s) = \frac{P(c|p)P(s|p)P(p)}{P(c)P(s)} = \lambda_p$$

Bayesian priors about the structure of the visual scene $P(c)$ and how the world behaves during a saccade $P(s)$ could be learned and updated through experience and stored in FEF networks. The conditional expectation λ_p would be convolved with a generative model Ψ to generate a prediction of the postsaccadic scene $\Psi(\lambda_p)$. The prediction would be compared with the actual input λ_a to yield a prediction error $\varepsilon = \lambda_a - \Psi(\lambda_p)$.

5.2.4 Physiological mechanism of the prediction map

Mechanistically, frontal modulatory control of the posterior lobes could be implemented through imposed patterns of synchronization mediated by cortico-cortical connections (Siegel et al., 2000; von Stein et al., 2000; Womelsdorf et al., 2007). Studies indicate that visually-evoked activity of single neurons is surprisingly quite deterministic (Arieli et al., 1996). The oft-encountered variability in single neuron responses emerges from the dynamics of ongoing network activity. This fact could be exploited by the prediction map for purposes of ensuring transsaccadic perception. The imposed predictions could alter the spatio-temporal properties of visual cortical network activity and thereby influence the specific visually-evoked responses that are ultimately integrated into the network and expressed as spikes. The FEF would initiate a specific synchronization pattern among the relevant visual neurons (those activated by features of the current scene) and this would serve to amplify behaviorally relevant signals and attenuate spatially disruptive signals in the cortex.

5.2.5 The sequence of events

A detailed account of what I propose occurs during every voluntary saccade is as follows. The imminent saccade would initiate an iteration of recurrent processing between the FEF and an assortment of visual cortical areas, beginning with receipt in the FEF of CD from the superior colliculus. This information represents the when and where of the imminent change in gaze and induces a transient alteration in local functional topology of the FEF network. At the center of the alteration would be FEF network hubs (h) (Sporns et al., 2007). FEF network hubs have access to information about the entire hemifield ($I_{hD(h)}(t)$) and are putatively the neurons with shifting RFs. The CD serves a gating function ($C_{hD(h)}(t)$) and routes the appropriate visual information through the hub ($f_{hD(h)}(t)$). (If CD is not present ($C_{hD(h)}(t)=0$), the hub simply passes on the visual information provided to it from node x.) These relationships may be written as:

$$f_{hD(h)}(t) = I_{hD(h)}(t)C_{hD(h)}(t), \text{ if } C_{hD(h)}(t) > 0$$

Otherwise: $f_{hD(h)}(t) = x, \text{ if } C_{hD(h)}(t) = 0$

The response field is said to shift and corresponds to a collection of visual information about the portions of space that the response field will encompass after the saccade. This information then would be combined with the causal estimates of the generative model embedded within the FEF network. A prediction would be generated and exported, manifested as a round of perisaccadic synchronized activity between the frontal and posterior lobes (Figure 30). The synchronized activity would alter the visual cortical network dynamics and effect how the visual stimulus-driven activity is integrated into the

network. The synchronized activity is equivalent to a prediction, the output of the generative model (blue line). If the actual visual input (black line) does not match this prediction, then residuals (prediction errors; orange line) are calculated by the FEF and iterative processes are continued. Perhaps something moved or due to noise or injury the system got it wrong. Persistent, systematic mismatches between the prediction and actual outcome would imply miscalibration of corollary discharge, generative model, or both. The brain could adjust its interpretation of the signals until mismatches were eliminated, a process of sensorimotor learning. More sporadic, atypical mismatches between prediction and outcome would imply, in contrast, that something was unstable in the outside world. Finally, compatible predictions and outcomes – the norm in everyday saccadic behavior – would signal both that internal calibration is correct and that the world is stable.

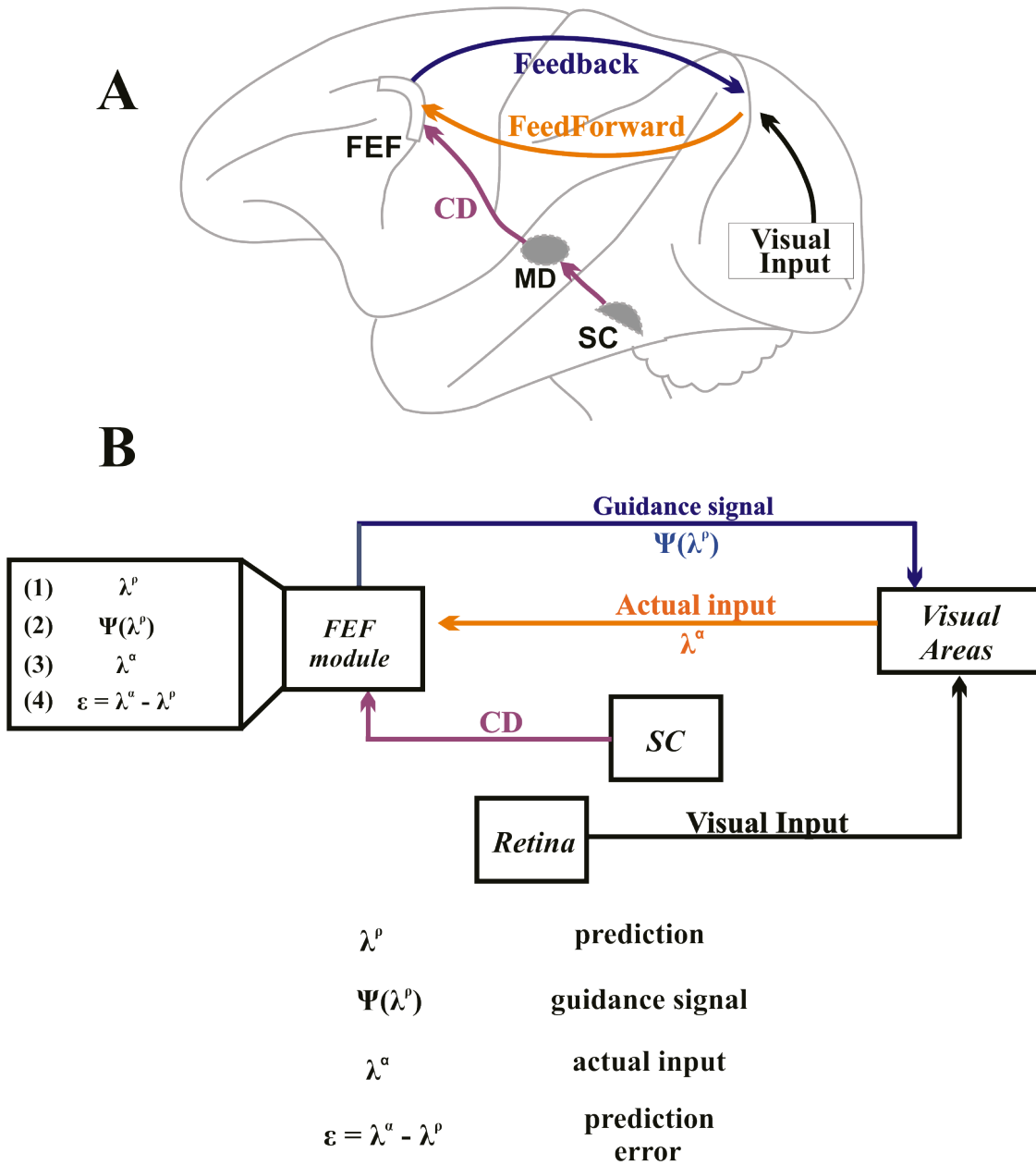


Figure 30 The frontal eye field as a prediction map. (A) Lateral view of macaque brain illustrating the interactions between the frontal eye field (FEF) and the posterior lobes. Triggered by CD, the FEF exports predictive signals to the posterior lobes via feedback connections. The posterior lobes report back to the FEF about the actual visual input via feedforward connection. (B). Corresponding schematic diagram depicting the computational roles of the FEF. FEF module inset: (1) A series of computations, triggered by CD from the midbrain and enabled by shifting RFs, results in a prediction of the postsaccadic scene (λ^p) based upon information extracted from the current or presaccadic scene. (2) The prediction is then convolved with a forward model (Ψ) to yield guidance signals ($\Psi(\lambda^p)$) that area imposed upon the posterior lobes. This signal constrains the state space of the posterior lobes and biases the operations performed therein. (3) Once the saccade is complete, information about the actually occurring postsaccadic scene (λ^a) is routed to the FEF. (4) The FEF compares the input representing the actual postsaccadic scene with the initial prediction ($\varepsilon = \lambda^a - \lambda^p$). This is useful for calibration, error correction, and the detection of unpredicted visual events.

5.26 Site of prediction error calculation

Aside from the FEF, prediction errors could be calculated at any number of visual cortical depots. Virtually every portion of the cortical mantle exhibits some degree of saccadic modulation (Baker et al., 2006). Dorsal stream components seem most likely for two reasons. First, the temporal structure of information flow through the primate visual system points to a dorsal stream speed advantage over the ventral stream (Bar, 2007; Bullier, 2001). Dorsal stream components exhibit activation latencies that often trail V1 responses by a meager 10 ms. Some even activate before V1 (Bullier et al., 2001; Schmolesky et al., 1998). This speed advantage would be optimal for the rapid detection and routing of prediction errors back to the FEF, if calculated elsewhere. Second, the dorsal stream is known as the where pathway (Ungerleider and Mishkin, 1982). Components are concerned with motion and the physical location of objects in the visual scene. Since I submit that the primary concern of the visual system during a saccade is to ensure a stable world, the dorsal stream would seem to be particularly important in controlling the illusory percept of motion concomitant to saccade generation. Any errors related to the prediction could be a consequence of an object that actually moved on its own accord and thus was not predicted. The object would be with high probability worthy of further inspection. The FEF would then direct the allocation of attentional and targeting mechanisms to these objects via retrojections of activity to stations of the ventral stream such as V4 and IT (Hamker, 2005; Moore and Armstrong, 2003).

5.2.7 Relation to previous FEF studies

Previous studies have uncovered a number of FEF response properties consistent with the notion of a prediction map. One implication of prediction error in general is that single neurons should not respond if the stimulus falling in its RF is predicted. Burman and Segraves found that when monkeys rescanned a previously scanned image, visual activity was virtually unaffected by the contents of the image that fell within the response field (Burman and Segraves, 1994). In contrast, these same neurons fired during the initial scan and when a target light suddenly appeared in the response field. After the initial scanning, a memory trace of the image was likely formed, and only deviations from the predicted image components were subsequently signaled as visual bursts. This suggests that the visual response of FEF neurons signals prediction error, the unexpected.

Other components of a prediction map would be expected to store elements of past visuosaccadic experience. These patterns would assist in the rapid generation of future predictions. A past record might serve as a Bayesian prior in calculating the probability of what action is to occur next. Neurons have been found in the FEF and surrounding PFC that seem to do just that, they seem to track past performance as well as anticipate the action the monkey is likely to perform next (Bruce and Goldberg, 1985; Hasegawa et al., 2000). They exhibit no visual or movement related activity, but instead evince a type of anticipatory activity that develops gradually after several trials and decays gradually once task contingencies are changed. These neurons might be referred to as simulator cells and could very easily play a role in FEF predictive computations.

An additional implication of a prediction map applies to the movement related aspects of the FEF, generally. If a function of the FEF is to generate predictions, then movement responses too may be viewed probabilistically. In fact, some pure movement cells have been found that generate vigorous bursts even when the monkey errs and does not perform the saccade (Bruce and Goldberg, 1985). This is evidence that the movement signal in FEF is closely akin to a prediction or probability estimate of a saccade being generated into its movement field. It bears little relationship to saccade dynamics (Segraves and Park, 1993). Stimulating the FEF collapses this probability estimate to 1. I suggest that the forced manner in which FEF movement signals have been studied classically, counting spikes while monkeys make required eye movements into a neuron's response field, may mask this probabilistic aspect of FEF function and redirect focus on alleged deterministic aspects of movement generation.

5.2.8 Empirical tests of the prediction map theory

A number of empirically testable predictions are deducible from the FEF perisaccadic prediction map theory. Firstly, if the system truly is computing prediction error, then one might predict that systematically imposing mismatches between the presaccadic and postsaccadic scenes should result in an attenuation of the error signals. That is, if the mismatch becomes predictable, then the system should cease to signal when any sort of presaccadic/postsaccadic mismatch occurs. This could be explored within the context of the saccadic translation task outlined in Chapter 3. For that task, we interleaved trials in which the stimulus moved by varying degrees with trials in which the stimulus remained stable. As such, the system was kept in the dark, so to speak, and

could not anticipate whether a probe would be stable or unstable. But, if one were to perform an experiment in which the probe changed along a dimension consistently from trial to trial, then a prediction of the theory is that the neurons would eventually cease responding to the change as it has since become predictable. Prediction error would be zero.

A second prediction relates to the various types of perisaccadic response modulations that have been observed in neurons throughout striate and extrastriate cortex. According to the prediction map theory, these effects are mediated at least in part by predictive, guidance signals issuing from the FEF. It is already known that stimulation of the FEF results in response alterations throughout extrastriate cortex. This indicates that there are functional connections between the FEF and extrastriate cortex. These connections could easily be harnessed at the time of a saccade and mediate the proposed computations. This has a simple prediction: inactivation of the FEF should abolish these perisaccadic effects. At the perceptual level, such causal perturbation is predicted to alter the animal's percept of transaccadic stability.

A more correlative test that would provide deeper insights into subtle mechanics would involve simultaneous recording from the FEF and a given extrastriate area during various saccadic tasks. For example, at the time of a saccade a certain degree of spiking coherence is predicted to emerge between the FEF and visual cortical neurons (such as V4, V2, and V1). Such coherence would betray a functional interaction. Upon arrival the guidance signals are proposed to influence oscillatory network dynamics of the recipient visual area. Oscillations effectively control neuronal excitability by opening windows of opportunity that selectively emphasize or deemphasize incoming sensory information.

For the case of transaccadic visual perception FEF guidance signals are predicted to modify network oscillatory phase dynamics of visual cortical areas to ensure that incoming sensory transients reflecting the displacement of the retinal image are attenuated and restricted from further network processing. This has the physiological prediction that a phase alteration of oscillatory behavior should occur throughout the visual cortex at the time of a saccade due to the modulatory influence of the FEF.

5.3 Summary and Conclusion

Visual stability is thought to rely on an active process by which motor information is integrated with visual information. Together these signals can initiate a computational chain of events that results in spatially-correct vision. We have studied one area that is located at the intersection of action and vision. Our results reveal that this area possesses a number of computational properties that render it a likely participant in visual stabilization mechanisms. Visual stabilization seems to require predictive computations. Accordingly, we found that FEF neurons appear to anticipate the visual outcome of a saccade and signal when the outcome does not match the anticipation. These signals were not just a lab curio devoid of any causal efficacy; they were found to be tightly correlated with and predictive of monkey psychophysics. To be of any functional utility these perisaccadic signals must interact with those posterior brain areas traditionally associated with higher-order, cognitive vision. The proposed model makes an attempt to incorporate the FEF within such a larger visual network and details how this interaction might occur at the physiological level. Future work should attempt to assess the validity of the computational claims and make an effort at circuit level interventions that bridge

the neuron-perceptual gap. Such interventions would provide a causal test of the role of these processes in mechanisms of transaccadic visual stability.

6.0 Bibliography

- Amiez, C., and Petrides, M. (2009). Anatomical organization of the eye fields in the human and non-human primate frontal cortex. *Prog Neurobiol* 89, 220-230.
- Anstis, S.M. (1974). Letter: A chart demonstrating variations in acuity with retinal position. *Vision Res* 14, 589-592.
- Arieli, A., Sterkin, A., Grinvald, A., and Aertsen, A. (1996). Dynamics of ongoing activity: explanation of the large variability in evoked cortical responses. *Science* 273, 1868-1871.
- Armstrong, K.M., Fitzgerald, J.K., and Moore, T. (2006). Changes in visual receptive fields with microstimulation of frontal cortex. *Neuron* 50, 791-798.
- Baker, J.T., Patel, G.H., Corbetta, M., and Snyder, L.H. (2006). Distribution of activity across the monkey cerebral cortical surface, thalamus and midbrain during rapid, visually guided saccades. *Cereb Cortex* 16, 447-459.
- Banks, M.S., Sekuler, A.B., and Anderson, S.J. (1991). Peripheral spatial vision: limits imposed by optics, photoreceptors, and receptor pooling. *J Opt Soc Am A* 8, 1775-1787.
- Bar, M. (2007). The proactive brain: using analogies and associations to generate predictions. *Trends Cogn Sci* 11, 280-289.
- Barlow, H. (2001). Redundancy reduction revisited. *Network* 12, 241-253.
- Batschelet, E. (1981). *Circular Statistics in Biology* (London, Academic Press).
- Bays, P.M., and Husain, M. (2007). Spatial remapping of the visual world across saccades. *Neuroreport* 18, 1207-1213.
- Becker, W., and Jurgens, R. (1979). An analysis of the saccadic system by means of double step stimuli. *Vision Res* 19, 967-983.

Benevento, L.A., and Fallon, J.H. (1975). The ascending projections of the superior colliculus in the rhesus monkey (*Macaca mulatta*). *J Comp Neurol* *160*, 339-361.

Berman, R.A., Heiser, L.M., Dunn, C.A., Saunders, R.C., and Colby, C.L. (2007). Dynamic circuitry for updating spatial representations. III. From neurons to behavior. *Journal of neurophysiology* *98*, 105-121.

Berman, R.A., Heiser, L.M., Saunders, R.C., and Colby, C.L. (2005). Dynamic circuitry for updating spatial representations. I. Behavioral evidence for interhemispheric transfer in the split-brain macaque. *J Neurophysiol* *94*, 3228-3248.

Boire, D., Theoret, H., and Ptito, M. (2001). Visual pathways following cerebral hemispherectomy. *Prog Brain Res* *134*, 379-397.

Bridgeman, B., Hendry, D., and Stark, L. (1975). Failure to detect displacement of the visual world during saccadic eye movements. *Vision Res* *15*, 719-722.

Bruce, C.J., and Goldberg, M.E. (1985). Primate frontal eye fields. I. Single neurons discharging before saccades. *J Neurophysiol* *53*, 603-635.

Bruce, C.J., Goldberg, M.E., Bushnell, M.C., and Stanton, G.B. (1985). Primate frontal eye fields. II. Physiological and anatomical correlates of electrically evoked eye movements. *J Neurophysiol* *54*, 714-734.

Bullier, J. (2001). Integrated model of visual processing. *Brain Res Brain Res Rev* *36*, 96-107.

Bullier, J., Hupe, J.M., James, A.C., and Girard, P. (2001). The role of feedback connections in shaping the responses of visual cortical neurons. *Prog Brain Res* *134*, 193-204.

- Burman, D.D., and Segraves, M.A. (1994). Primate frontal eye field activity during natural scanning eye movements. *J Neurophysiol* *71*, 1266-1271.
- Bushnell, M.C., Goldberg, M.E., and Robinson, D.L. (1981). Behavioral enhancement of visual responses in monkey cerebral cortex. I. Modulation in posterior parietal cortex related to selective visual attention. *J Neurophysiol* *46*, 755-772.
- Canedo, A. (1997). Primary motor cortex influences on the descending and ascending systems. *Prog Neurobiol* *51*, 287-335.
- Clower, D.M., West, R.A., Lynch, J.C., and Strick, P.L. (2001). The inferior parietal lobule is the target of output from the superior colliculus, hippocampus, and cerebellum. *J Neurosci* *21*, 6283-6291.
- Colby, C.L., Berman, R.A., Heiser, L.M., and Saunders, R.C. (2005). Corollary discharge and spatial updating: when the brain is split, is space still unified? *Prog Brain Res* *149*, 187-205.
- Connor, C.E., Gallant, J.L., Preddie, D.C., and Van Essen, D.C. (1996). Responses in area V4 depend on the spatial relationship between stimulus and attention. *Journal of neurophysiology* *75*, 1306-1308.
- Crapse, T.B., and Sommer, M.A. (2008a). Corollary discharge across the animal kingdom. *Nat Rev Neurosci* *9*, 587-600.
- Crapse, T.B., and Sommer, M.A. (2008b). Corollary discharge circuits in the primate brain. *Curr Opin Neurobiol* *18*, 552-557.
- Crapse, T.B., and Sommer, M.A. (2008c). The frontal eye field as a prediction map. *Prog Brain Res* *171*, 383-390.

- Crapse, T.B., and Sommer, M.A. (2009). Frontal eye field neurons with spatial representations predicted by their subcortical input. *J Neurosci* 29, 5308-5318.
- Crist, C.F., Yamasaki, D.S., Komatsu, H., and Wurtz, R.H. (1988). A grid system and a microsyringe for single cell recording. *Journal of neuroscience methods* 26, 117-122.
- Deubel, H., Bridgeman, B., and Schneider, W.X. (1998). Immediate post-saccadic information mediates space constancy. *Vision Res* 38, 3147-3159.
- Deubel, H., Schneider, W.X., and Bridgeman, B. (1996). Postsaccadic target blanking prevents saccadic suppression of image displacement. *Vision Res* 36, 985-996.
- Douglas, R.J., and Martin, K.A. (2004). Neuronal circuits of the neocortex. *Annu Rev Neurosci* 27, 419-451.
- Duhamel, J.R., Colby, C.L., and Goldberg, M.E. (1992). The updating of the representation of visual space in parietal cortex by intended eye movements. *Science* 255, 90-92.
- Engel, A.K., Fries, P., and Singer, W. (2001). Dynamic predictions: oscillations and synchrony in top-down processing. *Nat Rev Neurosci* 2, 704-716.
- Felleman, D.J., and Van Essen, D.C. (1991). Distributed hierarchical processing in the primate cerebral cortex. *Cereb Cortex* 1, 1-47.
- Fenske, M.J., Aminoff, E., Gronau, N., and Bar, M. (2006). Top-down facilitation of visual object recognition: object-based and context-based contributions. *Prog Brain Res* 155, 3-21.
- Ferrier, D. (1875). Experiments on the basis of monkeys. *Proceedings of the Royal Society of London B Biological Sciences* 23, 409-430.

Fries, W. (1984). Cortical projections to the superior colliculus in the macaque monkey: a retrograde study using horseradish peroxidase. *J Comp Neurol* 230, 55-76.

Friston, K. (2005). A theory of cortical responses. *Philos Trans R Soc Lond B Biol Sci* 360, 815-836.

Friston, K.J., and Price, C.J. (2001). Dynamic representations and generative models of brain function. *Brain Res Bull* 54, 275-285.

Gandhi, N.J., and Keller, E.L. (1997). Spatial distribution and discharge characteristics of superior colliculus neurons antidromically activated from the omnipause region in monkey. *J Neurophysiol* 78, 2221-2225.

Giguere, M., and Goldman-Rakic, P.S. (1988). Mediodorsal nucleus: areal, laminar, and tangential distribution of afferents and efferents in the frontal lobe of rhesus monkeys. *J Comp Neurol* 277, 195-213.

Gilbert, C.D., and Sigman, M. (2007). Brain states: top-down influences in sensory processing. *Neuron* 54, 677-696.

Gold, J.I., and Shadlen, M.N. (2007). The neural basis of decision making. *Annu Rev Neurosci* 30, 535-574.

Goldberg, M.E., and Bruce, C.J. (1990). Primate frontal eye fields. III. Maintenance of a spatially accurate saccade signal. *J Neurophysiol* 64, 489-508.

Goldberg, M.E., and Bushnell, M.C. (1981). Behavioral enhancement of visual responses in monkey cerebral cortex. II. Modulation in frontal eye fields specifically related to saccades. *J Neurophysiol* 46, 773-787.

Goldberg, M.E., and Wurtz, R.H. (1972). Activity of superior colliculus in behaving monkey. II. Effect of attention on neuronal responses. *J Neurophysiol* 35, 560-574.

Gottlieb, J.P., Kusunoki, M., and Goldberg, M.E. (1998). The representation of visual salience in monkey parietal cortex. *Nature* 391, 481-484.

Gould, H.J., 3rd, Cusick, C.G., Pons, T.P., and Kaas, J.H. (1986). The relationship of corpus callosum connections to electrical stimulation maps of motor, supplementary motor, and the frontal eye fields in owl monkeys. *J Comp Neurol* 247, 297-325.

Hall, W.C., and Moschovakis, A.K., eds. (2004). *The Superior Colliculus: New Approaches for Studying Sensorimotor Integration* (Boca Raton, CRC Press).

Hallett, P.E., and Lightstone, A.D. (1976). Saccadic eye movements to flashed targets. *Vision Res* 16, 107-114.

Hamker, F.H. (2005). The reentry hypothesis: the putative interaction of the frontal eye field, ventrolateral prefrontal cortex, and areas V4, IT for attention and eye movement. *Cereb Cortex* 15, 431-447.

Hanes, D.P., and Schall, J.D. (1996). Neural control of voluntary movement initiation. *Science* 274, 427-430.

Hanes, D.P., Thompson, K.G., and Schall, J.D. (1995). Relationship of presaccadic activity in frontal eye field and supplementary eye field to saccade initiation in macaque: Poisson spike train analysis. *Exp Brain Res* 103, 85-96.

Hasegawa, R.P., Blitz, A.M., Geller, N.L., and Goldberg, M.E. (2000). Neurons in monkey prefrontal cortex that track past or predict future performance. *Science* 290, 1786-1789.

Hays, A.V., Optican, L.M., and Richmond, B.J. (1982). A UNIX-based multiple process system for real-time data acquisition and control. *WESCON Conference Proceedings* 2, 1-10.

Heiser, L.M., Berman, R.A., Saunders, R.C., and Colby, C.L. (2005). Dynamic circuitry for updating spatial representations. II. Physiological evidence for interhemispheric transfer in area LIP of the split-brain macaque. *J Neurophysiol* 94, 3249-3258.

Heiser, L.M., and Colby, C.L. (2006). Spatial updating in area LIP is independent of saccade direction. *J Neurophysiol* 95, 2751-2767.

Helmholtz, H. (1925). *Helmholtz's Treatise on Physiological Optics*, 3rd edn (New York, Optical Society of America).

Herter, T.M., and Guitton, D. (2004). Accurate bidirectional saccade control by a single hemicortex. *Brain* 127, 1393-1402.

Hikosaka, O., and Wurtz, R.H. (1983). Visual and oculomotor functions of monkey substantia nigra pars reticulata. III. Memory-contingent visual and saccade responses. *J Neurophysiol* 49, 1268-1284.

Hoffmann, K.P., Bremmer, F., Thiele, A., and Distler, C. (2002). Directional asymmetry of neurons in cortical areas MT and MST projecting to the NOT-DTN in macaques. *J Neurophysiol* 87, 2113-2123.

Holst, E., and Mittelstaedt, H. (1950a). The reafference principle. *Naturwissenschaften* 37, 464-467.

Holst, E.V., and Mittelstaedt, H. (1950b). The reafference principle. *Naturwissenschaften* 37, 464-467.

Hopp, J.J., and Fuchs, A.F. (2004). The characteristics and neuronal substrate of saccadic eye movement plasticity. *Prog Neurobiol* 72, 27-53.

Hupe, J.M., James, A.C., Payne, B.R., Lomber, S.G., Girard, P., and Bullier, J. (1998). Cortical feedback improves discrimination between figure and background by V1, V2 and V3 neurons. *Nature* 394, 784-787.

Hwang, E.J., and Shadmehr, R. (2005). Internal models of limb dynamics and the encoding of limb state. *J Neural Eng* 2, S266-278.

Irwin, D.E. (1991). Information integration across saccadic eye movements. *Cognitive psychology* 23, 420-456.

Izawa, Y., Suzuki, H., and Shinoda, Y. (2004). Suppression of visually and memory-guided saccades induced by electrical stimulation of the monkey frontal eye field. I. Suppression of ipsilateral saccades. *J Neurophysiol* 92, 2248-2260.

Kleinschmidt, A., Buchel, C., Zeki, S., and Frackowiak, R.S. (1998). Human brain activity during spontaneously reversing perception of ambiguous figures. *Proc Biol Sci* 265, 2427-2433.

Knill, D.C., and Pouget, A. (2004). The Bayesian brain: the role of uncertainty in neural coding and computation. *Trends Neurosci* 27, 712-719.

Kusunoki, M., and Goldberg, M.E. (2003). The time course of perisaccadic receptive field shifts in the lateral intraparietal area of the monkey. *Journal of neurophysiology* 89, 1519-1527.

Lamantia, A.S., and Rakic, P. (1990). Cytological and quantitative characteristics of four cerebral commissures in the rhesus monkey. *J Comp Neurol* 291, 520-537.

Lee, T.S. (2002). Top-down influence in early visual processing: a Bayesian perspective. *Physiol Behav* 77, 645-650.

Lee, T.S., and Mumford, D. (2003). Hierarchical Bayesian inference in the visual cortex. *J Opt Soc Am A Opt Image Sci Vis* 20, 1434-1448.

Li, W., and Matin, L. (1997). Saccadic suppression of displacement: separate influences of saccade size and of target retinal eccentricity. *Vision Res* 37, 1779-1797.

Li, W.X., and Matin, L. (1990). The influence of saccade length on the saccadic suppression of displacement detection. *Perception & psychophysics* 48, 453-458.

Liu, J., and Newsome, W.T. (2003). Functional organization of speed tuned neurons in visual area MT. *Journal of neurophysiology* 89, 246-256.

Lynch, J.C., Hoover, J.E., and Strick, P.L. (1994). Input to the primate frontal eye field from the substantia nigra, superior colliculus, and dentate nucleus demonstrated by transneuronal transport. *Exp Brain Res* 100, 181-186.

Lynch, J.C., and Tian, J.R. (2005). Cortico-cortical networks and cortico-subcortical loops for the higher control of eye movements. *Prog Brain Res* 151, 461-501.

Maunsell, J.H., and Van Essen, D.C. (1983). Functional properties of neurons in middle temporal visual area of the macaque monkey. I. Selectivity for stimulus direction, speed, and orientation. *Journal of neurophysiology* 49, 1127-1147.

Mays, L.E., and Sparks, D.L. (1980). Dissociation of visual and saccade-related responses in superior colliculus neurons. *J Neurophysiol* 43, 207-232.

McPeck, R.M., and Keller, E.L. (2001). Short-term priming, concurrent processing, and saccade curvature during a target selection task in the monkey. *Vision Res* 41, 785-800.

Merigan, W.H., and Katz, L.M. (1990). Spatial resolution across the macaque retina. *Vision Res* 30, 985-991.

- Miall, R.C., and Wolpert, D.M. (1996). Forward Models for Physiological Motor Control. *Neural Networks* 9, 1265-1279.
- Mohler, C.W., Goldberg, M.E., and Wurtz, R.H. (1973). Visual receptive fields of frontal eye field neurons. *Brain Res* 61, 385-389.
- Moore, T., and Armstrong, K.M. (2003). Selective gating of visual signals by microstimulation of frontal cortex. *Nature* 421, 370-373.
- Moore, T., and Fallah, M. (2001). Control of eye movements and spatial attention. *Proc Natl Acad Sci U S A* 98, 1273-1276.
- Movshon, J.A., and Newsome, W.T. (1996). Visual response properties of striate cortical neurons projecting to area MT in macaque monkeys. *J Neurosci* 16, 7733-7741.
- Mumford, D. (1992). On the computational architecture of the neocortex. II. The role of cortico-cortical loops. *Biol Cybern* 66, 241-251.
- Nagy, A.L., and Wolf, S. (1993). Red-green color discrimination in peripheral vision. *Vision Res* 33, 235-242.
- Nakamura, K., and Colby, C.L. (2002). Updating of the visual representation in monkey striate and extrastriate cortex during saccades. *Proc Natl Acad Sci U S A* 99, 4026-4031.
- Nambu, A., Kaneda, K., Tokuno, H., and Takada, M. (2002). Organization of corticostriatal motor inputs in monkey putamen. *J Neurophysiol* 88, 1830-1842.
- Niemeier, M., Crawford, J.D., and Tweed, D.B. (2003). Optimal transsaccadic integration explains distorted spatial perception. *Nature* 422, 76-80.
- O'Regan, J.K., and Levy-Schoen, A. (1983). Integrating visual information from successive fixations: Does transsaccadic fusion exist? *Vision Res* 23, 765-768.
- Olszewski, J. (1952). *The Thalamus of the Macaca Mulatta* (Basel, S. Karger).

Pandya, D.N., and Vignolo, L.A. (1971). Intra- and interhemispheric projections of the precentral, premotor and arcuate areas in the rhesus monkey. *Brain Res* 26, 217-233.

Perrone, J.A., and Thiele, A. (2001). Speed skills: measuring the visual speed analyzing properties of primate MT neurons. *Nat Neurosci* 4, 526-532.

Poppel, E., Held, R., and Frost, D. (1973). Leter: Residual visual function after brain wounds involving the central visual pathways in man. *Nature* 243, 295-296.

Pouget, A., Dayan, P., and Zemel, R. (2000). Information processing with population codes. *Nature reviews* 1, 125-132.

Poulet, J.F.A., and Hedwig, B. (2006). The cellular basis of a corollary discharge. *Science* 311, 518-522.

Preuss, T.M., and Goldman-Rakic, P.S. (1987). Crossed corticothalamic and thalamocortical connections of macaque prefrontal cortex. *J Comp Neurol* 257, 269-281.

Rao, R.P., and Ballard, D.H. (1999). Predictive coding in the visual cortex: a functional interpretation of some extra-classical receptive-field effects. *Nat Neurosci* 2, 79-87.

Rensink, R.A. (2002). Change detection. *Annual review of psychology* 53, 245-277.

Robinson, D.A. (1972). Eye movements evoked by collicular stimulation in the alert monkey. *Vision Res* 12, 1795-1808.

Robinson, D.A., and Fuchs, A.F. (1969). Eye movements evoked by stimulation of frontal eye fields. *J Neurophysiol* 32, 637-648.

Roelfsema, P.R., Lamme, V.A., and Spekreijse, H. (2000). The implementation of visual routines. *Vision Res* 40, 1385-1411.

Roitman, J.D., and Shadlen, M.N. (2002). Response of neurons in the lateral intraparietal area during a combined visual discrimination reaction time task. *J Neurosci* 22, 9475-9489.

Sanger, T.D. (2003). Neural population codes. *Current opinion in neurobiology* 13, 238-249.

Schall, J.D. (2002). The neural selection and control of saccades by the frontal eye field. *Philos Trans R Soc Lond B Biol Sci* 357, 1073-1082.

Schall, J.D., Hanes, D.P., Thompson, K.G., and King, D.J. (1995a). Saccade target selection in frontal eye field of macaque. I. Visual and premovement activation. *J Neurosci* 15, 6905-6918.

Schall, J.D., Morel, A., King, D.J., and Bullier, J. (1995b). Topography of visual cortex connections with frontal eye field in macaque: convergence and segregation of processing streams. *J Neurosci* 15, 4464-4487.

Schall, J.D., and Thompson, K.G. (1999). Neural selection and control of visually guided eye movements. *Annu Rev Neurosci* 22, 241-259.

Schiller, P.H., and Koerner, F. (1971). Discharge characteristics of single units in superior colliculus of the alert rhesus monkey. *Journal of neurophysiology* 34, 920-936.

Schlag-Rey, M., Schlag, J., and Dassonville, P. (1992). How the frontal eye field can impose a saccade goal on superior colliculus neurons. *J Neurophysiol* 67, 1003-1005.

Schlag, J., Dassonville, P., and Schlag-Rey, M. (1998). Interaction of the two frontal eye fields before saccade onset. *J Neurophysiol* 79, 64-72.

Schlag, J., and Schlag-Rey, M. (2002). Through the eye, slowly: delays and localization errors in the visual system. *Nat Rev Neurosci* 3, 191-215.

- Schmolesky, M.T., Wang, Y., Hanes, D.P., Thompson, K.G., Leutgeb, S., Schall, J.D., and Leventhal, A.G. (1998). Signal timing across the macaque visual system. *J Neurophysiol* 79, 3272-3278.
- Schultz, W., and Dickinson, A. (2000). Neuronal coding of prediction errors. *Annu Rev Neurosci* 23, 473-500.
- Segraves, M.A., and Park, K. (1993). The relationship of monkey frontal eye field activity to saccade dynamics. *J Neurophysiol* 69, 1880-1889.
- Seidemann, E., Arieli, A., Grinvald, A., and Slovin, H. (2002). Dynamics of depolarization and hyperpolarization in the frontal cortex and saccade goal. *Science* 295, 862-865.
- Sherman, S.M., and Guillery, R.W. (1998). On the actions that one nerve cell can have on another: distinguishing "drivers" from "modulators". *Proceedings of the National Academy of Sciences of the United States of America* 95, 7121-7126.
- Siegel, M., Kording, K.P., and Konig, P. (2000). Integrating top-down and bottom-up sensory processing by somato-dendritic interactions. *J Comput Neurosci* 8, 161-173.
- Simons, D.J., and Rensink, R.A. (2005). Change blindness: past, present, and future. *Trends Cogn Sci* 9, 16-20.
- Smith, C.U.M. (2000). *Biology of Sensory Systems* (New York, John Wiley & Sons, LTD).
- Sommer, M.A. (1994). Express saccades elicited during visual scan in the monkey. *Vision research* 34, 2023-2038.
- Sommer, M.A. (1997). The spatial relationship between scanning saccades and express saccades. *Vision research* 37, 2745-2756.

Sommer, M.A., and Wurtz, R.H. (1998). Frontal eye field neurons orthodromically activated from the superior colliculus. *J Neurophysiol* 80, 3331-3335.

Sommer, M.A., and Wurtz, R.H. (2000). Composition and topographic organization of signals sent from the frontal eye field to the superior colliculus. *J Neurophysiol* 83, 1979-2001.

Sommer, M.A., and Wurtz, R.H. (2001). Frontal eye field sends delay activity related to movement, memory, and vision to the superior colliculus. *J Neurophysiol* 85, 1673-1685.

Sommer, M.A., and Wurtz, R.H. (2002). A pathway in primate brain for internal monitoring of movements. *Science* 296, 1480-1482.

Sommer, M.A., and Wurtz, R.H. (2004a). What the brain stem tells the frontal cortex. I. Oculomotor signals sent from superior colliculus to frontal eye field via mediodorsal thalamus. *J Neurophysiol* 91, 1381-1402.

Sommer, M.A., and Wurtz, R.H. (2004b). What the brain stem tells the frontal cortex. II. Role of the SC-MD-FEF pathway in corollary discharge. *Journal of neurophysiology* 91, 1403-1423.

Sommer, M.A., and Wurtz, R.H. (2006). Influence of the thalamus on spatial visual processing in frontal cortex. *Nature* 444, 374-377.

Sommer, M.A., and Wurtz, R.H. (2008a). Brain circuits for the internal monitoring of movements. *Annual Reviews in Neuroscience* *In press*.

Sommer, M.A., and Wurtz, R.H. (2008b). Brain circuits for the internal monitoring of movements. *Annu Rev Neurosci* 31, 317-338.

Sparks, D.L. (2002). The brainstem control of saccadic eye movements. *Nat Rev Neurosci* 3, 952-964.

Sparks, D.L., and Hartwich-Young, R. (1989). The deep layers of the superior colliculus. *Reviews of oculomotor research* 3, 213-255.

Sperry, R. (1950). Neural basis of the spontaneous optokinetic response produced by visual inversion. *The Journal of Comparative and Physiological Psychology* 43, 482-489.

Sporns, O., Honey, C.J., and Kotter, R. (2007). Identification and classification of hubs in brain networks. *PLoS ONE* 2, e1049.

Stanton, G.B., Goldberg, M.E., and Bruce, C.J. (1988). Frontal eye field efferents in the macaque monkey: II. Topography of terminal fields in midbrain and pons. *J Comp Neurol* 271, 493-506.

Swadlow, H.A., Rosene, D.L., and Waxman, S.G. (1978). Characteristics of interhemispheric impulse conduction between prelunate gyri of the rhesus monkey. *Exp Brain Res* 33, 455-467.

Takahashi, M., Sugiuchi, Y., and Shinoda, Y. (2007). Commissural mirror-symmetric excitation and reciprocal inhibition between the two superior colliculi and their roles in vertical and horizontal eye movements. *Journal of neurophysiology* 98, 2664-2682.

Tehovnik, E.J., Sommer, M.A., Chou, I.H., Slocum, W.M., and Schiller, P.H. (2000). Eye fields in the frontal lobes of primates. *Brain Res Brain Res Rev* 32, 413-448.

Thompson, K.G., and Bichot, N.P. (2005). A visual salience map in the primate frontal eye field. *Prog Brain Res* 147, 251-262.

Tian, J., Schlag, J., and Schlag-Rey, M. (2000). Testing quasi-visual neurons in the monkey's frontal eye field with the triple-step paradigm. *Exp Brain Res* 130, 433-440.

Tolias, A.S., Moore, T., Smirnakis, S.M., Tehovnik, E.J., Siapas, A.G., and Schiller, P.H. (2001). Eye movements modulate visual receptive fields of V4 neurons. *Neuron* 29, 757-767.

Umeno, M.M., and Goldberg, M.E. (1997). Spatial processing in the monkey frontal eye field. I. Predictive visual responses. *J Neurophysiol* 78, 1373-1383.

Umeno, M.M., and Goldberg, M.E. (2001). Spatial processing in the monkey frontal eye field. II. Memory responses. *J Neurophysiol* 86, 2344-2352.

Ungerleider, L.G., and Mishkin, M. (1982). Two cortical visual systems. In *Analysis of Visual Behavior*, D.J. Ingle, M.A. Goodale, and R.J.W. Mansfield, eds.

Virsu, V., and Rovamo, J. (1979). Visual resolution, contrast sensitivity, and the cortical magnification factor. *Exp Brain Res* 37, 475-494.

von Stein, A., Chiang, C., and Konig, P. (2000). Top-down processing mediated by interareal synchronization. *Proc Natl Acad Sci U S A* 97, 14748-14753.

Wade, N., and Tatler, B.W. (2005). *The moving tablet of the eye: the origins of modern eye movement research* (New York, Oxford University Press).

Womelsdorf, T., Anton-Erxleben, K., Pieper, F., and Treue, S. (2006). Dynamic shifts of visual receptive fields in cortical area MT by spatial attention. *Nat Neurosci* 9, 1156-1160.

Womelsdorf, T., Anton-Erxleben, K., and Treue, S. (2008). Receptive field shift and shrinkage in macaque middle temporal area through attentional gain modulation. *J Neurosci* 28, 8934-8944.

Womelsdorf, T., Schoffelen, J.M., Oostenveld, R., Singer, W., Desimone, R., Engel, A.K., and Fries, P. (2007). Modulation of neuronal interactions through neuronal synchronization. *Science* 316, 1609-1612.

Wurtz, R.H. (2008). Neuronal mechanisms of visual stability. *Vision Res* 48, 2070-2089.

Wurtz, R.H., and Goldberg, M.E. (1972). Activity of superior colliculus in behaving monkey. III. Cells discharging before eye movements. *J Neurophysiol* 35, 575-586.